Pleistocene-Holocene Sedimentation Along King Fahd Causeway Between Saudi Arabia and Bahrain

by

Ata Hasan Darwish

A Thesis Presented to the

FACULTY OF THE COLLEGE OF GRADUATE STUDIES

KING FAHD UNIVERSITY OF PETROLEUM & MINERALS

DHAHRAN, SAUDI ARABIA

In Partial Fulfillment of the
Requirements for the Degree of

MASTER OF SCIENCE

In

EARTH SCIENCES

August, 1988

Pleistocene-Holocene sedimentation along King Fahd causeway between Saudi Arabia and Bahrain

Darwish, Ata Hasan, M.S.

King Fahd University of Petroleum and Minerals (Saudi Arabia), 1988

PLEISTOCENE-HOLOCENE SEDIMENTATION ALONG KING FAHD CAUSEWAY BETWEEN SAUDI ARABIA AND BAHRAIN

BY

ATA HASAN DARWISH

A Thesis Presented to the

FACULTY OF THE COLLEGE OF GRADUATE STUDIES

KING FAHD UNIVERSITY OF PETROLEUM & MINERALS

DHAHRAN, SAUDI ARABIA

In Partial Fulfillment of the
Requirements for the Degree of

MASTER OF SCIENCE

In

EARTH SCIENCES

AUGUST, 1988

KING FAHD UNIVERSITY OF PETROLEUM AND MINERALS

DHAHRAN, SAUDI ARABIA

This thesis, written by Ata Hasan Ismail Darwish under the direction of his Thesis Advisor and approved by his Thesis Committee, has been presented to and accepted by the Dean of the College of Graduate Studies, in partial fulfillment of the requirements for the degree of MASTER OF SCIENCE in EARTH SCIENCES.

Thesis Committee

Prof. C. D. Conley, Thesis Advisor

Prof. G. W. Lynts, Member

Dr. M. N. Cagatay, Member

Dr. M. A. Al-Ukayli, Department Chairman

Dr. A. S. Al-Zakari, Dean, College of Graduate Studies

بِسْمِ اللَّهِ الرَّحْمَٰنِ الرَّحِيمِ

53. "He Who has made for you The earth like a carpet Spread out; has enabled you To go about therein by roads (And channels); and has sent Down water from the sky." With it have We produced Divers pairs of plants Each separate from the others.	ٱلَّذِى جَعَلَ لَكُمُ ٱلْأَرْضَ مَهْدًا وَسَلَكَ لَكُمْ فِيهَا سُبُلًا وَأَنزَلَ مِنَ ٱلسَّمَآءِ مَآءً فَأَخْرَجْنَا بِهِۦٓ أَزْوَٰجًا مِّن نَّبَاتٍ شَتَّىٰ ﴿٥٣﴾

THIS THESIS IS DEDICATED TO MY MOTHER

ACKNOWLEDGEMENT

First and foremost, praise and thanks be to Almightly Allah, the most Gracious,the most Merciful, and Peace be Upon His Prophet.

I wish to express my sincere appreciation to Prof. C.D. Conley, my major Thesis advisor, for his invaluable and continuous guidance and encouragement throughout this study. I also wish to thank the other members of my Thesis Commitee, Dr. Mehmet Cagatay and Prof. G.W.Lynts for their cooperation and helpful suggestion.

I would like to express my deep appreciation to Dr. M.A. Ukayli, the Chairman of the Earth Sciences Departement. Also special thanks are due to Prof. Z.El-Naggar, Dr. A.A.Qahwash and Dr. M. G. Davis, The Branch Manager of Balast-nedam group, for their help in obtaining the marine rock samples under King Fahd causeway between Saudi Arabia and Bahrain.

Special thanks are due to Dr. Nourdin Abbass, CAL Manager R.I., Dr.H. Khatri, Mr. Nuguen and Mr. Metra for continoue help during SEM and XRD analysis in Research Institute, KFUPM.

I would like to thank Dr. Ibrahim Alam, Manager of Environmental Protection Program, and Dr. M. Sadiq for their helpful guidance during chemical work. My sinceres thanks for Dr. Hamid Qunebi, from the Arabian Journal of Science and Engineering, for his help in preparing the Arabic abstract.

I would like to express my gratitude and thanks to Earth Sciences Laboratory technicians, Ali Abdullatif, Zafar Kaplan, and Orhan Demeros for their help in laboratory work. Special thanks are due to Departement secretaries, Ryad Beg and Gulam Khan, for their help in printing this manuscript.

My sincere thanks to My wife for her moral support throughout all phases of this work.

Lastly, I sincerely acknowledge my brothers in law Husni Shehata and Gazi Al Teepy who motivated and assisted me in different phases during my stay at the university.

Support of King Fahd University of Petroleum & Minerals is hereby acknowledged.

TABLE OF CONTENTS

Page

CHAPTER III

LITHOFACIES

CHAPTER 1V

DIAGENETIC CHANGES IN THE ROCKS

LIST OF FIGURES

LIST OF PLATES

ABSTRACT

This study was conducted on a series of 10 rock cores, as much as 44 meters long, along King Fahd causeway between Saudi Arabia and Bahrain at the entrance of Gulf of Salwa (26° N-50° 20 E) on the Arabian Shallow Shelf. The cores penetrate Pleistocene-Holocene rocks and sediments in that area of the Arabian Gulf. These cores show two mineralogical units;

1- A lower dolomite interval, as much as 40 meters thick.
2- An upper non-dolomite interval, three to nine meters thick, which consists of interbedded quartz sandstone, calcitic skeletal grainstone, quartz sand, and aragonitic skeletal and oolitic sand and grainstone.

The dolomitic interval comprises several depositional cycles. Each cycle includes upward shallowing sequence consisting of, from base to top; skeletal packstone, wackestone/mudstone, pelletal grainstone and green mudstone with thin horizons of white mudstone fragments (breccia).

The depositional environments start with a shallow open marine subtidal environment shallowing progressively to extremely shallow, restricted lagoonal environment with brief periods of subaerial exposure that produced desiccation breccias. The dolomitic lithofacies, in general, suggest a shallow water origin and was probably deposited at sea level slightly lower than today, as suggeted by the presence of several subaerial exposure periods. Moreover, the dolomitic lithofacies appear to represent deposition in two shallow lagoon between recurring oolitic paleoshoals.The dolomitic lithofacies are thought to have been deposited in mid-Pleistocene and before the first major lowering of sea level.

Following the cyclical shallow marine deposition, after dolomitization, a discontinuous, thin quartz sand was deposited during brief low stand o sea level (110,000-90,000 y.b.p.). Skeletal grainstone was deposited during later transgression (90,000- 75,000 y.b.p.). Next, the entire Gulf was emptied during the major late Pleistocene regression. Rainfall during late Pleistocene pluvial periods supplied fresh water, which caused the leaching of aragonitic constituents, precipitation of calcite cement and calcitizing deeper dolomite horizons

As the climate became more arid, a blanket of dune sand accumulated in coastal Arabia, Bahrain, Qatar and UAE including the studied area. Aragonitic oolitic and skeletal sand and grainstone were deposited during the Flandrial Transgression after the Gulf of Salwa was flooded (6,000 y.b.p). The lithostratigraphy of the non-dolomitic layers and profile of sea level changes of Fairbridge (1961) can be matched well.

(الخلاصه)

لقد اجريت،هذه الدراسة الجيولوجية،على عينات صخرية مختارة من عدد من الثقوب الاستكشافية المستخرجة من اسفل جسر الملك فهد البحري علي الساحل الغربي للخليج العربي الذي يربط البحرين بالمملكة العربية السعودية ، والواقع في مدخل خليج سلوى مابين خط عرض ٢٦ درجة شمالا وخط طول ٥٠ درجة و٢٠ ثانية شرقا . والجدير بالذكر ان هذه الثقوب الاستكشافية تخترق كلا من صخور وترسبات عصر البلايستوسين والهولوسين (الحديث) وتتكون من نوعين من الصخور :

اولا : صخور غير دولوماتية وتقع في الجزء الاعلى ويتراوح سمكها مابين ثلاثة الى تسعة امتار ، وهي مرتبة طبقيا كالاتي بدءا بالاحدث .

ا) صخور وترسبات الاراجونايت وتشمل :
- ترسبات وصخور السرئيات (الاوولايت)
- ترسبات وصخور الهياكل الإحفورية .

ب) رمال غير متماسكة من الكوارتز (المرو).

ج) صخور كلسية حبيبية وغنية بالهياكل الإحفورية.

د) حجر رملي متماسك (المادة اللاحمة غالبا الكالسيت).

ثانيا: صخور دولوماتية وتقع في الجزء الاسفل ويبلغ سمكها ٤٠ مترا على الاقل وهي تشمل عدة سحن صخرية ذات انسجة مختلفة طبقا لاختلاف بيئات الترسيب.والواقع ان الصخور الدولوماتية تمثل عدة دورات ترسيبية (خمس على الاقل) وكل دورة تتضمن عدد من السحن الصخرية ذات الانسجه المختلفة والتي تمثل في مجملها سلسله ترسيبية متدرجة في الضحالة اذ يبدا الترسيب عادة ببيئة شاطئية غير عميقة نسبيا وذات طاقة عالية (نشطة) وهي في الغالب مفتوحة على الحوض الرئيسي للمياة (البحر أو الخليج) فتؤدي الي تكون ترسبات حبيبية غنية بالهياكل الإحفورية ومع إزدياد ضحالة المياه يزداد الحصر وتقل حركة الماء مما يقلل نسبة الأحافير ويزيد نسبة الطين الذى يميز البيئات ذات الطاقة المنخفضة . ثم يستمر التدرج في الضحالة وبالتالي الحصر مما يقلل حركة المياه مؤدياً إلى تكون بيئة اختزال خالية من الاوكسجين الضروري لحياة الكائنات فتترسب طبقة الطين الحجري الخضراء الخالية تماما من اي اثر للكائنات الحيه،وهذه الطبقة عادة ماتنتهي بطبقة بيضاء من الشقوق الطينية والتي تمثل الانحسار الكامل للمياة والتعرض الكامل للشمس . وهذا يعني ان الصخور الدولوماتية بصورة عامة تمثل بيئة شاطئية ضحلة يتخللها عدة فترات من الإنحسار الكامل للمياه وهذا مايؤكدة القطاع الجيولوجي للمنطقة والذى يظهر ان الدولومايت ترسب في برك شاطئية (اثنتين علي الاقل) يفصلها حواجز قديمة من السرئيات .

اما بالنسبه للصخور غير الدولوماتية فهناك توافق كامل مابين وضعها الطبقي وبيئاتها الترسيبية من جهة ومنحي التغير في سطح البحر الذى وضعه فيربرج سنة ١٩٦١ للفترة الرباعية والثلاثية (٥٠٠٠٠ سنه من الان). اذ تتبع الصخور الدولوماتية مباشرة طبقة غير متصلة من الحجر الرملي الذى ترسب خلال الإنحسار القصير للبحر مابين ١١٠٠٠٠ و٩٠٠٠٠ سنه من الان . تلاها فترة من طغيان البحر ادت الي ترسب طبقة سميكة من الهياكل الإحفورية وذلك مابين ٩٠٠٠٠ و ٧٥٠٠٠ سنة من الان . تلا ذلك فترة الإنحسار الرئيسي للبحر والتي ادت الى فراغ الخليج العربي تماما من المياه،وهي مابين ٧٥٠٠٠ و ١٠٠٠٠ سنة من الان . وخلال هذه الفترة والتي امتازت بالجفاف ترسبت طبقة رملية من الكوارتز والتي تمثل الفترة الرئيسية لزحف الرمال من الجزيرة العربية حيث غطت الكثبان الرملية شواطئ السعودية والامارات والبحرين وقطر بما فيها منطقة الدراسة بطبقة رملية بسمك يصل الى ٧ امتار .

واخيرا تُغطى الطبقة الرملية بطبقة غير مستمرة من السرئيات والهياكل الإحفورية الحديثة وهي من معدن الارجونات حيث انها ترسبت خلال الطغيان الاخير للبحر او مايسمى بطغيان (فلاندريان البحري) والذى بدا قبل ١٠٠٠٠ سنه من الان .

CHAPTER I

INTRODUCTION

1. General Geology

The Arabian (Persian) Gulf is a marginal sea with an average depth of 35 m, and a maximum depth of 100 m near its narrow entrance. Its elongat bathymetric axis separates two major geological provinces - the stable Arabian Foreland and the unstable Zagros Fold Belt - which are reflected in the contrasting coastal and bathymetric morphologies of Arabia and Iran (Fig. 1) . The Arabian Gulf has a gently inclined sea floor lacking "shelf edges" comparable with those of modern Caribbean carbonate provinces. (Purser and Seibold, 1973).

Arabian Gulf is bordered by one of the richest oil-producing regions of the world. Most of the oil is from sedimentary sequence deposited in a geosyncline to which sediments are still being added.

2. Structural Setting

The foundations of the modern Arabian Gulf were largely laid during the Plio-Pleistocene Zagros orogeny. The outline of the Gulf, with the Zagros range to the

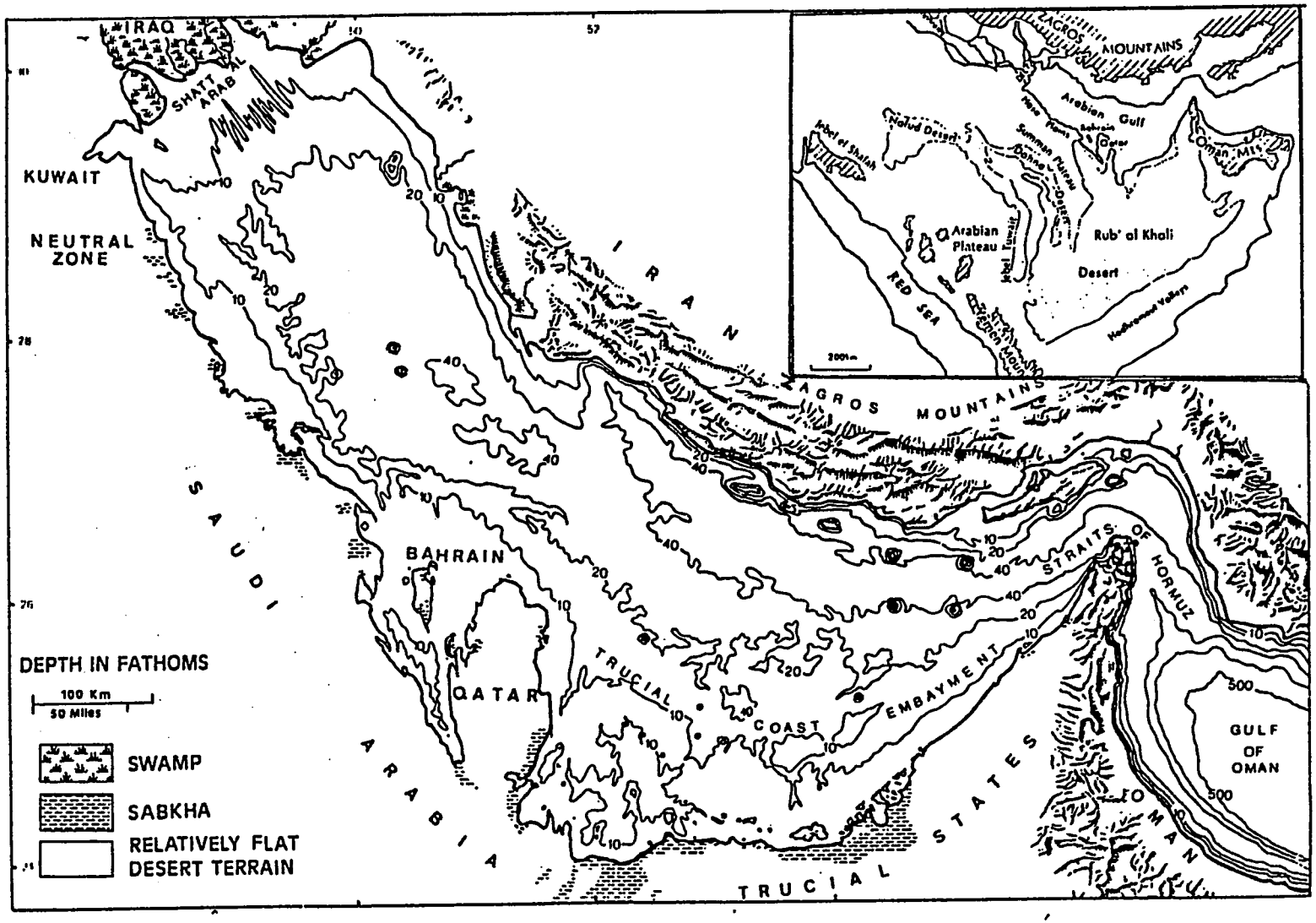

Fig.(1) - Map of the Arabian Gulf Region showing the principal morpholog-ical aspects of the basin and surrounding landmass (After Purser 1973,fig.1).

north, the offshore islands of Iran and the possibly fault-controlled Hasa (Fig. 2) were formed during Plio-Pleistocene, as was the Oman Mountains uplift with its profound effect on circulation patterns within the Gulf. The main axis of the Arabian Gulf is a NW-SE Zagros feature. The effect of pre-Pliocene movements have, except the Bahrain and Qatar structures, been obscured by later tectonics and sedimentation. The Bahrain and Qatar structures seem to owe their present form largely to pre-Pliocene movements (Kassler, 1973).

Sparker profiles provide evidence of a fault and fracture system affecting Miocene and Pliocene rocks in Gulf of Salwa, Qatar, and Abu Dhabi. The trend is northwest, similar to that of a large portion of Saudi Arabian coastline, which may be controlled by faulting. The Gulf of Salwa subsided along its bounding fractures (Fig. 2) between 700,000 and 150,000 y.b.p. There is northwest trending anticlinal structure called Bahrain Ridge which passes through Bahrain island and the studied area (Fig. 2). It has been rising in the last few thousand years (Kassler, 1973)

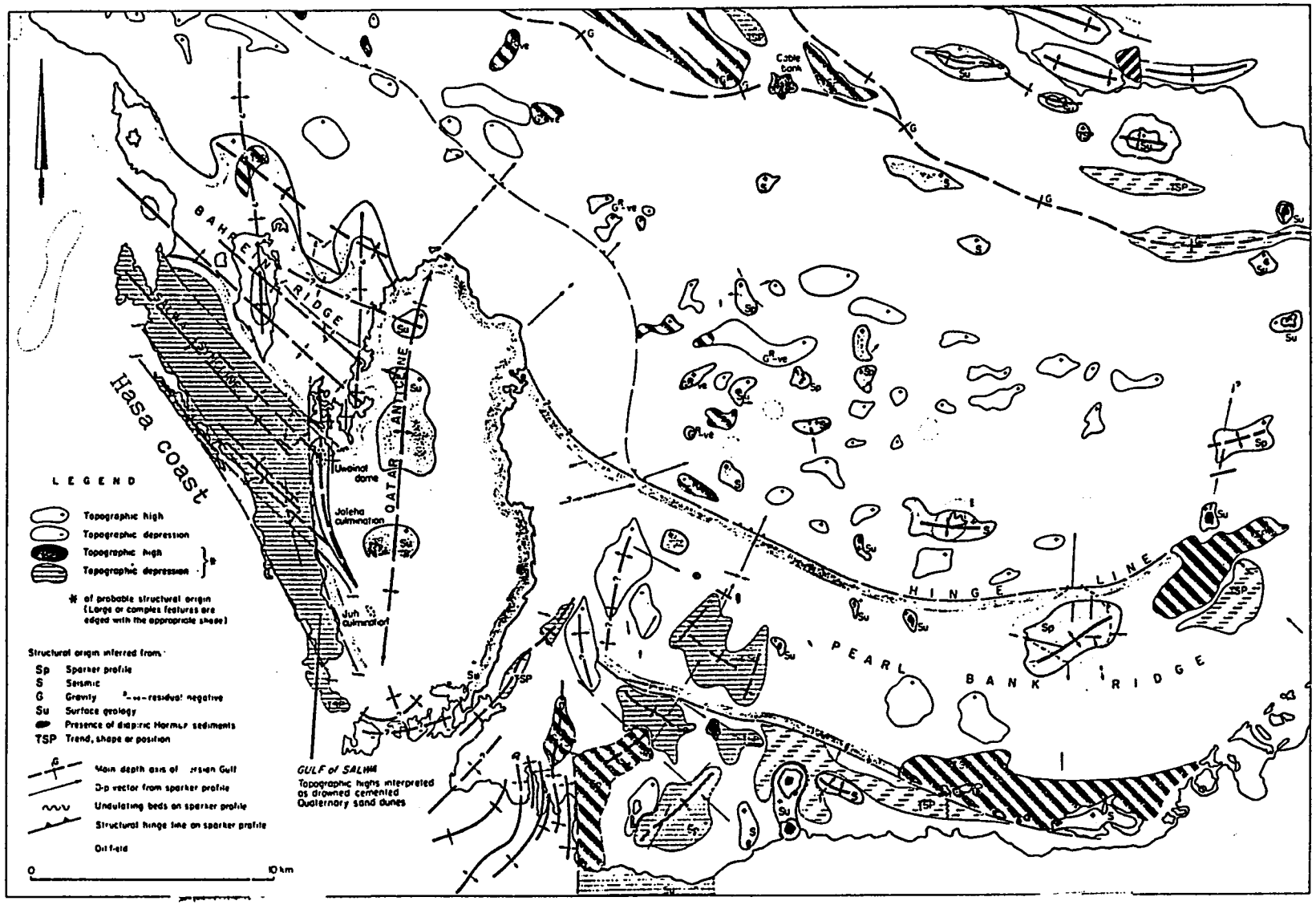

Fig.(2) - Shallow structure and topography of the central Arabian Gulf based on sparker profiles and echo-sounder (From Kassler in Purser,1973, Fig.4).

3. Sedimentary Setting

Carbonate sediments dominate the shallow water along the arid southwestern side of the Arabian Gulf, which is considered to be one of the important sites of present-day carbonate deposition in the world.

According to Purser and Seibold (1973) the present climate, being essentially continental, is characterised by marked seasonal fluctuations which, in the absence of oceanic circulation, impart a high degree of variability to the sedimentary environments in the Gulf basin. In general the Gulf is low in siliciclastic sediments. Evaporitic minerals are more dominant than terrigenous along the south-western side of the Gulf, especially in coastal sabkhas. Wagner and Togt (1973) recognised 14 sedimentary facies in the present-day sediments, of which 12 were carbonates, one was quartz sand, and one was sedimentary gypsum.

The largest areas of sand-size quartz in the present-day sediments are on the Arabian side of the Gulf, around the southern parts of Bahrain and the Qatar peninsula, and in patches off the Abu Dhabi coast. Dunes have been carried into the sea by northwesterly Shamal winds (Doornkamp et al., 1980). One of the largest of these sand bodies is in

the area south of Umm Said in Qatar, where the sand body is 30 m thick (Shinn,1973).

Over much of the 226.000 sq. kms. of the Gulf, carbonates are being deposited, but these are not evenly distributed, and can be considered to occur in three ill-defined belts (Fig.3). On the Iranian side, the annual rainfall is 200-500 mm, which is sufficient to transport clay and silt into the basin to produce marls. Roughly parallel to the axis of the Gulf but a little closer to the Arabian side, begins the Arabian Shallow Shelf. This shelf is characterised by the dominance of carbonate sediments. The carbonate sands or muddy sands on this shelf are generally only 20-50 cm thick, and between ripples and sand-patches there are often exposures of Neogene limestones and dolomites (Purser and Seibold, 1973). Most of the carbonate sands on lhis shelf are surfaced by hard-grounds (Shinn, 1969). The coastal belt of the Arabian Shallow Shelf contains several sabkha settings (Fig. 3). The study area is included in the Arabian Shallow Shelf. The third division includes terriginous sediments of the Shatt al Arab delta. These sediments enter the Gulf from the rivers at its heads and from the Zagros mountains on its north-east flank.

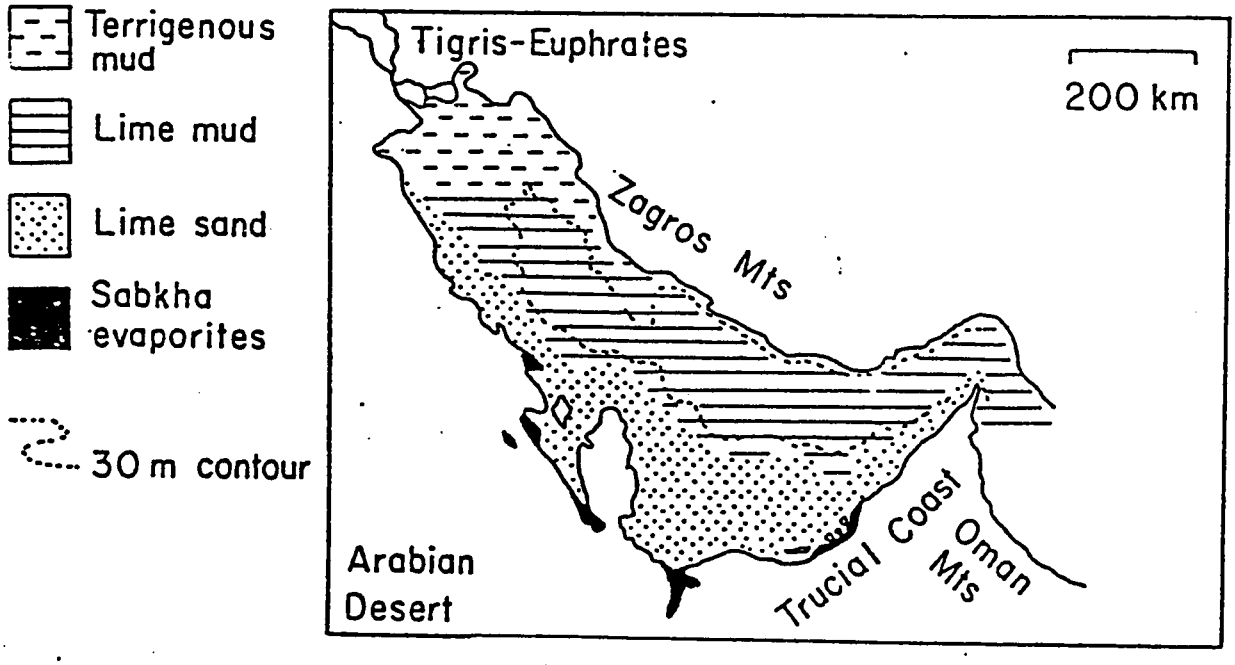

Fig.(3)- Map showing the present-day sediment distribution in the Arabian Gulf Region (from Emery, 1956).

4. Geographic setting of the study area

The Arabian Gulf has been subdivided into a series of bathymetric provinces (Seibold and Vollbrecht, 1969). These provinces include the Shat el Arab shallow shelf, Western Basin, Central Basin, Central Swell and Arabian Shallow Shelf (Arabian Homocline, Fig. 4). This study was conducted on the shallow sediments in the semi-restricted marine area between Saudi Arabia and Bahrain, which belongs to the Arabian Shallow Shelf (Fig. 4). The study area lies at the entrance of Gulf of Salwa (26° N-50° 20` E).

5. Principal environmental factors influencing Holocene sedimentation in the Gulf

The conditions that give rise to this facies association are:

(a) High temperatures;

Air temperatures in the summer normally reach 35° C, and can be over 40° C. Water temperatures range from 22°-37° C and can exceed 40° C in shallow lagoons (Evans et al., 1969; Purser and Seibold, 1973).

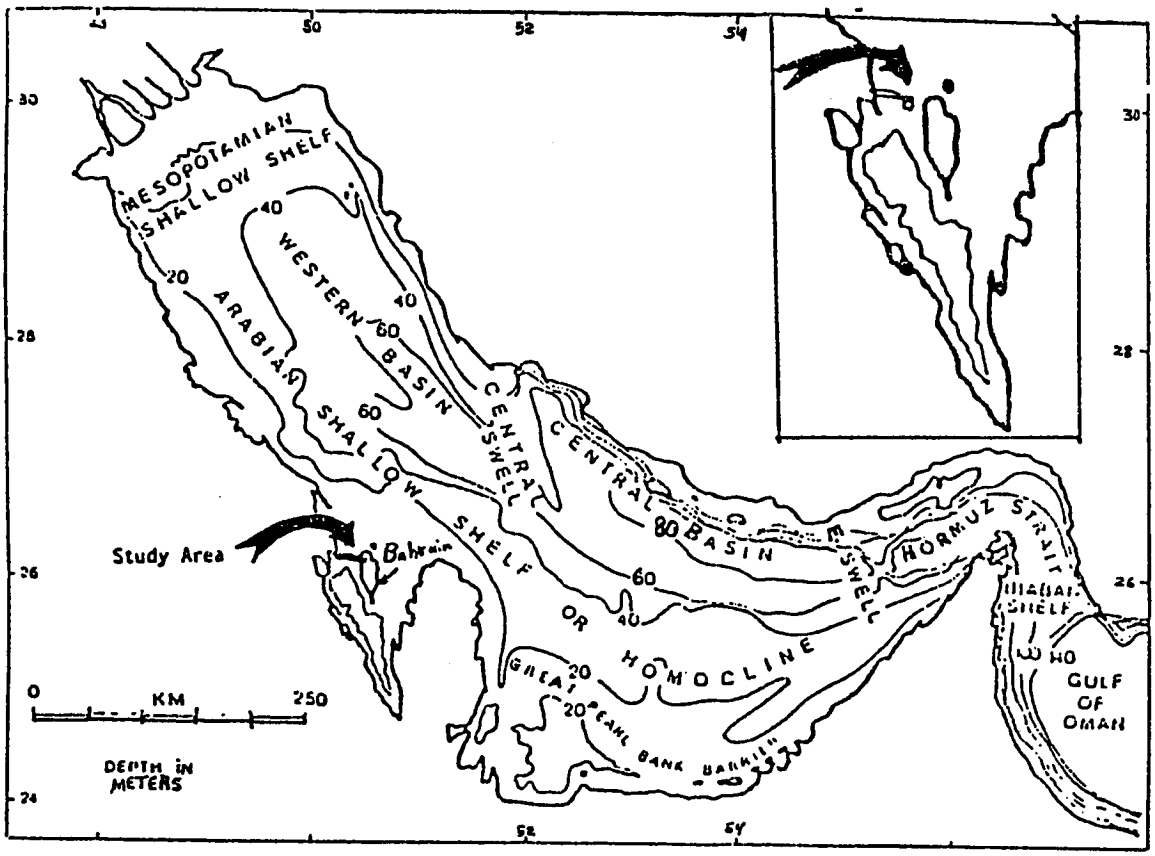

Fig.(4)- Map showing the study area along with the principal bathymetric provinces in the Arabian Gulf (After Purser,1973, Fig.3).

(b) Low rainfall;

The average annual rainfall along the Abu Dhabi coast is 34 mm (Evans et al., 1969). That in Bahrain is a little higher (72.5 mm) and it is both seasonal and concentrated into storms. However, rain water does not provide a significant influx of non-saline water into the sea.

(c) Wind;

The prevailing winds in the Arabian Gulf region are from the northwest. In the summer, these winds create waves and surface currents, and also carries some terrigenous material into the marine sediments.These summer winds are locally called the Shamal winds. In spite of the high relative humidities, averaging as high as 70-84%, such winds increase evaporation of surface water. The combined effects of frequent winds, high temperature, and low precipitation result in excessive evaporation of Arabian Gulf waters (124 mm/year, Butler, 1970).

(d) Shallow sea water;

Most of the coastal belt is less than 20 m deep. Light penetration is sufficient nearly everywhere for the existence of different types of carbonate producing organisms.

(e) Minimal oceanic influences;

The Gulf is largely surrounded by land, and there is very limited oceanic buffering through the Strait of Hormuz (Purser and Seibold, 1973). This results in large and rapid facies changes

6. Present status of the problem

Relatively few studies have been made on the Pleistocene-Holocene sediments of the Saudi Arabian shallow shelf, compared to the extensive work carried out on the Emirates coast and Iranian shores of the Arabian Gulf. However, most of these studies concentrated on supratidal areas and sedimentation pattern in sabkhas. Moreover those concerned with sedimentation in the Arabian shallow shelf dealt only with the surficial sediments (Purser, 1973) The present study focusses not only on modern subtial sediments but also coveres more than 20 m thickness of Pleistocene-Holocene rock cores in ten boreholes along 10 km length between Saudi Arabia and Bahrain.

7. Objectives of the study

Abrupt vertical lithological changes were encountered in a series of rock cores taken from the area. To identify and interpret these changes, a petrographic and mineralogical

study was carried out on these cores. The specific objectives of this study can be summarized as follows:

1- To determine the compositional and textural characteristics of the Pliestocene-Holocene sediments deposited between Saudi Arabia and Bahrain.

2- To understand the nature and distribution of these sediments.

3- To reveal the diagenetic processes in the carbonate sequences of these sediments.

4- To integrate and use the obtained data in interpretation of the depositional and diagenetic history of these sediments, which will in turn contribute to an understanding of Pleistoce-Holocene sea level changes in this part of the Arabian Gulf.

8. The previous works

Few geological studies have been done on the recent sedimentation in the study area. Fortunately, some studies have been made in the nearby areas, such as Qatar and United Arab Emirate (UAE) coasts. The UAE coast has received the most attention in the past few years. Studies conducted along that coast brought to the light an extensive region of

recent carbonate sediments (Evans et al., 1970, Kinsman, 1964). Houbolt (1957) has given a vivid picture of the relation between petrography and bathymetry of sediments near Qatar. Illing and Partner (1965) investigated the shallow deposits around Qatar including the lagoons and tidal flats. For more references on the recent carbonate studies in the Gulf; see particularly; Sugden, 1963; Kinsman, 1964; Evans et al., 1964; Wells and Illing, 1964; Evans, 1966; Evans and Bush, 1969; Taylor and Illing, 1969; Evans, 1970; Purser, 1973; Park, 1977; Al-Asfour, 1982 and Gunatilaka, 1986.

The most recent work on the sediments of the Arabian Gulf were presented at the Conference on Quaternary Sediments in the Arabian Gulf held at Kuwait University in February 1987. Only abstracts were available at the time of the study.

CHAPTER II

METHODS OF STUDY

1. Sampling

The studied rock samples were core samples from holes drilled in connection with the construction of the King Fahd causeway between Saudi Arabia and Bahrain. The King Fahd Causeway project was initiated by preliminary engineering site investigation in January, 1983, by Bàlastnedam groep n.v.(Fig. 5). After establishing the engineering properties of these rocks, some of the undisturbed cores were given to King Fahd University of Petroleum and Minerals and were used in this geological study.

These cores are labelled by three separated numbers {(e.g. 3/44 (7.5)}. The first indicates bridge number, the second gives borehole number, and the third gives the depth of the sample below sea bottom. The causeway includes five bridges separated by small man-made islands, which consist of compacted sediment fillings. The studied cores are from under bridges 1,2 and 3 in Saudi Arabian waters (Fig. 5).

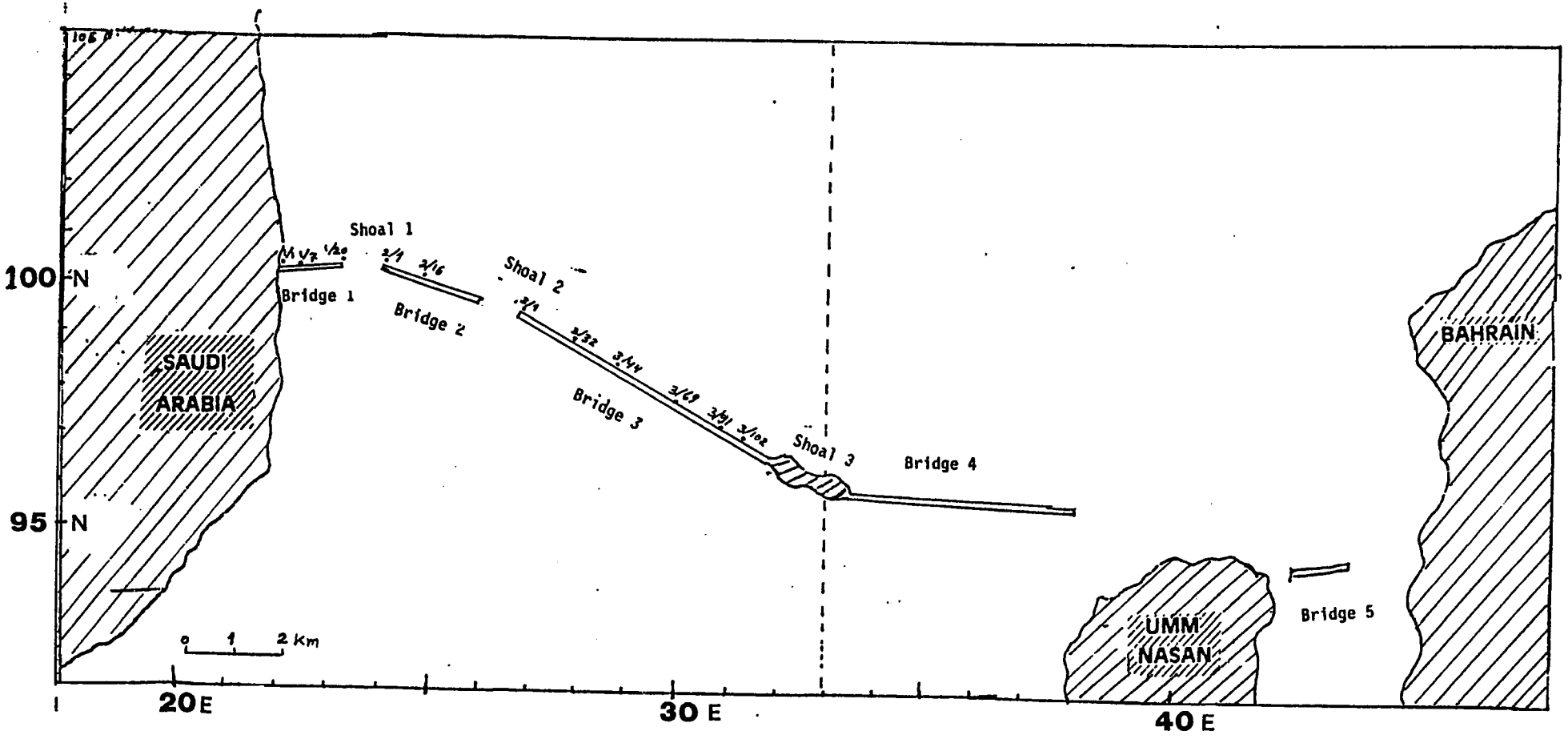

Fig.(5) - The location of the studied boreholes along with the bridges and shoales .

Engineering log descriptions, which were prepared by Balast-nedam groep, were available for all the drilled rock cores. An example of log description is given in Appendix D. These log descriptions were sometimes used in this study to correlate certain beds or layers.

2. Preparation of Thin Sections for Petrographic Analysis

A total of 100 rock samples were selected for petrographic analysis. One cm thick slabs were made from each rock samples, using a rock-cuttin machine. The dimensions of these slabs were later adjusted to fit the available glass slides. Most of the samples are porous, soft rock, so they were impregnated using Petropoxy (resine) in special teflon sleeves, with removable bottom (Fig. 6).

Thin sections were made from all the collected samples except those that are too soft and fine to withstand cutting. Most of the thin-sections were kept uncovered to facilitate applying minerals stains. Selected thin sections were stained using Alizarin Red "S". The thin-sections were examined under a petrographic microscope, and photographed using a Leitz Petrographical Photomicroscope.

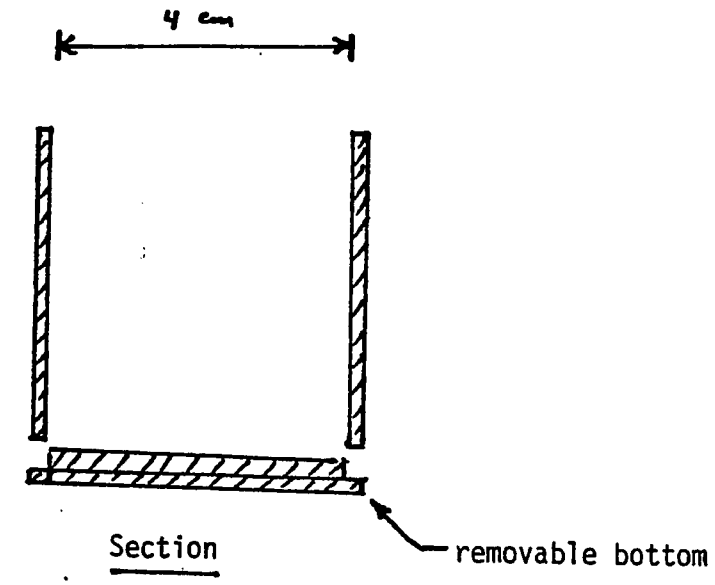

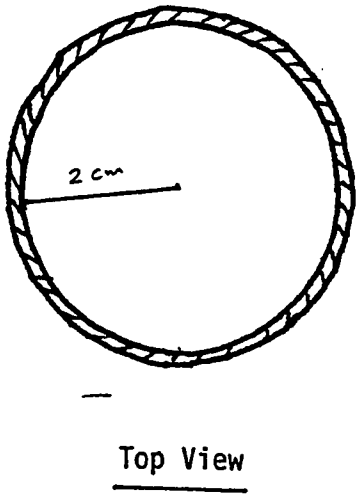

Fig.(6) - Teflon sleeve for soft rock impregnation by epoxy resin .

3. X-ray Powder Diffraction (XRD)

X-ray diffraction powder analysis (XRD) was used to identify the mineral contents of the rocks. Samples for the X-ray analysis were ground to powder using laboratory Vibrating Cup Mill. About 50 samples were investigated by a Phillips X-ray diffractometer, employing Ni-filtered, Cu radiation, and a goniometer speed of 1/min. The generator was run at 20 mv and 50 kv.

The clay fraction of selected samples were separated and identified by XRD using glycolation and heating (Warshaw, 1961) (Appendix B1). Table 1 gives the dominant X-ray diffraction peaks for aragonite, calcite and dolomite, in order of decreasing intensities. Figure 7 illustrates an example of X-ray diffractograms that were used in mineral identification. Sixteen samples were investigated by computerized XRD in the Research Institute (KFUPM), for a semi-quantitative mineralogical analysis of the samples (Appendices B5-B9). This analysis is done by comparing the intensity of the most intense peak of that phase with the standard. Amorphous compounds would not be detected by the XRD technique.

Table (1)- The dominant X-ray differaction peaks for aragonite, calcite and dolomite. in order of decreasing intensities (From Milliman, 1971, Table 9)

dÅ	Degrees 2 Θ	I/I_1	hkl
	Aragonite		
3.396	26.24	100	111
1.977	45.90	65	221
3.273	27.25	52	021
2.700	33.18	46	012
2.372	37.93	38	112
2.481	36.21	33	200
1.882	48.36	32	041
2.341	38.45	31	130
1.877	48.50	25	202
1.742	52.53	25	113
	Calcite		
3.035	29.49	100	104
2.285	39.43	18	113
2.095	43.18	18	202
1.913	47.53	17	108
1.875	48.55	17	116
2.495	36.00	14	110
3.860	23.04	12	102
	Dolomite		
2.886	30.98	100	104
2.192	41.18	30	113
1.781	51.30	30	009
1.786	51.15	30	116
1.804	50.60	20	018
2.015	44.99	15	202
2.670	33.56	10	006
2.405	37.39	10	110

. 2 Θ angles are for Cu-Kα radiation.

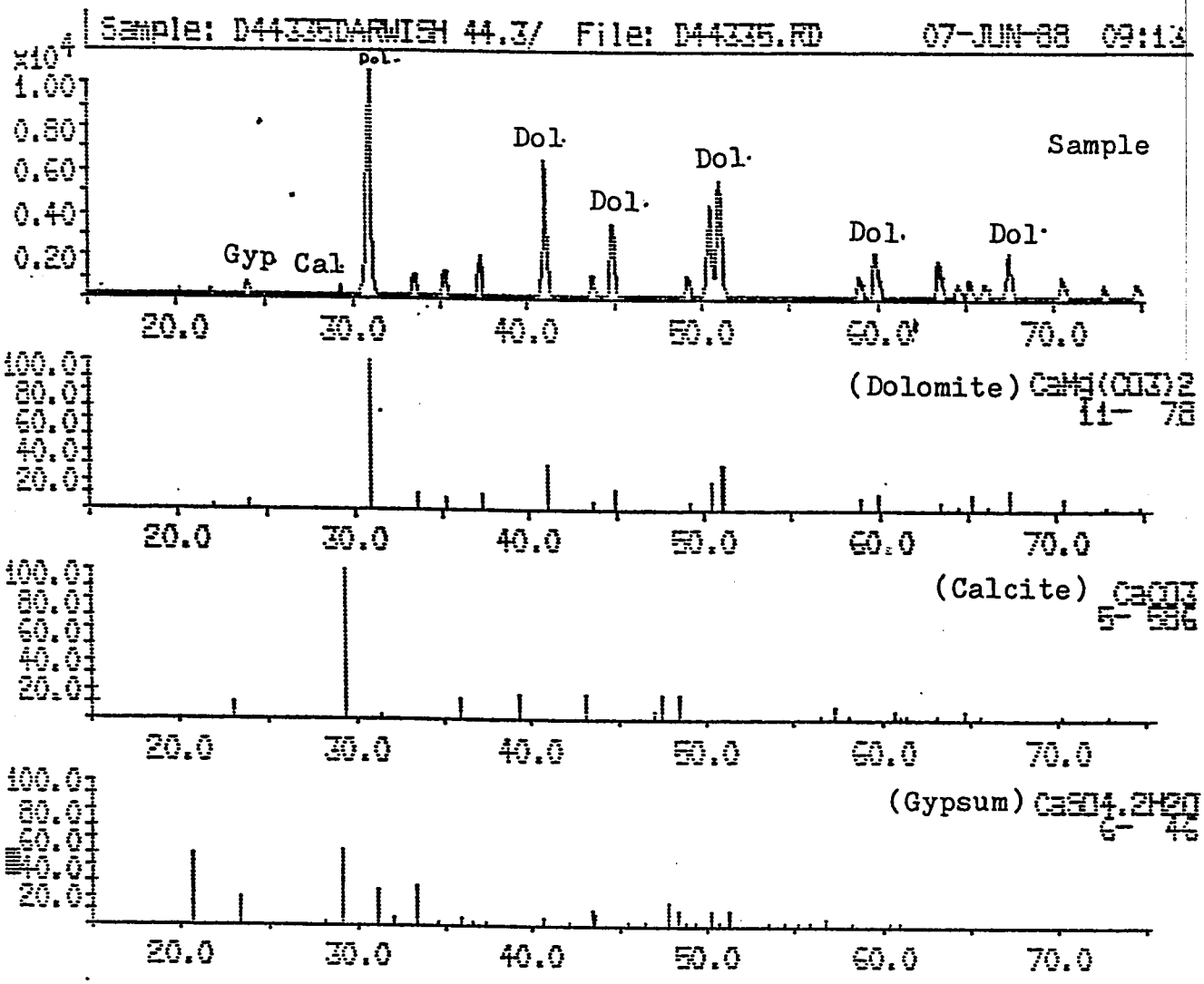

Fig.(7)- XRD diffractograms

An example of XRD diffractogram showing different mineral peaks. This sample contains mainly dolomite with a minor amount of calcite and gypsum, sample number 3/44 (35 m).

Standard diffractograms for dolomite, calcite and Gypsum are given below for comparison.

4. Scanning Electron Microscope (SEM)

Scanning electron microscope (SEM) examination provided detailed compositional and textural data on the selected rock samples. Sixteen rock samples, which were tested by XRD analysis, were further investigated by SEM (Geol-JSM 840 and Jeal-JSM-T300). The samples were cut into discs of about 2 cm in diameter, glued to SEM mounting stubs (holder) with fresh fracture surface upward. A thin conductive coat of gold was vapourized under vacuum onto the upper surface of the rock discs.

The secondary electron images of the samples were examined on the CRT screen and photographed. The SEM also provided compositional data by energy dispersive XRF analysis(Fig. 8)

5. Insoluble Residue Determination and Petrographic Staining Test

(a) Acid Wash

Eight different rock samples were treated by dilute HCL (1 normal) to study the insoluble residue and determine its content (Appendix F).

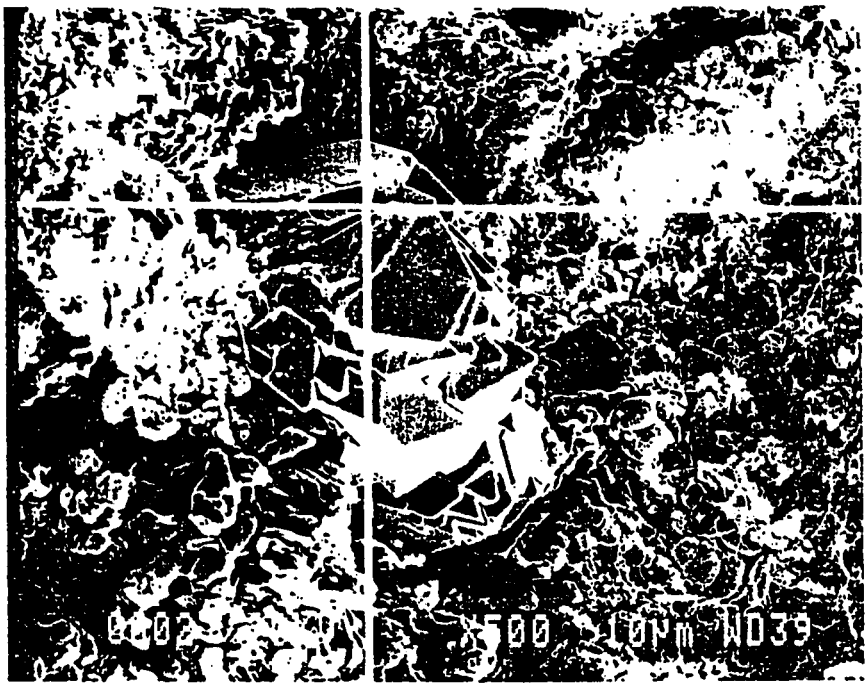

(a)

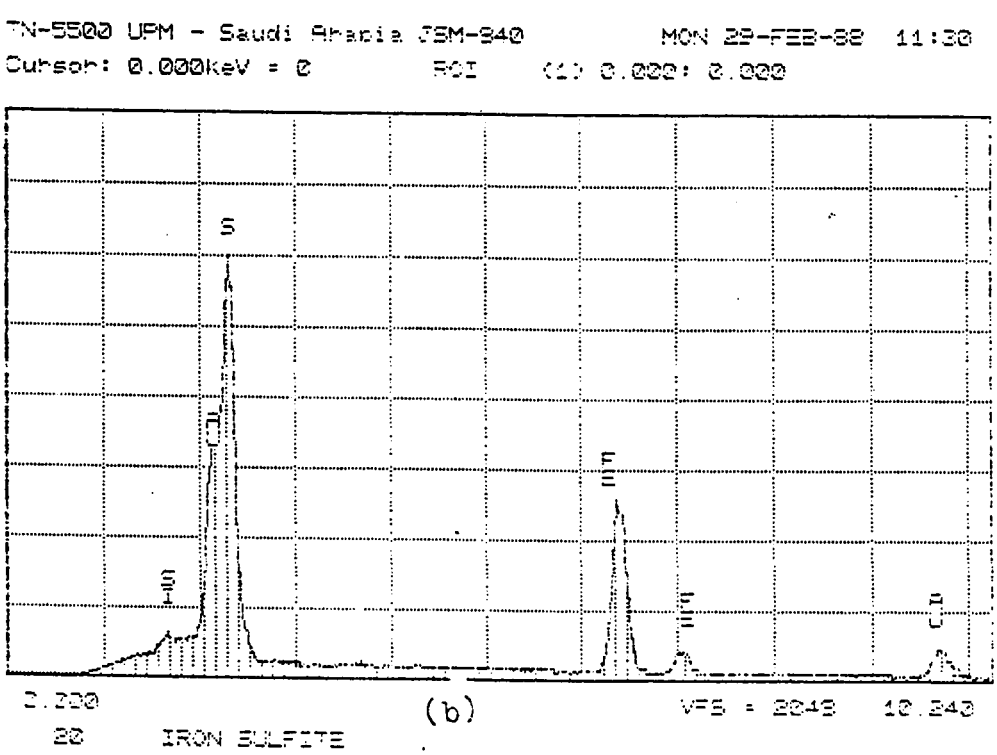

Fig.(8) SEM compositional data

(a) SEM secondary electron image of pyrite crystal in a matrix of dolomite.
(b) SEM compositional data by energy dispersive XRF for the above pyrite crystal, sample 3/32(12 m).

(b) Staining with Alizarine Red "S"

Selected thin sections and rock samples were stained using Alizarine Red "S" to distinguish between calcite and dolomite.

CHAPTER III

LITHOFACIES

Petrographic data were used to defined the various lithofacies that dominate this area of the Arabian Shallow Shelf. The studied rocks were classified according to the depositional textural classification of Dunham (1962), with some additions to indicate minerals content and constituents of the the rocks. For example,a calcitic skeletal grainstone indicates that the rock has grain-supported texture and a mainly calcite composition.

For a better understanding of the progressive diagenetic changes, stratigraph and depositional environment, the lithofacies were divided into two mineralogical units from the youngest to oldest as follows :

1. Non dolomitic sediments and rocks, which include the following lithofacies:

1) Aragonitic oolitic sand and grainstone
2) Aragonitic skeletal grainstone
3) Quartz sand
4) Calcitic skeletal grainstone
5) Quartz sandstone

2. *Dolomite rocks, which include the following lithofacies:*

1) Oolitic grainstone/packstone

2) Skeletal packstone

3) White skeletal wackestone/mudstone

4) Pelletal grainstone/packstone

5) Green mudstone

1. NON-DOLOMITIC ROCKS

1.1 Aragonitic oolitic sands and grainstone

Three oolitic tidal bars, each about four meters thick, are encountered in the study area. These sediments consist mainly of yellowish highly polished concentric ooids (Plate 1a). They contain some mollusca and formanifera, most of which are partially covered by cryptocrystalline aragonitic cement that obscures the exterior features (Plate 1b,c). The upper 20 cm is partiall lithified with acicular aragonitic and possibly micritic cement, with loose, uncemented ooids below (Plate 2).

The grain size of these ooids ranges from 750 um to 880 um. Grain size distribution is moderately to moderately well sorted (σ = -0.74 to -0.57). The skewness is near symmetrical to coarse skewed (Sk = -0.09 to - 0.2) (Folk,

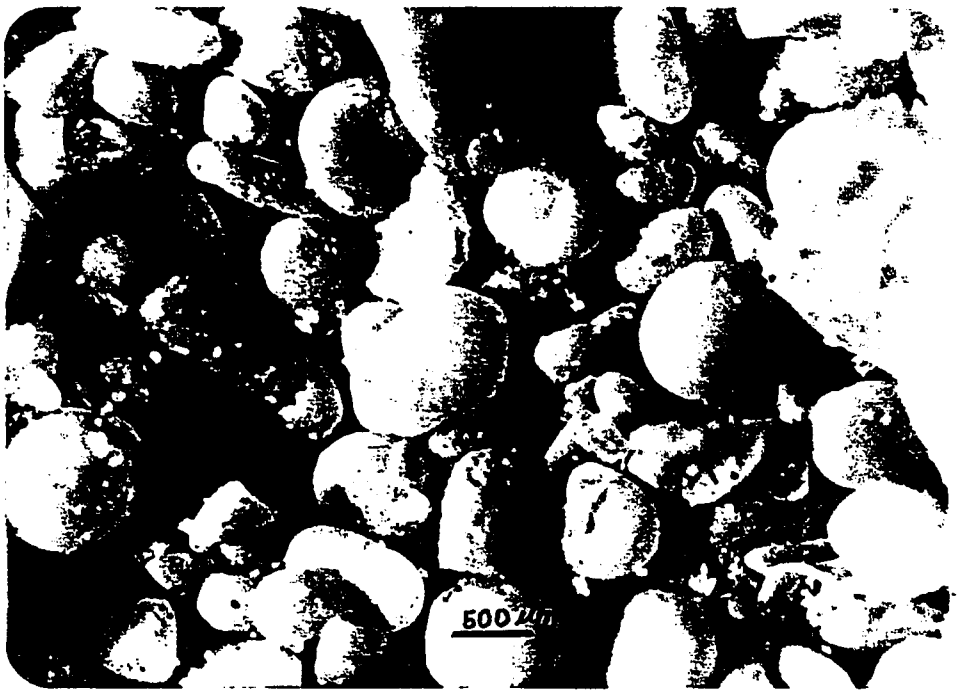

(a)

(b)

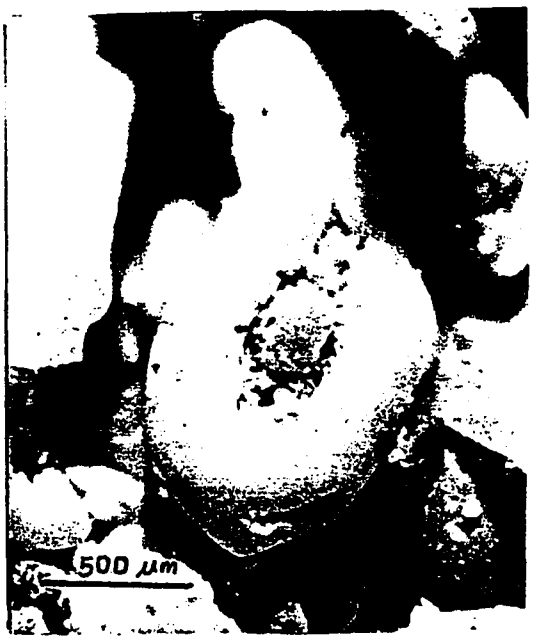

(c)

Plate 1. Aragonitic oolitic sand

(a) Oolitic sand, with highly polished grain surfaces.
(b) and (c) Foraminifera (milliolids and peneroplids), partially coated by cryptocrystalline aragonite in oolitic sand .

(a), (b) and (c) Reflected light, scale, 500 um, sample number 3/102(0 m) .

(a)

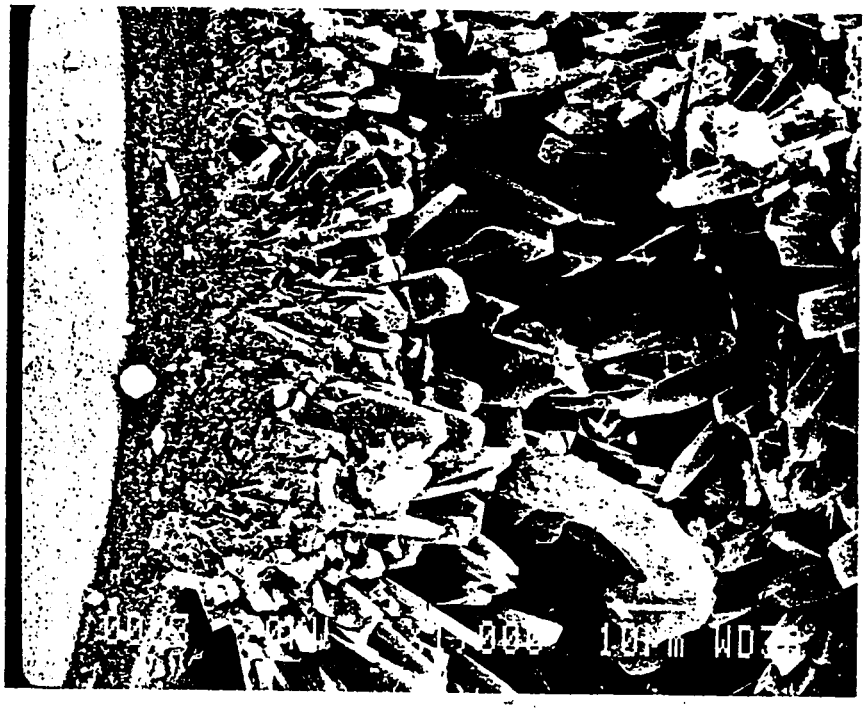

(b)

Plate 2. Aragonitic oolitic grainstone

(a) SEM photograph shows the oolitic grainstone, with intergranular aragonitic cement.
(b) Magnified view of the aragonitic cement in (a) showing the acicular aragonite crystals.

SEM, scale 100 um in (a) and 10 um in (b), sample 3/102(.5 m).

1974). Figure 9 shows the grain size distribution of these ooids at different depths. The result shows identical grain size distribution within 150 cm depth in bore hole 3/102.

The thin sections show oolitic grains vary in size due to varying size of the nucleus. The oolitic grains often have a quartz nucleus. The shape of ooids tend to resemble the shape of nucleus (Plate 3). The oolitic coatings are relatively thin compared to their nuclei, and when compared to the oolitic coating of Abu Dhabi ooids (Purser, 1973, p. 297). The mineral content, determined by XRD analysis, are 60% aragonite, 20% calcite and about 20% quartz. Carbon dating (by Shell Research) of the Saudi-Bahrain oolitic tidal bars sand gave given an age of 430+170 year (Loreau and Purser, 1973).

1.2 Aragonitic skeletal grainstone

This lithofacies is a brown to light grey, highly skeletal grainstone. The skeletal constituents are mainly pelecypods and gastropods (Plate 4). Other skeletal constituents include foraminifera (milliolids and peneroplids), coralline algae, barnacles, worm tubes, ostracods, and echinoids. There is about 10 to 20% of subangular quartz sand. There is also some mud matrix. This lithofacies contains about 60% aragonite, 20% calcite,

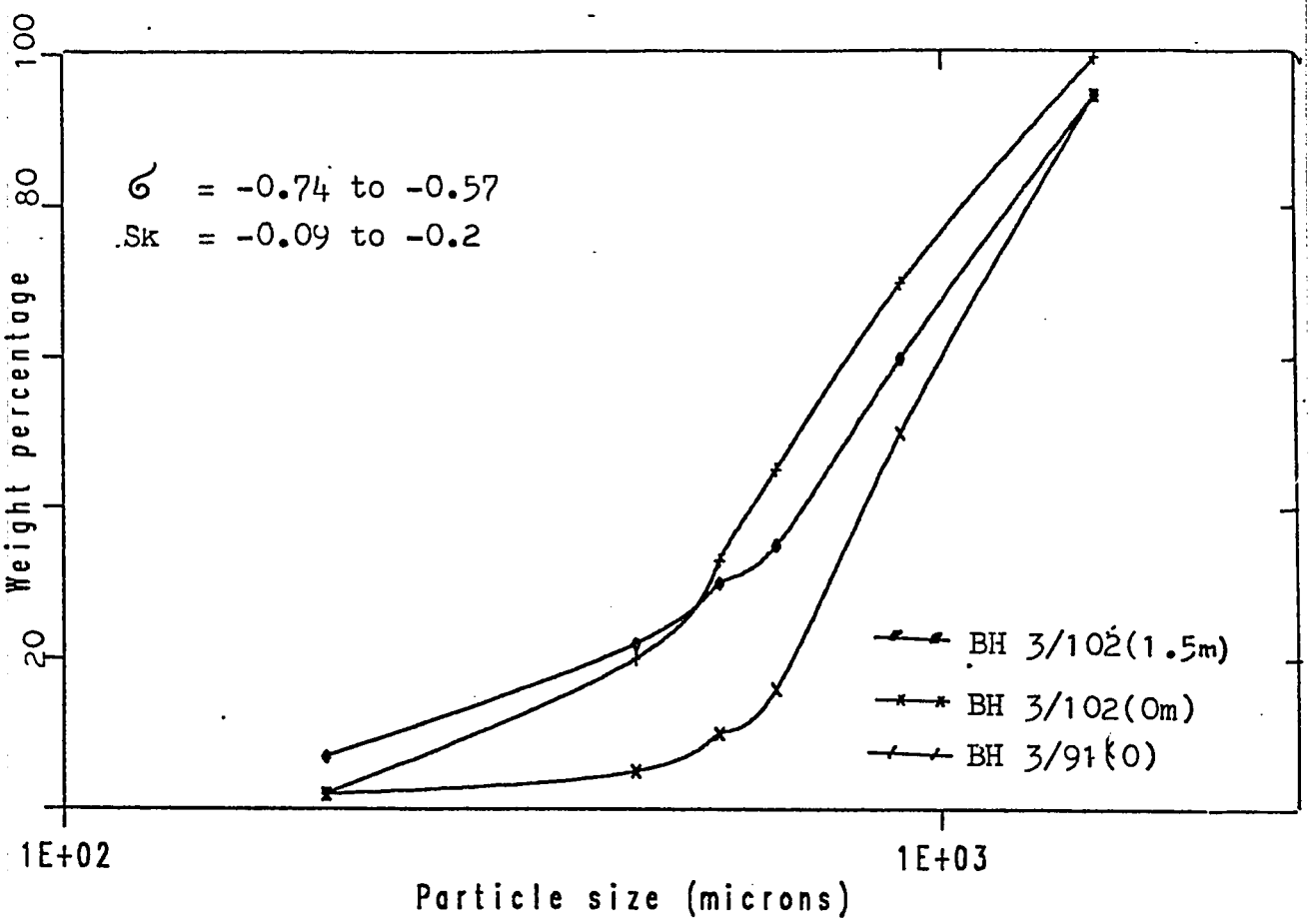

Fig.(9) - Grain size distribution for three oolitic sand samples.
σ = Standard deviation, Sk= Skewness value

(a)

(b)

Plate 3. Aragonitic oolitic grainstone

(a) Oolitic grainstone with concentric and cryptocrystalline oolitic coating. Transmitted light, plane polarized.

(b) This photomicrograph shows the quartz and skeletal grains as oolitic nuclei. Transmitted light, cross polarized.

(a) and (b) Scale 500 um, sample number 3/102(1 m).

(a)

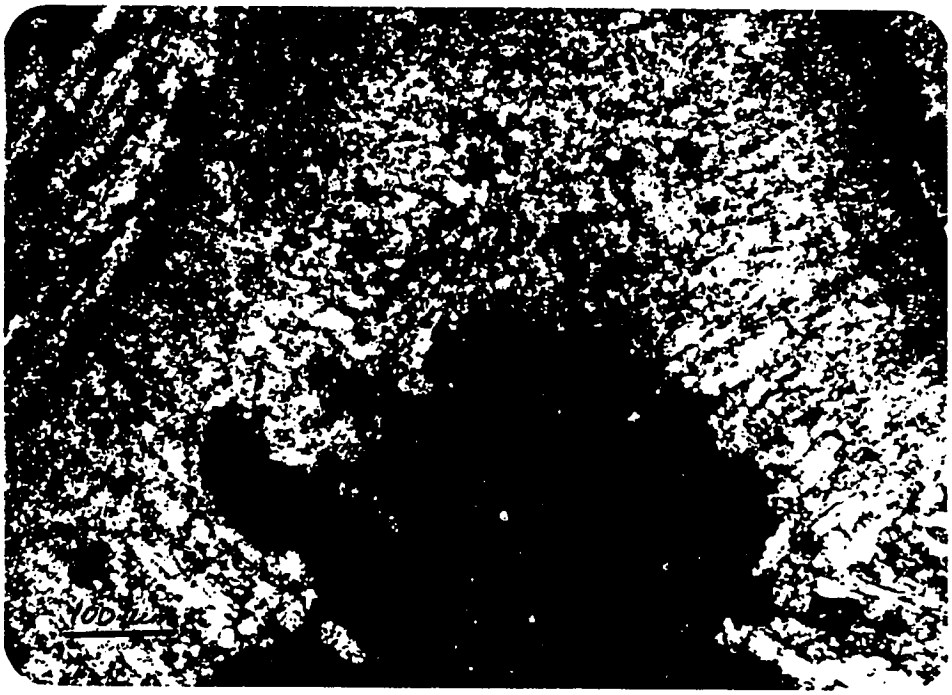

(b)

Plate 4. Aragonitic skeletal grainstone

(a) Acicular aragonitic cement radiates outward from skeletal grains and inward into chambers.

(b) Magnified view of the rectanguler area in photomicrograph (a) showing the intergranular aragonitic cement.

(a) and (b) Transmitted light, cross polarized, scale 500 um in (a) and 100 um in (b), sample number 3/24(0.5 m).

and 10-20% quartz. Micritized margins exist in some molluscan shells. All components are cemented together by well developed acicular aragonite and possibly some micrite cements (Plate 4). Maximum thickness of this lithofacies is 1.5 m.

1.3 Quartz sands

Quartz sands are yellow to grey, poorly sorted loose sand. The mean grain size is 450 um with standard deviation of 250 um (Fig.10). All the seived samples are coarsely skewed, with skewness value ranging between 2 and 2.7 (Folk, 1974). This layer is highly variable in thickness, ranging from a few centimeters to five meters. The sand becomes somewhat coarser in a landward direction. The coarser grains are rounded and spherical (Plate 5), whereas the finer grains are subangular In general the rounded to subrounded grains are dominant. Some grains ar grains are partially covered by very thin carbonate cement. X-ray diffraction analysis shows that this lithofacies contain about 75% quartz and 15% feldspar with, a minor amount of aragonite, which is due to the presence of some molluscan shells and aragonitic cement (Plate 5).

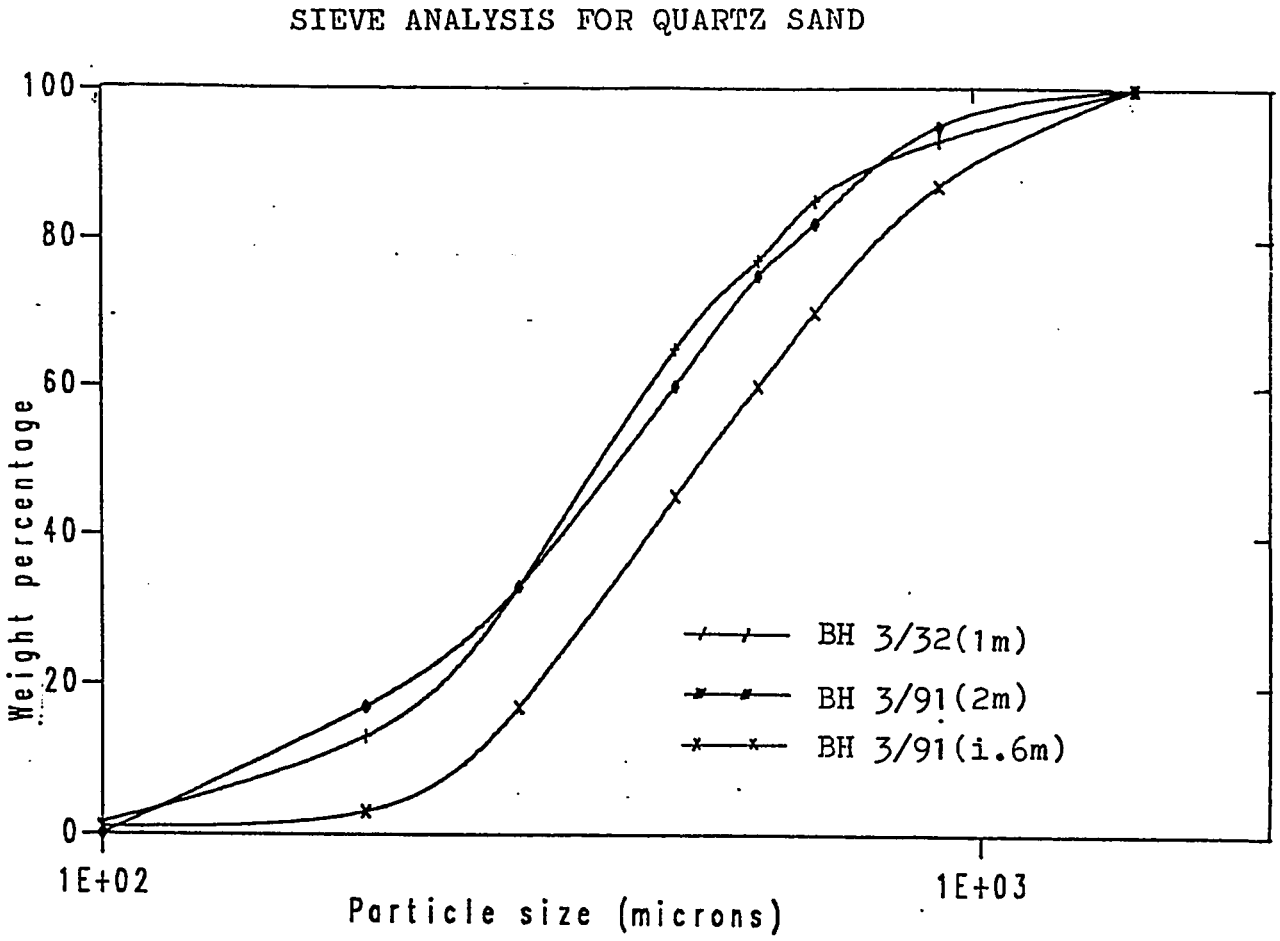

Fig.(10) - Grain size distribution for three quartz sand samples.

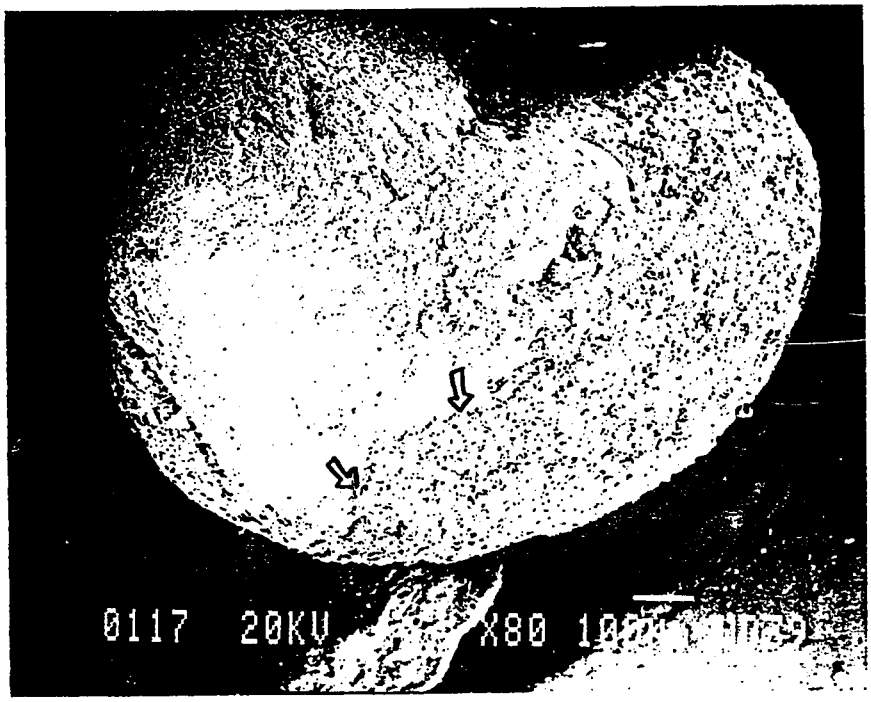

Plate 5. Quartz sand

Quatz sand grain partially coated by a crust of aragonitic cement in the lower part (arrows). SEM, scale 100 um, sample 3/91(4 m).

1.4 Calcitic skeletal grainstone

This lithofacies is yellowish white in color, with abundant skeletal fragments. Calcitic skeletal grainestone contains mainly mollusca and barnacles. There is about 10-20% sub-angular to sub-rounded, medium quartz sand.

All the constituents of this rock are cemented by euhedral to subhedral, bladed sparry calcite cement, about 20-80 um long (Plate 6 b). The lower parts of this layer often contains some oolitic grains. Staining and XRD indicate a composition of about 80% calcite and 20% quartz.

This lithofacies is highly leached. All the molluscan shells have been leached completely leaving unfilled moldic pores outlined by crystalline calcite cement (Plate 6 a,b). Here and there, fragments of unleached organisms (e.g barnacles) are still recognizable The thickness of this layer is variable, averaging 2.5 m.

(a)

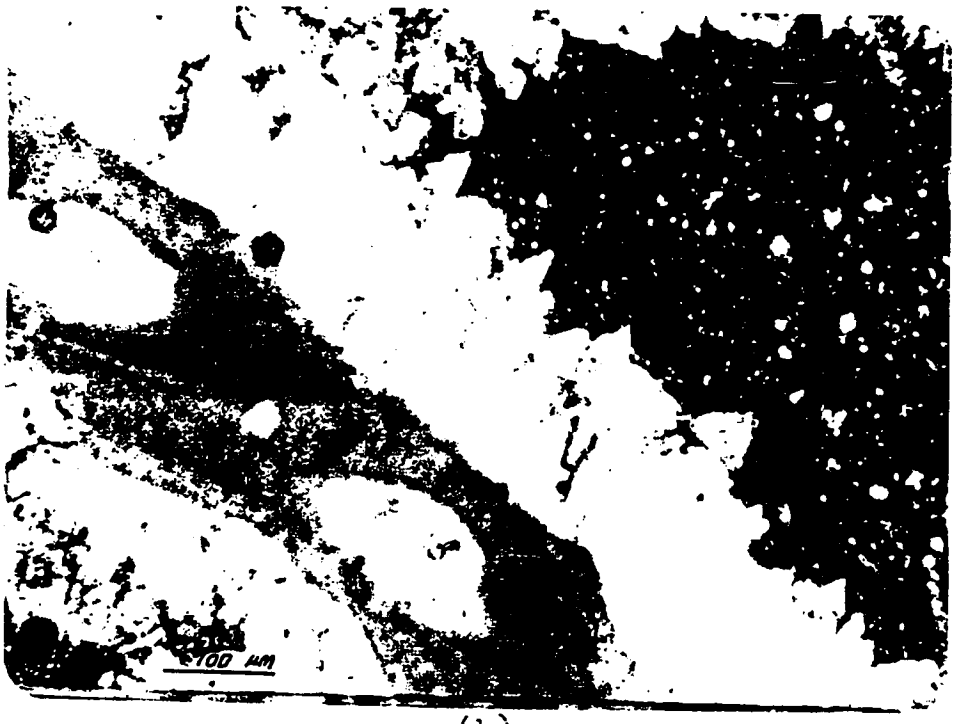

(b)

Plate 6. Calcitic skeletal grainstone

(a) This photomicrograph shows the sparry calcite cement, which outlines molds of organisms. Stained with Alizarine red-s. Transmitted light, plane polarized, scale 100 um, sample 3/44.3(3 m).

(b) Photomicrograph shows undissolved barnacle fragment surrounded by bladed calcite cement. Transmitted light, cross polarized, scale 100 um, sample number 3/44.3(3 m).

1.5 Quartz sandstone

This lithofacies is a grey, highly lithified, moderately sorted quartz sand stone. The grains are subangular to subrounded, with a diameter of 300 to 700 um. It is cemented either by calcite or dolomite microspar (20-40 um diameter) (Plate 7). The layer is discontinuous and averages one meter in thickness.

2. DOLOMITIC LITHOFACIES

In general, these lithofacies are made up of mainly dolomite, with variable, amounts of calcite, gypsum , quartz or clay minerals.

2.1 Dolomitic oolitic grainstone

There are several thin oolitic grainstone beds in dolomitic layers (Chapter V). This lithofacies is yellowish white, slightly skeletal, dolomitic grainstone/packstone. Ooids are generally spherical, moderately to well sorted, with a diameter of 300 to 1000 um. Low angle thin cross laminations (3 mm thick) are occasionally seen in oolitic horizons.

Most oolite nuclei are pellets. Grains are cemented by a

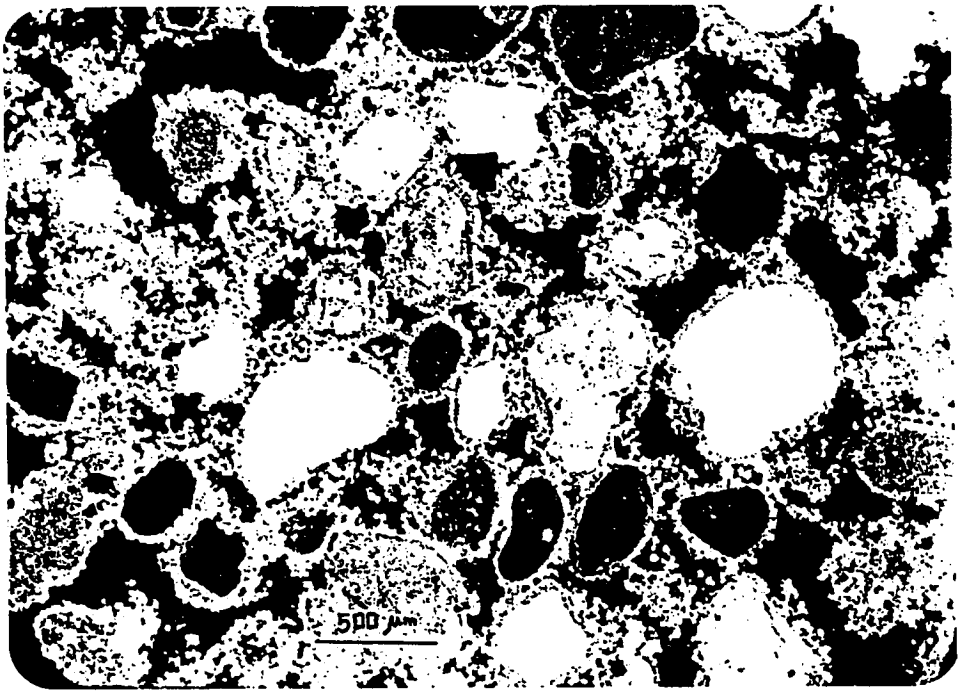

(a)

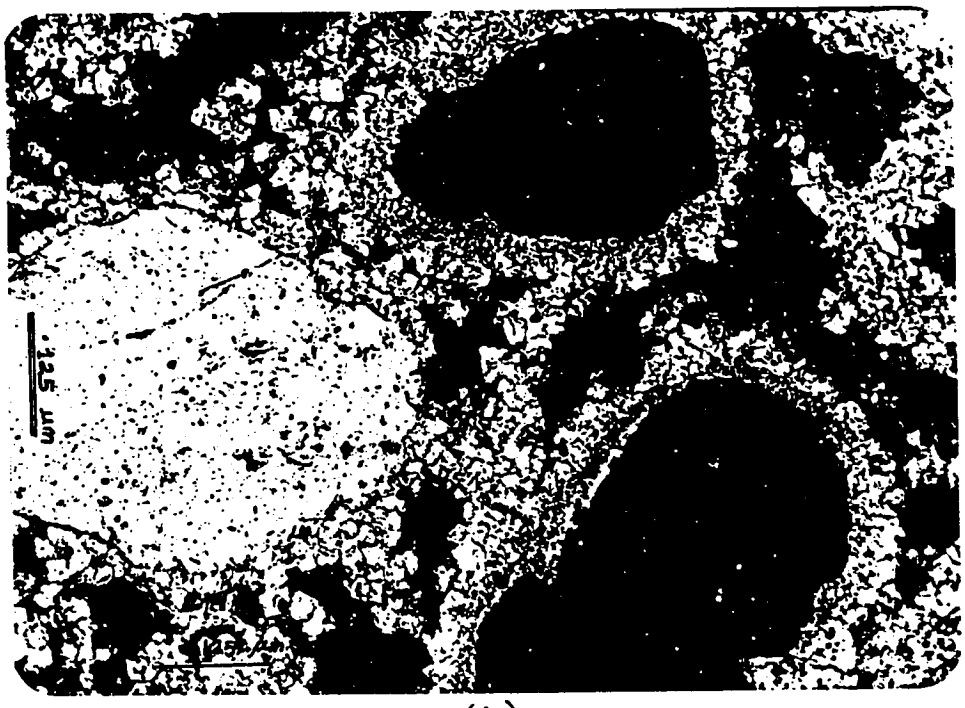

(b)

Plate 7. Quartz sandstone

(a) Quartz sandstone cemented by isopachous drusy calcite microspar.
(b) Magnified view of the calcitic isopachous cement in photomicrograph (a).

(a) and (b) Transmitted light, cross polarized, scale 500 um in (a) and 125 um in (b), sample 3/32(4 m).

rim of fine sparry dolomite (Plate 8). This lithofacies has been affected by intensive diagenetic processes, which include leaching of skeletal fragments and some ooids, as well as complete dolomitization and neomorphism. Thus some oolitic textural features have been obscured. Consequently, ooids are identified on the basis of size, shape, coating, and sorting (Plate 9). The average thickness of this layer is 50 cm. It ranges from 0.35 m to 0.7 m.

2.2 Dolomitic skeletal packstone

This lithofacies is a yellowish to light greyish white abundantly skeletal packstone. It is mainly dolomite with minor amounts of quartz silt and calcite crystals. Despite intensive leaching, high spired gastropods, pelecypods, scaphopods, ostracods, and benthonic foramanifera can be recognised. In most cases, the solid shells of the organisms were leached leaving interior sediment casts. Fine dolomitic microspar cement developed inside molds and between grains (Plate 10). Dolomitic packstone layers are highly variable in thickness ranging from a few centimeters to two meters.

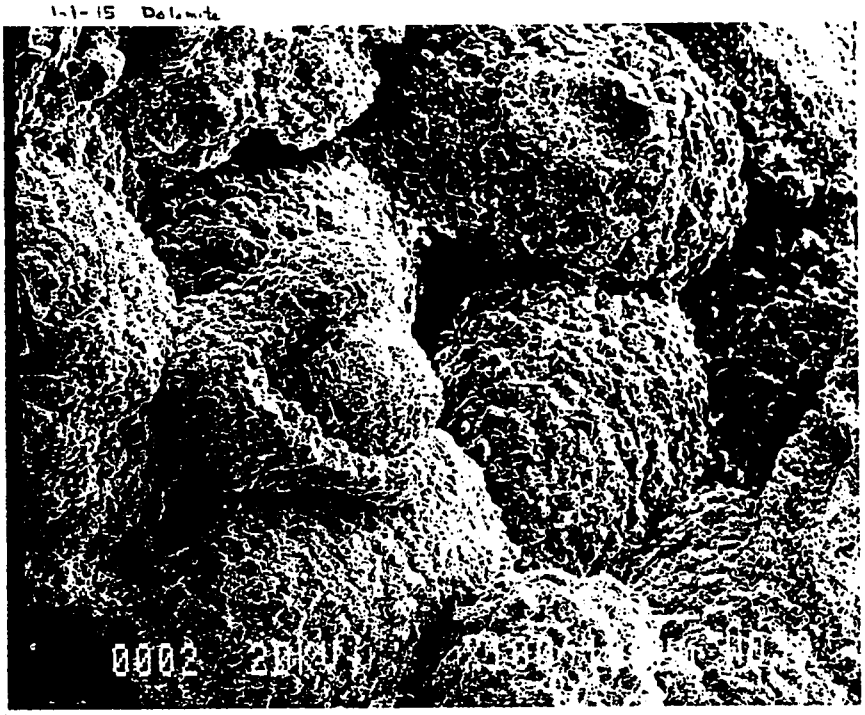

Plate 8. Dolomitic oolitic grainstone

Surface features and microstructure of dolomitic oolitic grainstone, cemented by a crust of blocky dolomite crystals. SEM, scale 100 um, sample 1/1(15 m).

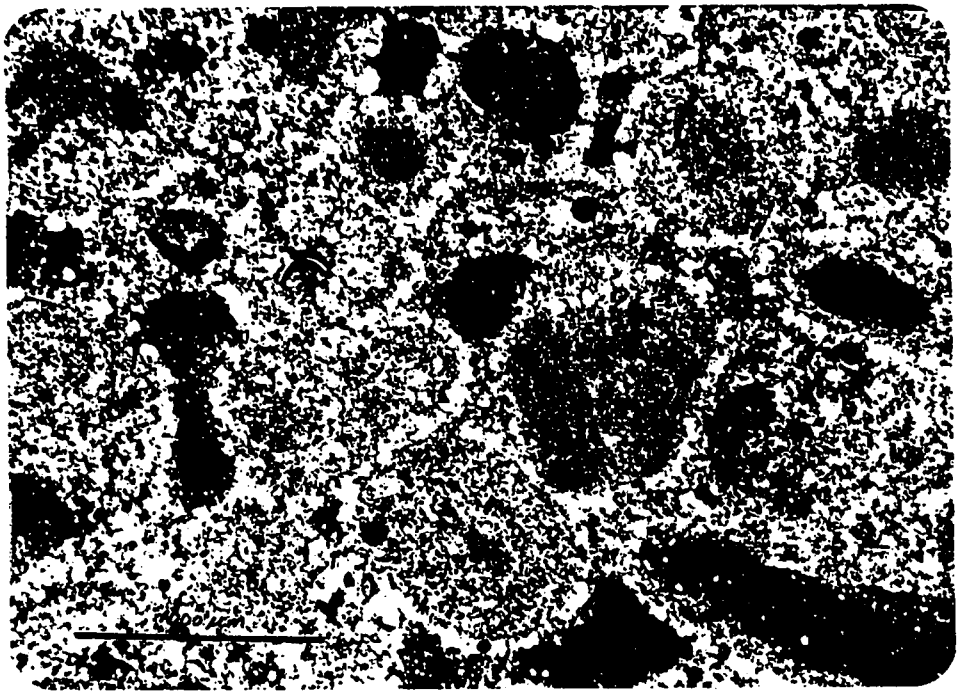

(a)

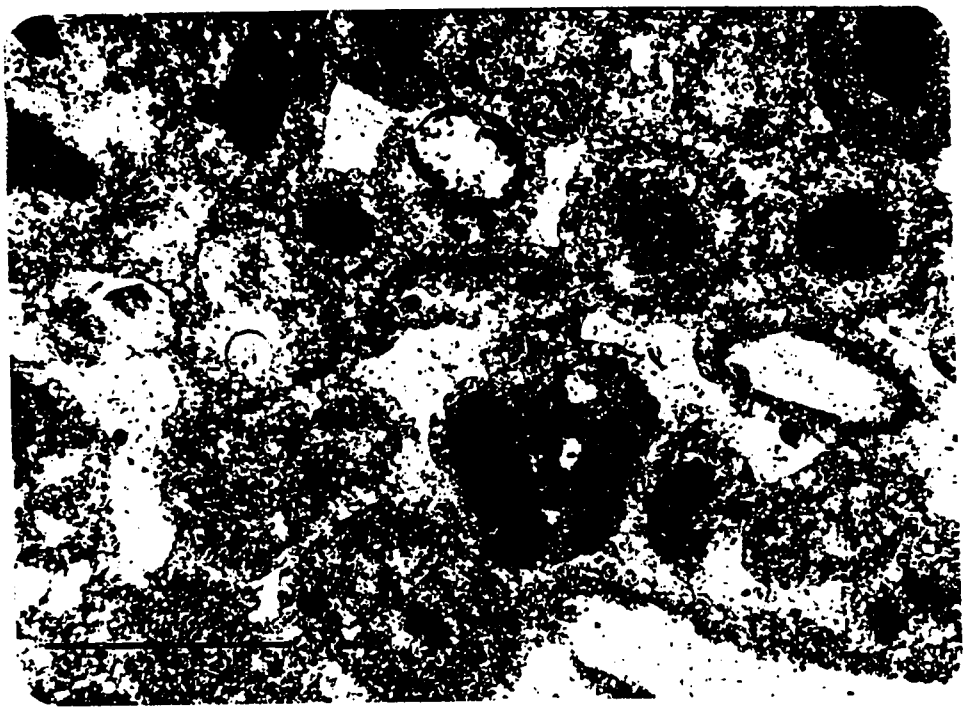

(b)

Plate 9. Dolomitic oolitic grainstone

(a) Dolomitic oolitic grainstone, cemented by blocky dolomite crystals, which form rims around the ooids. Transmitted light, Cross polarized, scale 1000 um, sample number 1/1(15 m).

(b) The same section in (a) with plane polarized light. Scale 1000 um.

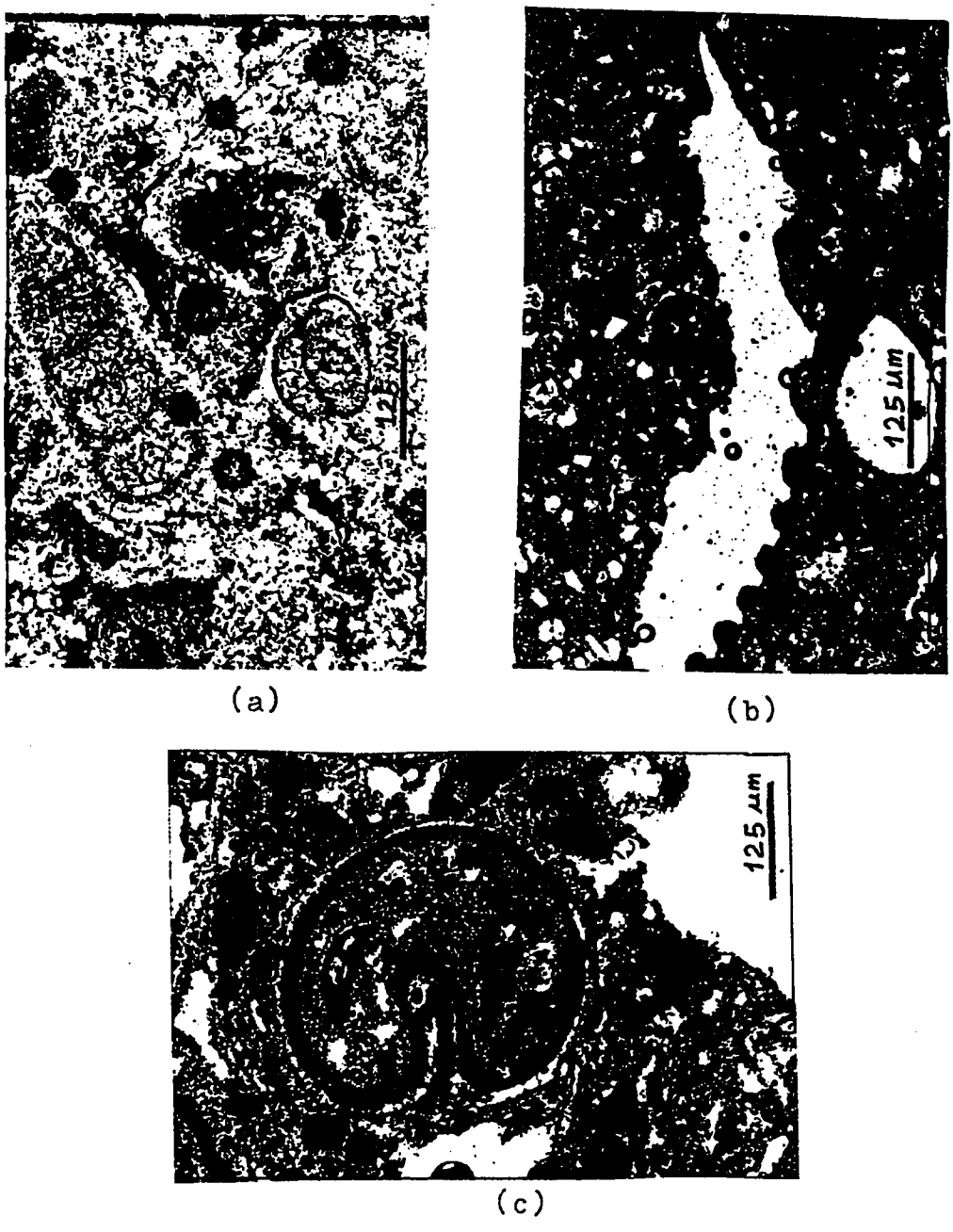

(a) (b)

(c)

Plate 10. Dolomitic skeletal packestone

(a) Some benthonic foraminiferids surrounded by dolomitic microspar cement. Transmitted light, cross polarized, scale 125 um.
(b) Empty mold of leached molluscan shell. The accurate preservation of the molds suggest early cementation of mud. Transmitted light, plane polarized, scale 125 um.
(c) Interior sediment cast of gastropod. Transmitted light, plane polarized, scale 125 um.

(a), (b) and (c) Sample number 1/1(20 m).

2.3 Dolomitic skeletal wackestone/mudstone

This lithofacies is the dominant dolomitic lithofacies. Color varies from creamy white to greyish white. This wackestone/mudstone contains skeletal fragments with a minor amount of soft pellets in some horizons (Plate 11a). Dolomite is dominant, but may include minor amounts of gypsum and quartz, which increase slightly landward. Gypsum fills some intergranular pores. There are well developed calcite crystals (maximum 10%) (Plate 11b), especially in the boreholes under bridge 3.

2.4 Pelletal grainstones/packstone

This lithofacies is light greyish white in color. Pellets are ovoidal to spherical with some irregular, distorted pellets (Plates 12, 13, 14). Average grain size is about 200 um in longest dimension, moderately to well sorted. Pelletal grainstone contains mainly dolomite with minor amounts of calcite and gypsum, filling some intergranular pores (Plate 13). There are some skeletal fragments, including benthonic foraminifera and molluscan molds.

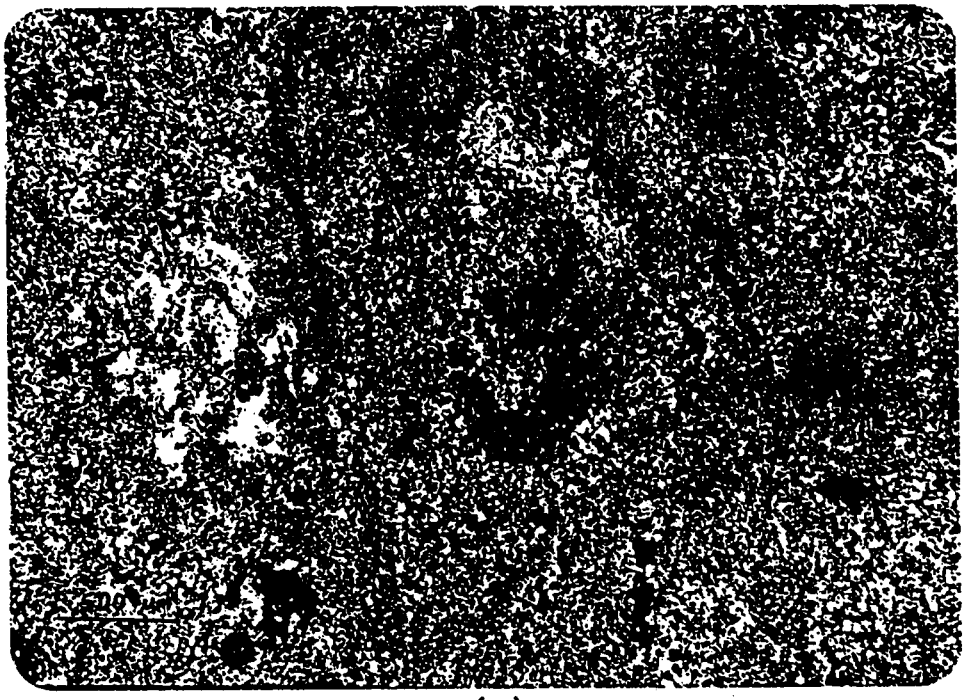

(a)

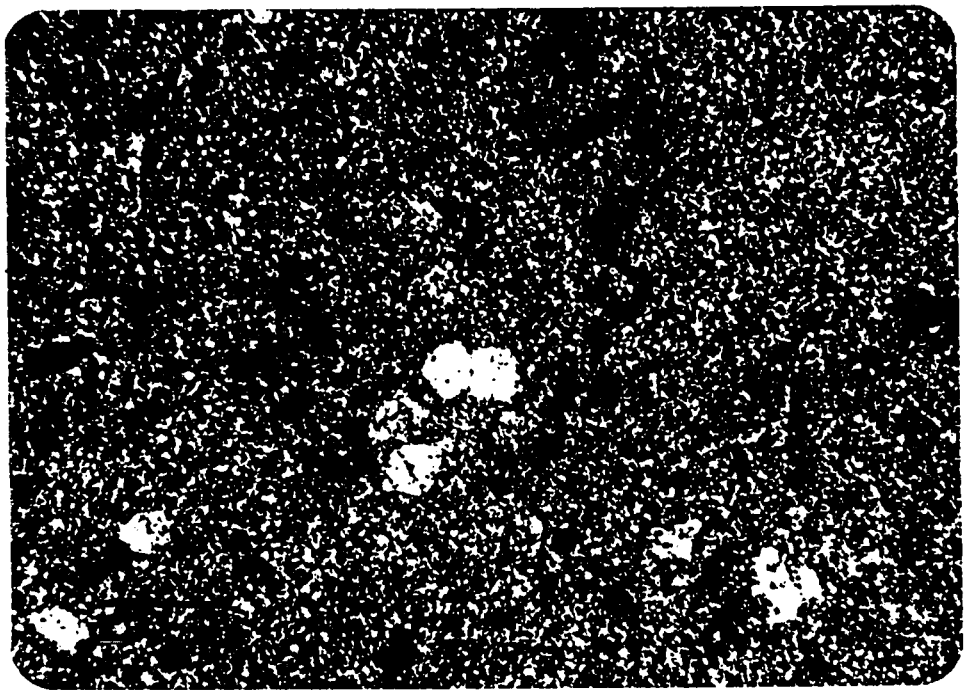

(b)

Plate 11. Skeletal wackestone/mudstone

(a) Skeletal wackestone/mudstone containing skeletal fragment (echinoid). Transmitted light, cross polarized, scale 500 um, sample number 3/ 44.3(10 m).

(b) Some well developed calcite crystals scattered in dolomitic matrix. Transmitted light, cross polarized, scale 125 um, sample number 3/102(11.5 m).

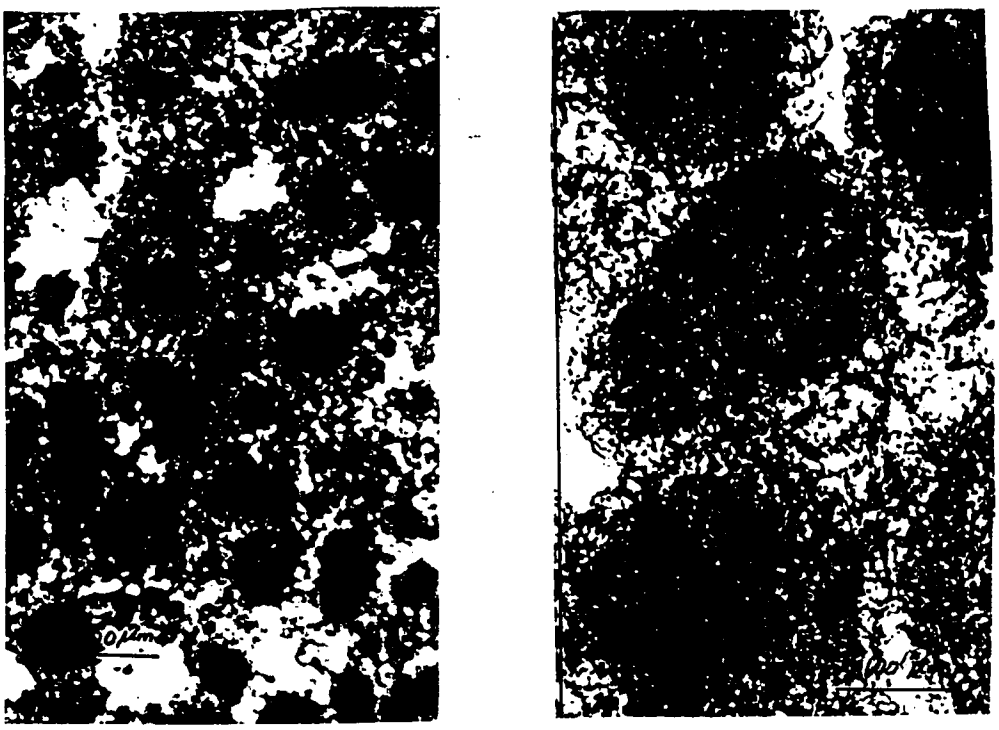

(a) (b)

Plate 12. Pelletal grainstone/packstone

(a) Photomicrograph shows the ovoidal to spherical pellets, well sorted, with average diameter of about 170 um.

(b) Magnified view of photomicrograph (a) illustrates the dolomitic microspar cementing the pellets.

Transmitted light, plane polarized, scale 500 um in (a) and 100 um in (b), sample number 3/44.3(26 m).

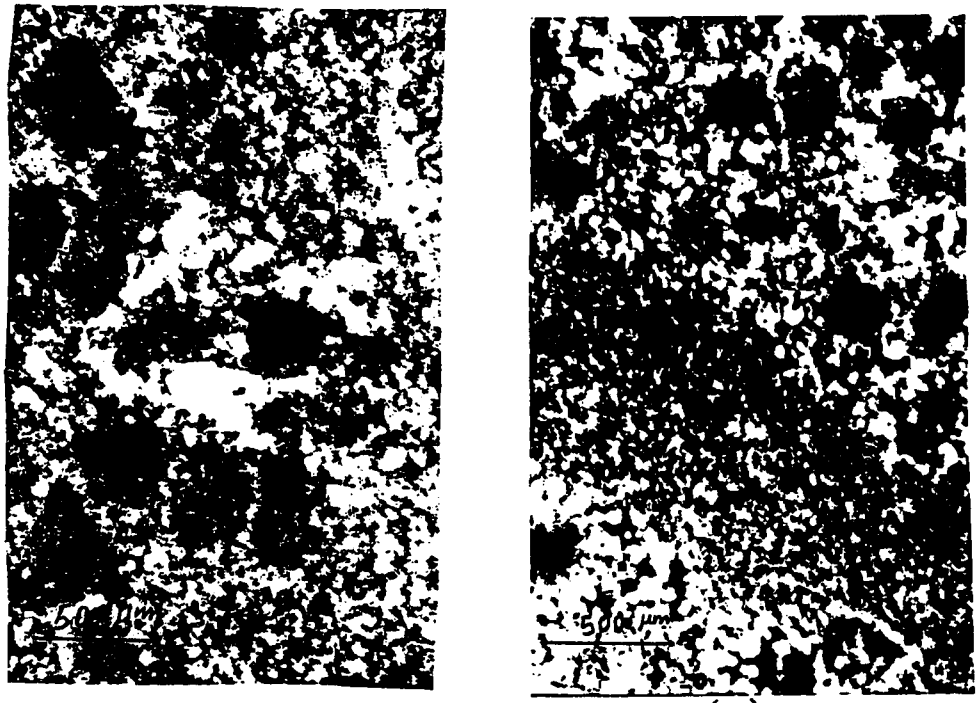

Plate 13. Pelletal grainstone/packstone

(a) Photomicrograph shows intergranular pores filled with gypsum.
(b) Interior sediments cast of unidentified fossil in pelletal grainstone.

Transmitted light, cross polarized, scale 500 um in (c) and (d), sample number 3/44.4(26 m).

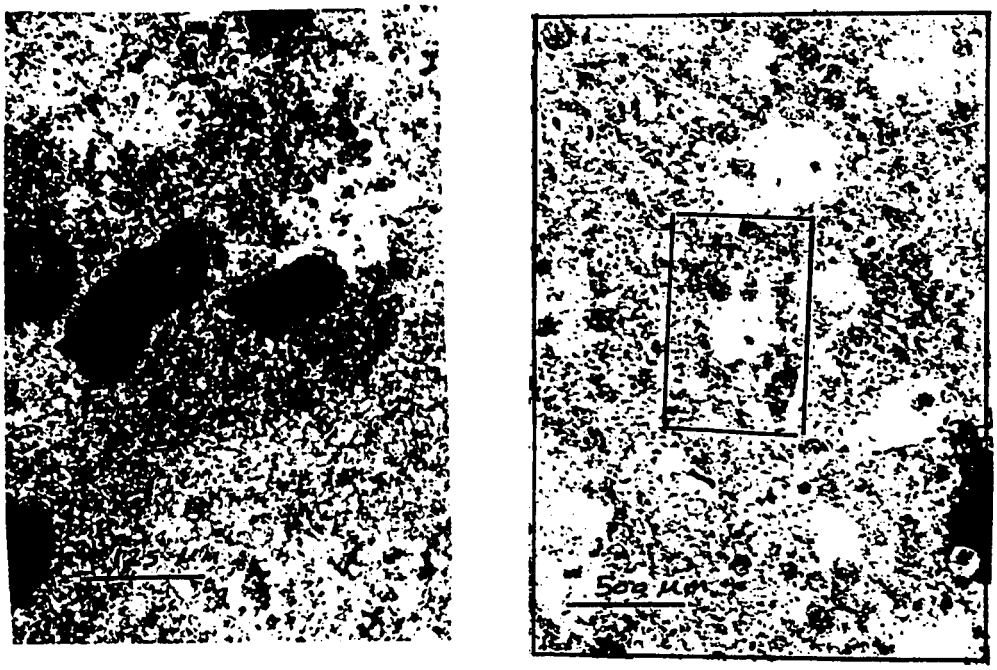

(a)

(b)

(c)

Plate 14. *Pelletal grainstone/*packstone

(a) Photomicrograph shows some irregular and distorted pellets. Transmitted light, cross polarized, scale 125 um, sample 3/44.3(26 m).

(b) Photomicrograph shows pellets inside a calcite crystal. Transmitted light, cross polarized, scale 500 um, sample number 3/102(14 m).

(c) Magnified view of the rectangular area in (b) showing clearly the pellets inside the crystal. Cross polarized, scale 125 um.

2.5 Dolomitic green mudstone (Green mudstone)

This lithofacies is pale green to greyish green in color. Green mudstone occurs in at least five horizons, with their thickness ranging between 0.25 m and 2 m. This rock is principally microcrystalline dolomite (Plate 15), with smaller amounts of clay minerals (4-15%), mainly palygorskite and illite. Palygorskite in the green mudstone is believed to have formed in-situ and not of detrital origin because of the delicate fibrous morphology of this mineral in the samples (Plate 16). Green mudstone also contains a variable amount of quartz silt and fine grained subrounded sand ranging from 7% to 38%.

Well developed calcite crystals, ranging from 150 um to 400 um in maximum dimension, were encountered in all green mudstone layers under bridge 3 (Plate 15). Calcite crystals are absent from borehole 3/1 and shoreward (Fig. 5). Calcite contents ranges between 10% and 40%. There is about 10% gypsum in the coastal green mudstone samples. Gypsum content decreases, to less than 5% a way from shore.

Most thin sections of green mudstone contain some yellowish brown spots of iron staining. SEM photographs show some well developed pyrite crystals (Appendix C4).

(a)

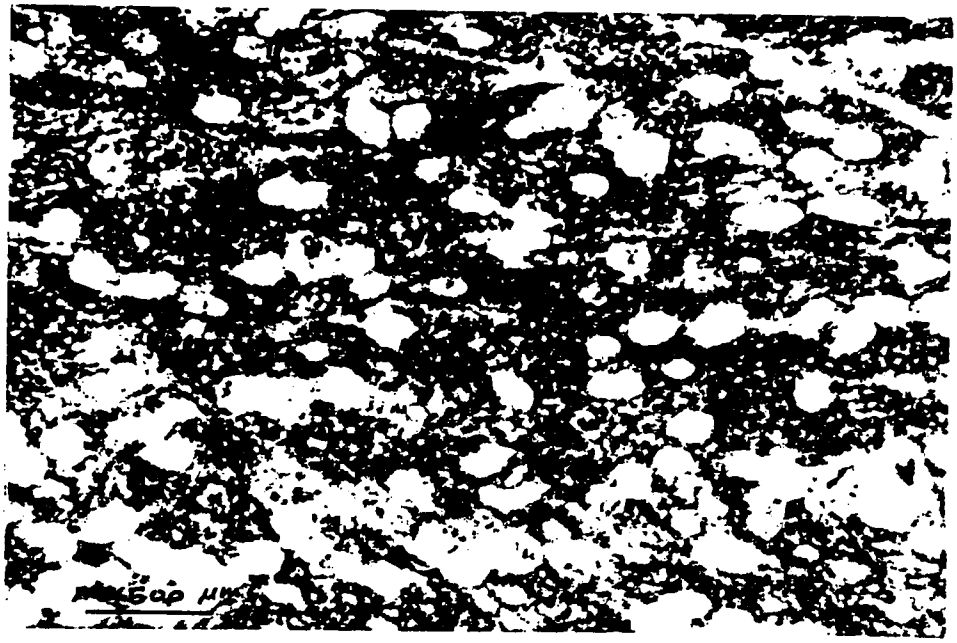

(b)

Plate 15. Dolomitic green mudstone

(a) Photomicrograph shows the microcrystalline to crypto-crystalline texture of the green mudstone (brownish in photo). Well developed calcite crystals are concentrated in more porous areas. Transmitted light, cross polarized, scale 125 um, sample number 3/44.3(15 m).

(b) Uniform distribution of calcite crystals in green dolomitic mudstone matrix. Transmitted light, cross polarized, scale 125 um, sample number 3/44.3(24 m).

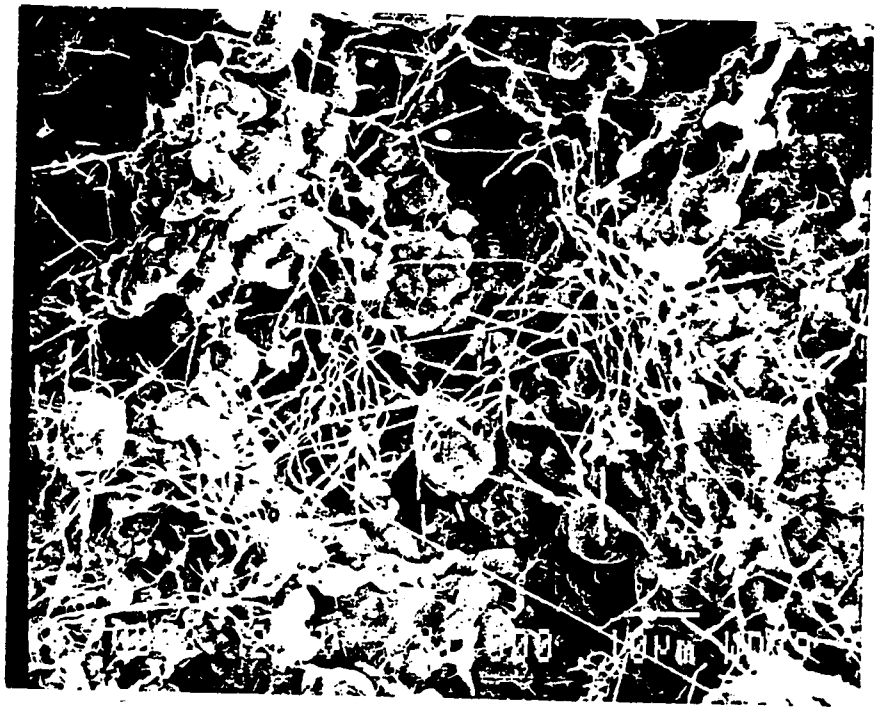

Plate 16. Dolomitic green mudstone

Green mudstone contains microcrystalline dolomite and fibrous clay mineral (palygorskite) . The delicate fibers suggest their authigenic origin. SEM, scale 10 um, sample 2/1 (19 m).

Green mudstone almost always contains thin mudstone breccia horizons, which include distorted, wispy, and angular to subangular white dolomitic mudstone fragments, 1 cm to 7 cm in longest dimension, in a matrix of dolomitic green mudstone (Plate 17).

(a)

(b)

Plate 17. Breccia horizons in green mudstone

(a) Irregular, subrounded and wispy white mudstone fragments in green mudstone matrix.
(b) Angular, white mudstone fragments in a matrix of green mudstone.

(a) and (b) Reflected light, scale in centimeters, sample number 3/44.3 (40 m).

CHAPTER 1V

DIAGENETIC CHANGES IN THE ROCKS

The studied rocks have been pervasively altered by several diagnetic processes. These processes include cementation, micritization, dissolution, precipitation, dolomitization, and calcitization.

1. DIAGENESIS IN NON-DOLOMITIC ROCKS

1.1 Early diagenetic changes in aragonitic skeletal and oolitic sands

(a) Cementation

The aragonitic skeletal and oolitic sands, which represent the present-day sediments include bands of lithified grainstone as much as 20 cm thick. These are cemented by two types of cement. The first is acicular aragonite, which radiates outward from grains and inward into chambers (Plate 4). It also forms fan-like (botryoidal) cement (Plate 18a), which is a common early submarine cement in sediments of coastal Arabia (Shinn, 1969). The second is small amounts of fine-graine micritic cement (Plate 18b).

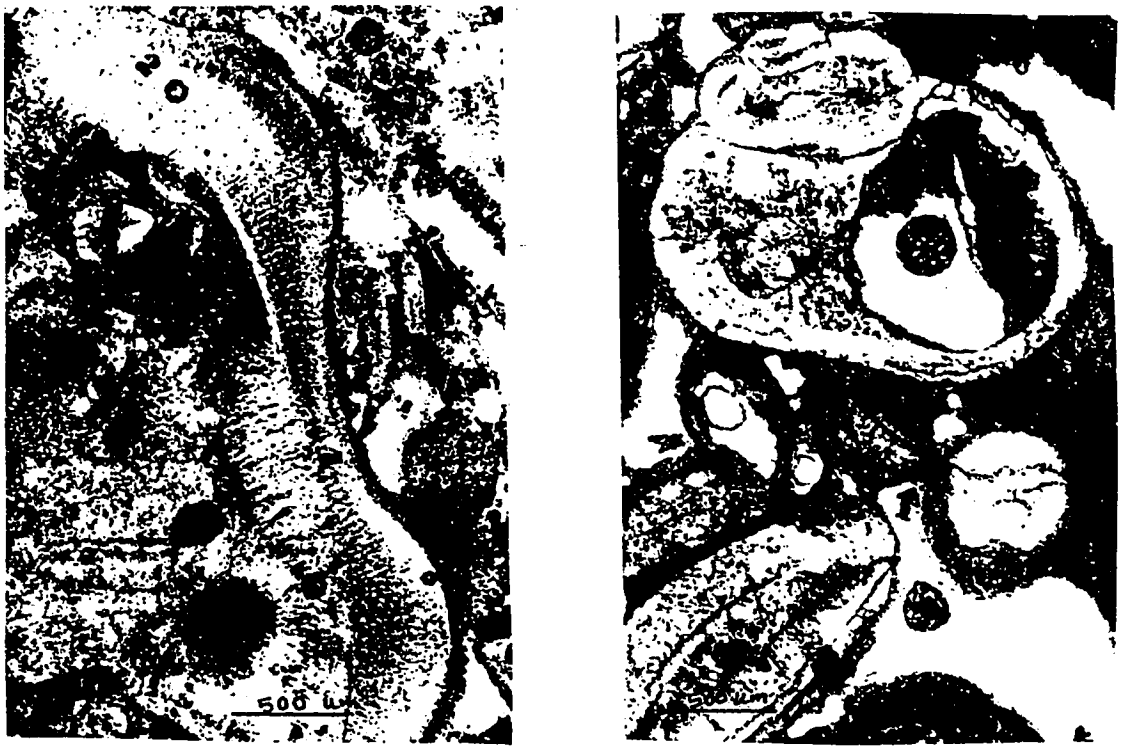

(a) (b)

Plate 18. Cements in aragonitic skeletal grainstone

(a) Fan-like (botryoidal) aragonite cement on molluscan shell, marked (1) and (2). Transmitted light, plane polarized, scale 500 um, sample number 3/24 (0.5 m).

(b) Skeletal grains cemented by micritic cement (arrows). Transmitted light, plane polarized, scale 500 um, sample number 3/32/ (0.3 m).

(b) Micritization

Micritization is one of the earliest diagenetic processes to affect the recent carbonate sediment particles resulting in alteration of the original skeletal and oolitic grains to homogeneous cryptocrystalline (micritic) fabric. Plate 19 illustrates some micritic spots in oolitic coatings representing partial micritization. Micritization may result from the activity of boring algae (Bathurst, 1971).

1.2 Diagenetic changes in calcitic skeletal grainstone

Calcitic skeletal grainstone appears to be affected by as many as four stages of diagenesis:

(a) Early cementation stage

An early cement, possibly aragonitic origin, is assumed by analogy with the early submarine cementation of recent aragonitic skeletal grainstone discussed above. There is no clear evidence of this generation of cement due to subsequent diagenetic effects.

(b) Dissolution-precipition stage

In this stage aragonitic cement was either leached or recrystallized as result of meteoric water, and concurrently, bladed sparry calcite cement was deposited.

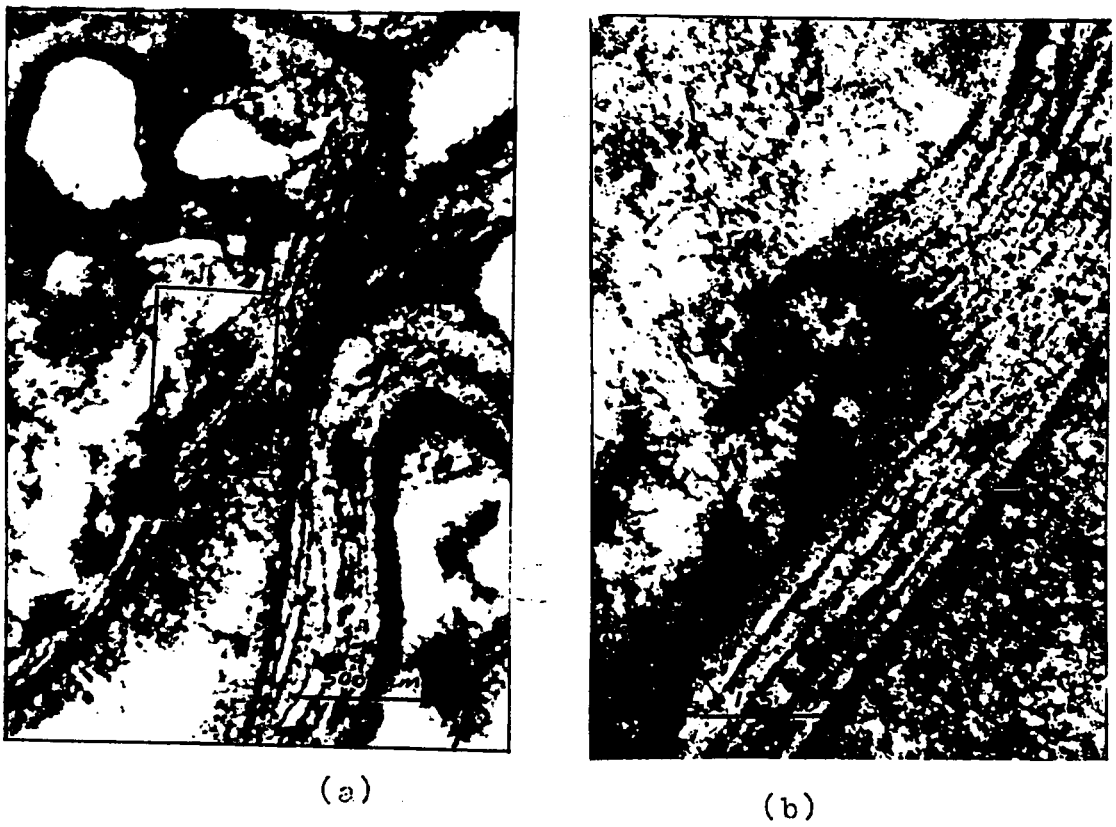

(a) (b)

Plate 19. Micritization in oolitic grainstone

(a) Micritic spots in the concentric oolitic coating representing partial micritization.
(b) Magnified view of the rectangular area in (a) showing partial micritization.

Transmitted light, plane polarized, scale 500 um in (a) and 125 um in (b), sample 3/102(0.5 m).

These bladed calcite crystals are euhedral to subhedral with dimensions about 10 um by as much as 80 um (Plate 6). The intergranular fabric remains reasonably constant due to the deposition of the calcite cement on shell surfaces (Land, in Bathurst, 1971). The aragonitic shells are later dissolved (Taylor, in Bricker, 1971) leaving shell molds. Scattered calcite cement was then precipitated inside some skeletal molds (Plate 6). However, these processes may take place more or less concurrently.

1.3 Diagenesis in quartz sandstone

(a) Cementation

Quartz sandstone is cemented by isopachous drusy, calcite microspar (20-40 um) (Plate 7). This type of cement is usually developed in a fresh water phreatic zone (Scoffin, 1987).

(b) Replacement of quartz by calcite

Margins of a few quartz grains were replaced by calcite cement (Plate 7b).

2. DIAGENESIS IN DOLOMITIC ROCKS

Some points should be mentioned before discussing diagenesis in dolomitic rocks:

(a) There are two varieties of dolomitic lithofacies, depending on colour and associated minerals:

1. White dolomitic lithofacies, which include skeletal mudstone/wackestone, pelletal grainstone/packstone, oolitic grainstone/packstone and skeletal packstone. All these lithofacies contain mainly dolomite (Chapter III).

2. Green dolomitic mudstone (Green mudstone). In this lithofacies, dolomite is the main mineral with 4-15% clay minerals (Chapter III). It may include thin breccia horizons of white dolomitic mudstone fragments in green mudstone groundmass.

(b) All the calcite in the dolomite layers is secondary and resulted from calcitization of dolomite. It is abundant under bridge 3 towards the Bahrain Island and disappears towards shore.

2.1 Outlines of diagenetic processes in dolomitic rocks.

Dolomitic rocks appear to be intensively affected by as many as five diagenetic stages. Details will be included within the diagenesis of each lithofacies . Dolomitization and calcitization will be discussed separately.

(*a*) *Early marine cementation*

(*b*) *Early neomorphism*

(i) Micritization (degrading neomorphism)

(ii) Aggrading neomorphism

(*c*) *Dissolution-precipitation stage*

(*d*) *Complete dolomitization*

(*e*) *Partial calcitization of dolomite*

2.2 Diagenetic changes in dolomitic mudstones

Dolomitic mudstone includes both the white skeletal mudstone/wackestone and the green mudstone.

Dolomite microspar, which results from aggrading neomorphism of micrite, is the principal component of dolomitic mudstone. Plates 20 and 25 illustrate microspar that is equant, anhedral to subhedral, and about 10 um

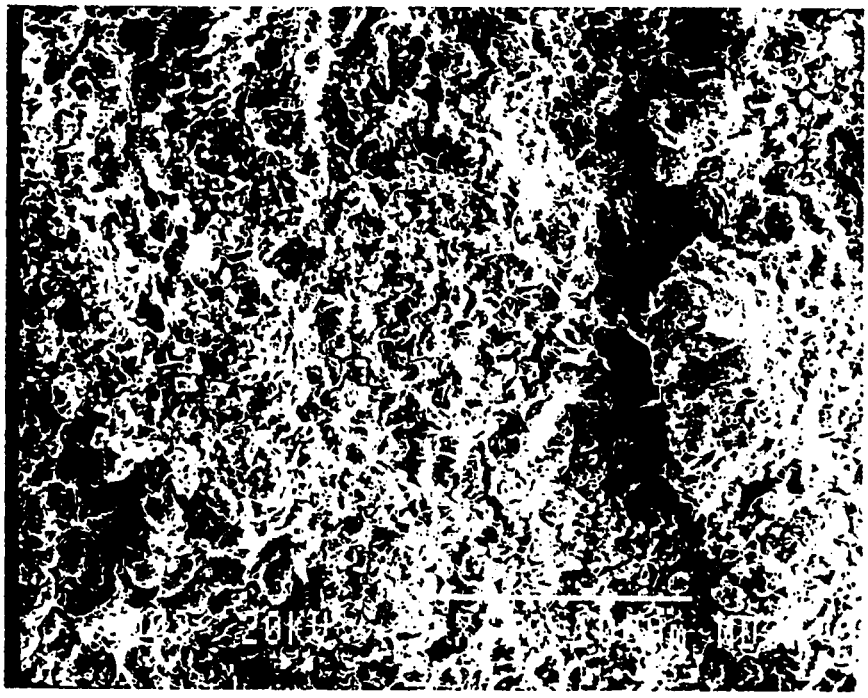

(a)

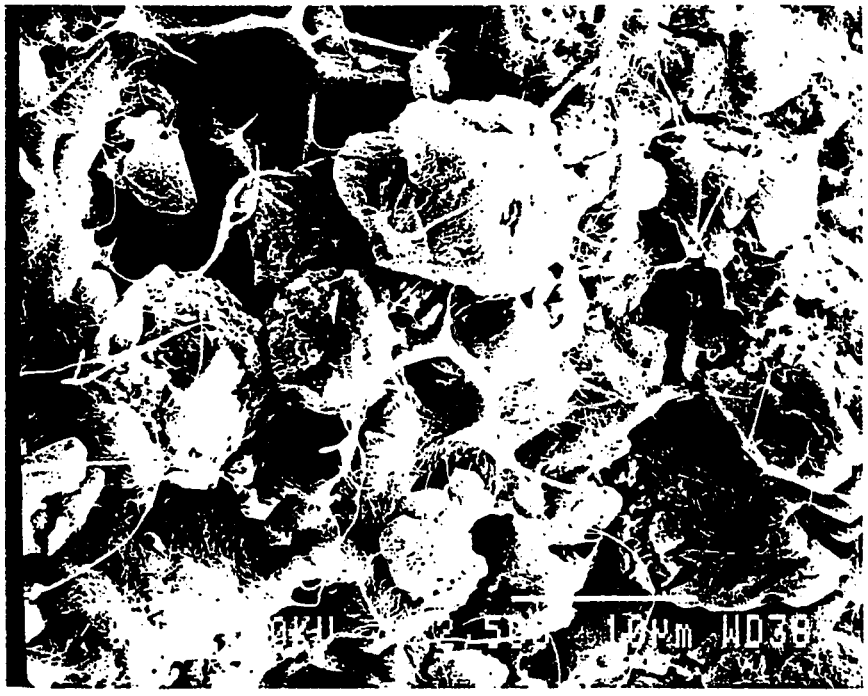

(b)

Plate 20. Dolomitic microspars in mudstone.

(a) SEM photograph illustrates equant, anhedral to subhedral dolomitic microspar (10 um) in dolomitic green mudstone.

(b) Magnified view of photograph (a) showing dolomitic microspar associated with fibrous clay mineral (palygorskite) in green mudstone.

SEM, scale 100 um in (a) and 10 um in (b), sample number 3/44.3(37 m)

across. In green mudstone, dolomitic microspar (Plate 19b) is almost always associated with fibrous clay minerals (palygorskite and/or illite).

Dolomitization, and aggrading neomorphism are believed to have occurred concurrently. Dolomitic mudstone shows partial later calcitization (Plate 15).

2.3 Diagenetic changes in oolitic grainstone

Analogous to the present-day oolitic sand discussed previously, the dolomitic oolitic grainstone appears to be affected by the following diagenetic processes:

(*a*) *Micritization*.

Micritization is one of the earliest diagenetic process resulting in transformation of the concentric oolitic coating to cryptocrystalline, randumly oriented, coating (Plate 21).

(*b*) *Dissolution-precipitation stage*

Some oolitic nuclei and coatings, as well as aragonitic skeletal fragments were dissolved leaving molds (Plates 8, 21). At the same time, crusts of blocky calcite spar (20-40 um) were precipitated around and between the oolitic grains replacing a previous early cement (?). This stage was probably the result of fresh water percolation.

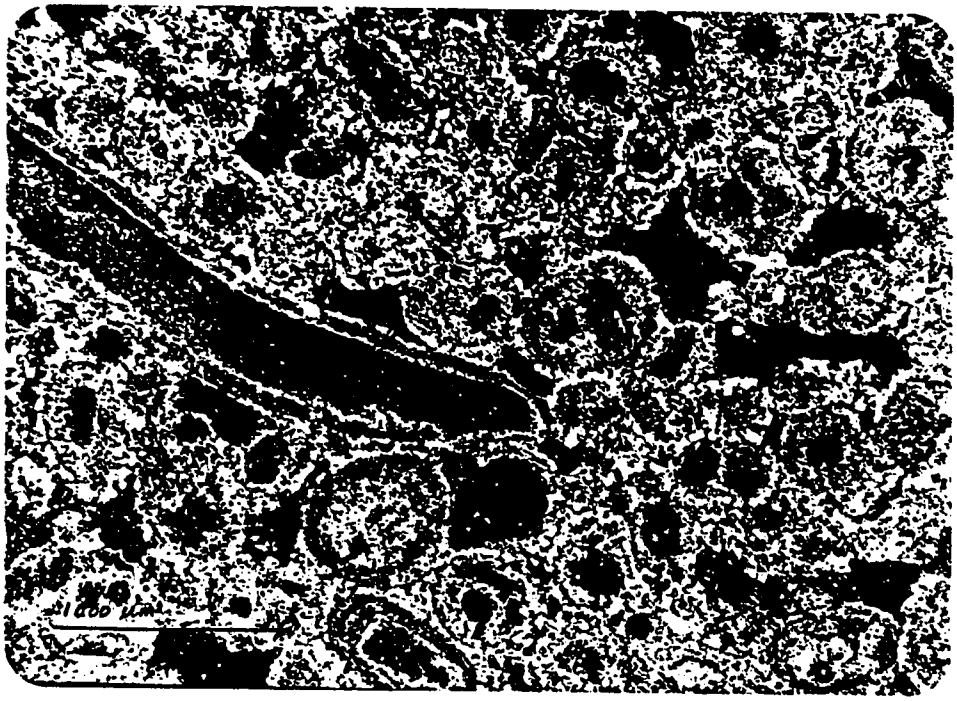

(a)

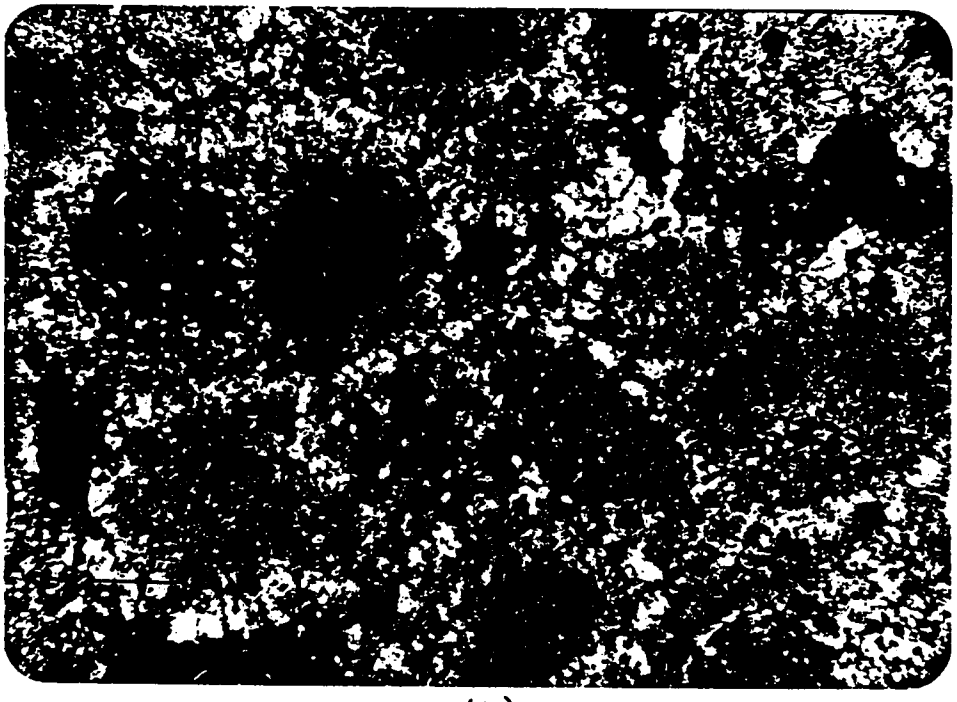

(b)

Plate 21. Diagenesis in oolitic grainstone

(a) Photomicrograph illustrates the empty molds of some dissolved oolitic nuclei and skeletal fragments. The internal structure of oolitic grains is not clear due to the intensive neomorphism. Transmitted light, cross polarized, scale 1000 um, 1/1(15 m).

(b) This photomicrograph shows crusts of blocky calcite spar cement (20-40 um) around the oolitic grains. Transmitted light, cross polarized, scale 100 um, sample 1/1 (15 m).

2.4 Diagenetic changes in pelletal grainstone/packstone

(a) Cementation by coarse dolomitic microspar, about 20 to 40 um across (Plate 22a).

(b) Partial aggrading neomorphism of pellets.

Some individual pellets show partial or complete aggrading neomorphism to microspar (5-10 um), which may partially obscure the outline of the neomorphosed pellet. Moreover large patches of pellets and matrix are neomorphosed to microspar leaving ghosts of the previous pelletal texture (Plate 22 b).

2.5 Diagenetic changes in skeletal packstone

(a) Early lithification

Early lithification is suggested by the good preservation of skeletal molds. The nature and type of this cement is not known due to later diagenetic processes.

(b) Dissolution-precipitation stage

In this stage all aragonitic shells were dissolved leaving empty molds or molds with interior mud casts (Plate 23). Microspar cement (5-10 um) partially lines the molds (Plate 24) and coats exterior grain surfaces.

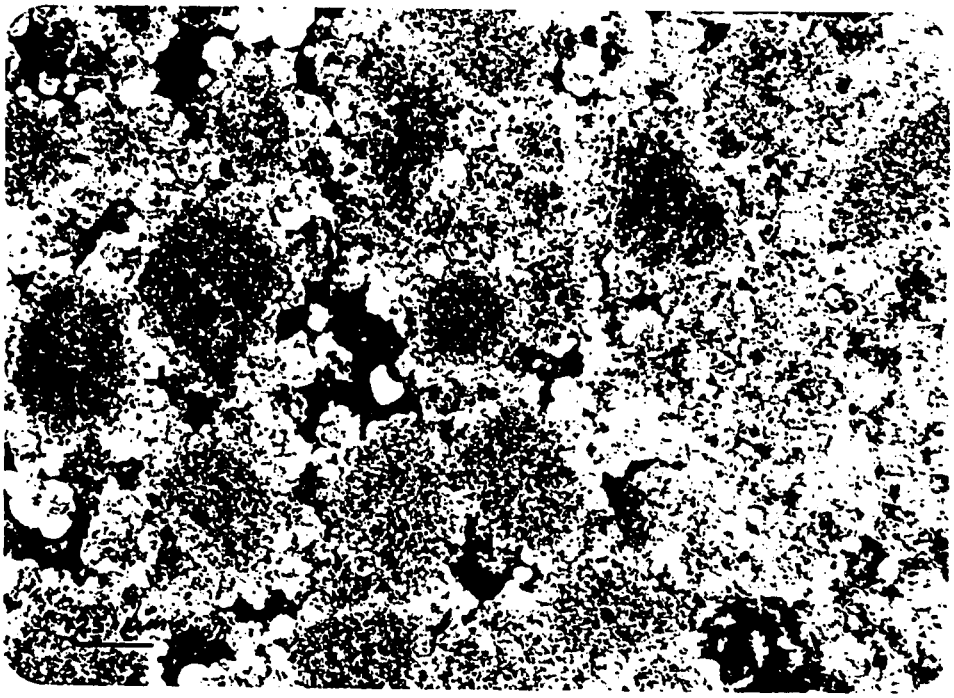

(a)

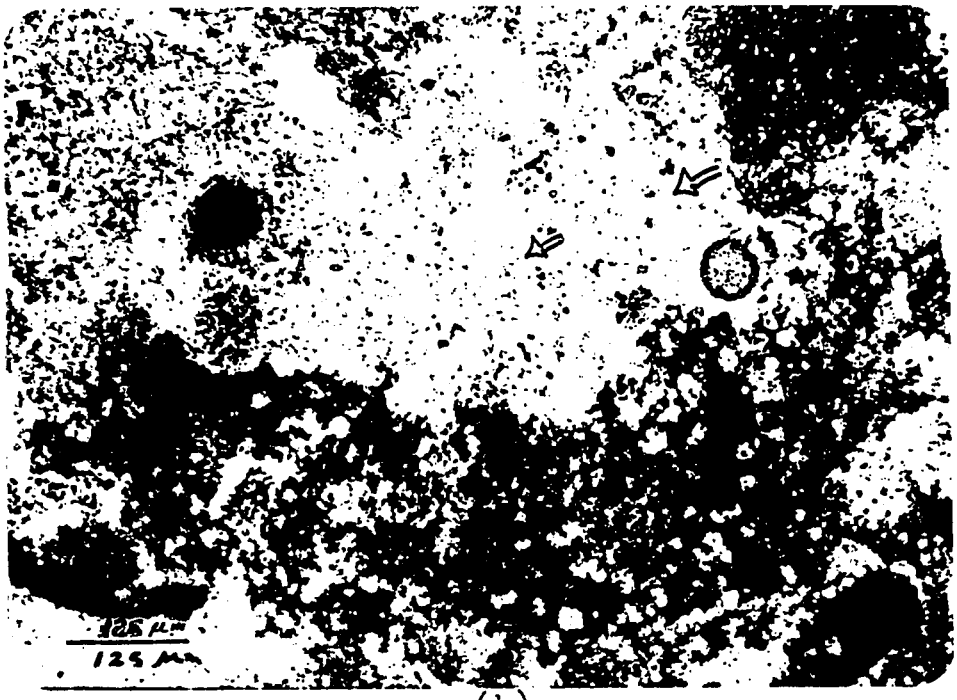

(b)

Plate 22. Diagenesis in pelletal grainstone

(a) Coarse dolomitic microspar (20-40 um) cement in pelletal grainstone. Transmitted light , cross polarized, scale 125 um, sample number 3/69 (13 m).

(b) Completely recrystalized patches in pelletal grainstone. The ghost of the recrystallized pellets can still be recognized (arrows). Transmitted light, plane polarized, scale 125 um, sample number 3/44.3 (25.5m).

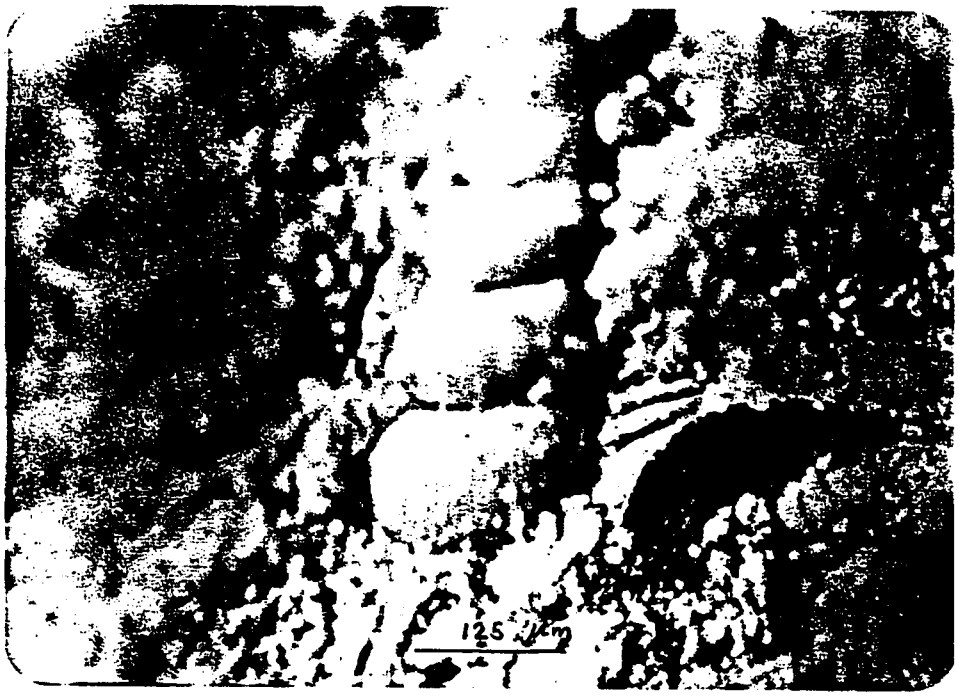

(a)

(b)

Plate 23. Shell dissolution in skeletal packstone

(a) and (b) Shells dissolved leaving empty molds and internal mud casts (pelecypod cast in photograph a and gastropod in b). Reflected light, scale 125 um, sample 1/20(15 m).

(a)

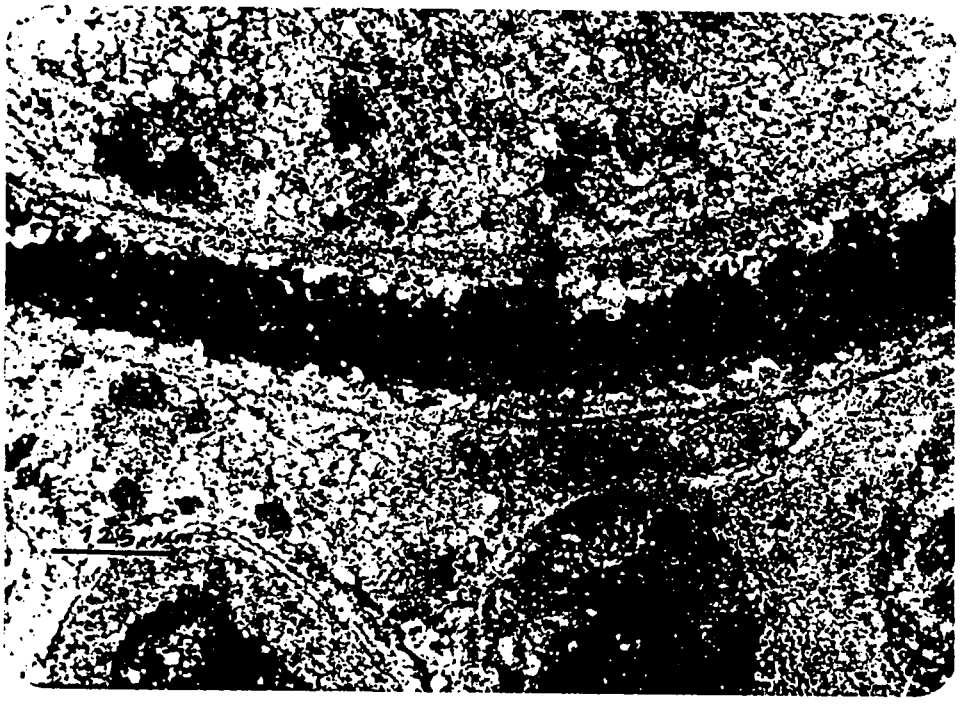

(b)

Plate 24. Shell dissolution in skeletal packstone

(a) Dolomitic microspar cement lining internal surface of skeletal mold.
(b) Magnified view of the rectangular area in (a) showing the microspar cement inside skeletal mold.

Transmitted light, cross polarized, scale 500 um in (c) and 125 um in (d), sample 1/1(20 m).

2.6 Dolomitization

Dolomitization may have occurred during or shortly after deposition of carbonate sediments as an early diagenetic process. This is supported by the following petrographic observations:

1- The original textural features are well preserved. Fossils, ooids and intergranular fabric can be recognized easily, which is good evidence of its early diagenetic origin (Doornkamp et al,1980).

2- The boundary between the dolomitic facies and non-dolomitic facies is a sharp stratigraphical boundary, which is good evidence for its early diagenetic origin. That means, dolomitization took place before the deposition of the overlying limestone.

Before suggesting a dolomitization model the following points should be considered:

1- Finding a reasonable source for the Mg-bearing solution, which was responsible for dolomitizing this thick dolomite sequence (> 40 m). One of the primary requirements for regional dolomite formation is a large supply of magnesium.

2- Finding an acceptable mechanism for transporting this

magnesium and distributing it through the host limestone and into the less permeable green mudstones.

2.6.1 Possible dolomitization model:

Taking in consideration the previous points two possible models may be applicable.

(i) Seepage reflux.

Dolomitization may be occurred by seepage reflux of Mg-rich brines from coastal sabkhas (Adams and Rhodes,1960; Zenger, 1975, Illing et al., 1965) through the calcitic rocks (Fig.11). The coastal sabkhas were formed around the Gulf of Salwa during, and perhaps after, the time of deposition of dolomitized rocks (Fig. 3). Kassler (1973) indicate several generations of sabkhas on the Arabian coast between 200,000 and 5000 y.b.p. (see Fig. 20).

Coastal sabkhas were flooded with sea water as result of tides and storms. The extensive evaporation resulted in deposition of gypsum, which increased the concentration of Mg in the sabkha solution. That lead to the formation of high-Mg brines in these sabkhas. The specific gravity of sabkha solusions increased as the brines were concentrated. The brines, in the supratidal sabkhas, may have seeped down by the following mechanisms:

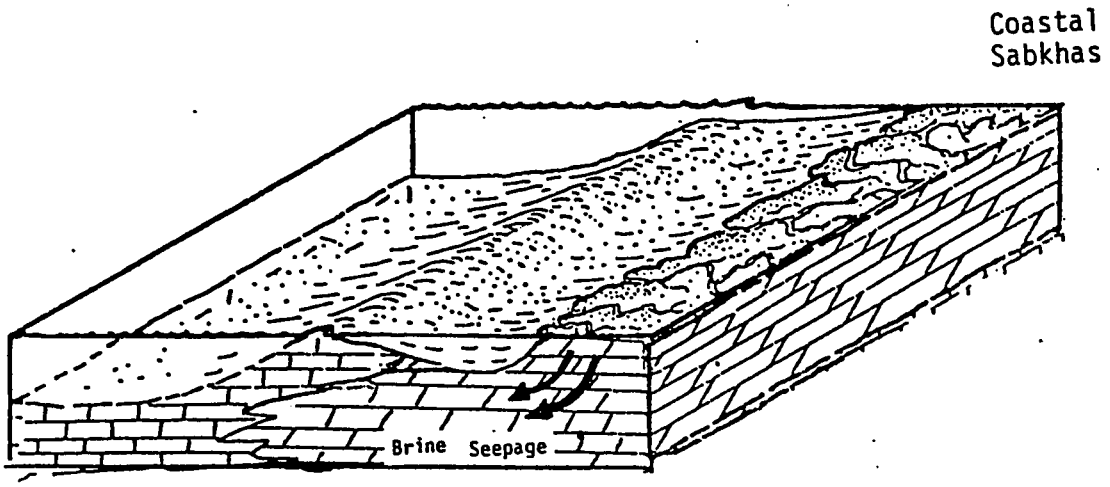

MODEL OF DOLOMITIZATION

Fig.(11)- Proposed model of dolomitization by seepage reflux (After Adam and Rhodes,1960; Zenger,1975).

(a) Density difference

Density difference was developed between lagoonal sea water and sabkha brines due to intensive evaporation (Scoffin, 1987).

(b) Head difference

There is slight head difference between the elevated supratidal sabkhas and the lagoonal sea water.

(c) The presence of porous horizons

The leaching of aragonitic shells provided the pathway for heavy brine to seep through the rocks.

The brines may have been diffused to less porous layers by concentration difference. To support this model, Adams and Rhodes (1960) mentioned that, the brines should have left "foot prints" behind it. The presence of gypsum, occupying some intergranular pores and fossils molds supports seepage reflux model. Gypsum content reached as high as 10%, especially in nearshore boreholes and about 1% in seaward boreholes. This gypsum was believed to have been precipitated during migration of brines from the nearby coastal sabkhas, which have been documented by Kassler (1973).

However, the lack of gypsum in general may be attributed to later leaching by fresh water, which may have caused partial calcitization of dolomite. This interpretation for the absence of gypsum could be valid only in the case of seepage reflux mechanism.

(ii) Mixing of fresh water and salt water

A plausible mechanism for dolomite formation is by mixing of fresh and salt marine water. Several studies dealing with mixing zone dolomites have appeared in the literature, including those of Hsu,1963, 1966; Land, 1973; Land and Epstein, 1970; Land et al., 1975; Dunhan and Olson, 1978, and others. The proponents of this model proposed that the mixing of marine pore water with meteoric-derived ground water or brackish water would lead to dolomitization of calcium carbonate in the subsurface, without precipitation of evaporites. Folk and Land (1975) proposed that ground water was derived from subaerially exposed areas during rainy periods. Figure 12 shows a model for dolomitization by mixing mechanism (Dunhan and Olson, 1978).

2.6.2 Discussion

In the studied rocks, the lack of evaporites and the presence of some relatively large (> 5 um) dolomite crystal

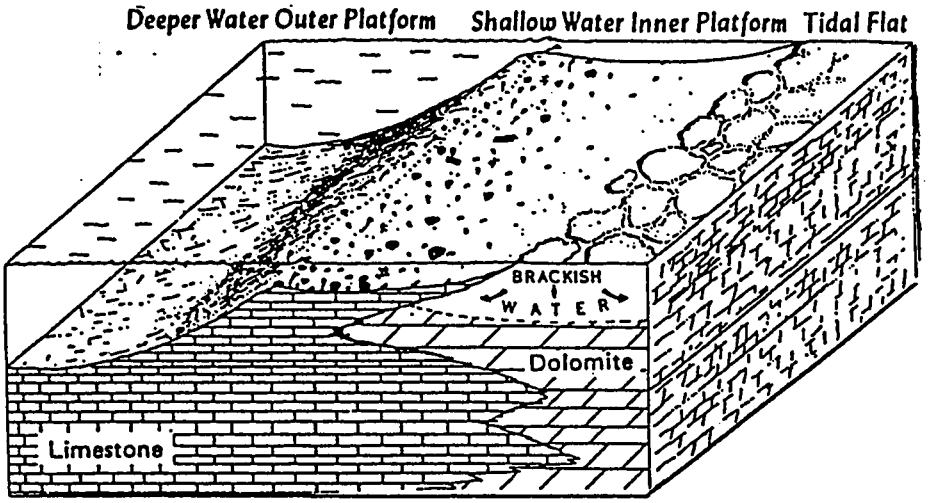

Model of dolomitization

Fig. (12).1. Proposed model of dolomitization by mixing fresh and salt water (Brackish water) (From Dunham and Olsons, 1978).

have been considered as supportive petrographic evidence for the mixing mechanism (Folk and Land, 1975; Marrow, 1975). But the dominance of microcrystalline dolomitic crystals, constituting the oolitic and pelletal grainstone, argues against this petrographic evidence.

In general, there is much uncertainty over the two proposed mechanisms and factors that control the genesis of the early dolomite. Most current models of dolomitization are incapable of explaining the genesis of dolomite that lacks evidence of supratidal origin and evaporites (Badiozamani, 1973). For that reason I suggest further study on dolomitization with the help of oxygen and carbon isotope (Doornkamp et al., 1980) to clarify the model and the nature of dolomitization (Fig.13).

2.7 Calcitization of dolomite

2.7.1 Nature and distribution of calcite

Large scale replacement of dolomite by calcite was encountered in all dolomitic lithofacies under bridge 3, but replacement calcite disappears shoreward. All the calcite in dolomitic rocks resulted from calcitization. Calcite content ranged between 10-50% in the green mudstone horizons, and did not exceed 10% in the white dolomitic

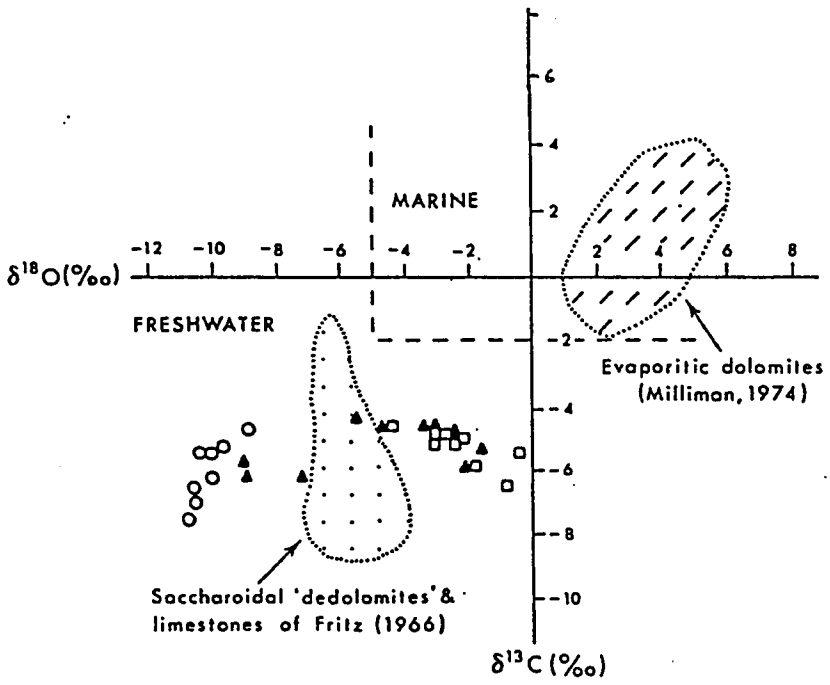

Fig.(13)- Aa example of carbon and oxygen isotops studies, which were used in determining the environment and nature of dolomitization processes (From Doornkamp et al ,1980,Fig.5.3).

lithofacies. This was probably because the white dolomite was better cemented and less permeable than the weakly lithified green mudstone. The concentration of replacement calcite was higher in deeper horizons, and there was no calcite in the upper two meters of the dolomitic interval (Appendix A8). In the green mudstones the calcite crystals were concentrated in the more porous area (Plates 15a). Less commonly, the calcite showed uniform distribution through out the green mudstone (Plate 15b). Calcite crystals are 150 um to 400um in longest dimension and euhedral to subhedral, some have cloudy centers.

Development of a single large calcite crystal is initiated in two ways. First, by gradual replacement of dolomite microspar from the central portions, then continues toward the margin to form a single, large calcite crystal (Plate 25). Second, calcite gradually replaces dolomite from the marginal portions to form the rhombic outline of a large calcite crystal leaving dark micritic residue in the centers of some crystals, which causes the cloudy appearance of the crystals (Plate 26). Doornkamp et al.(1980) called the first type of calcite crystal, centrifugal replacement, and centripetal for the second.

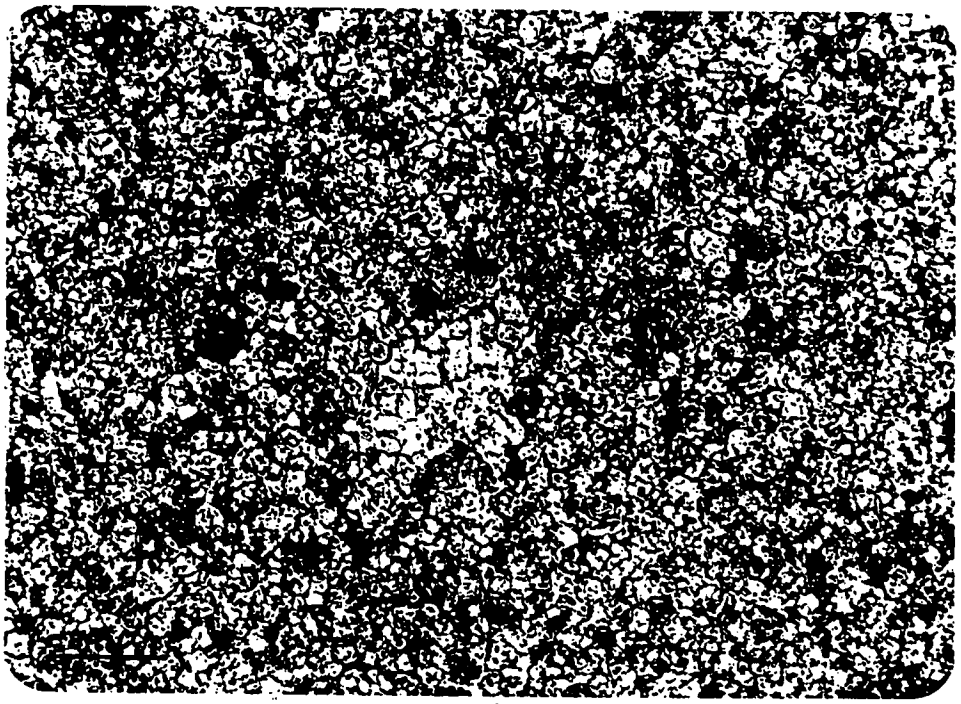

(a)

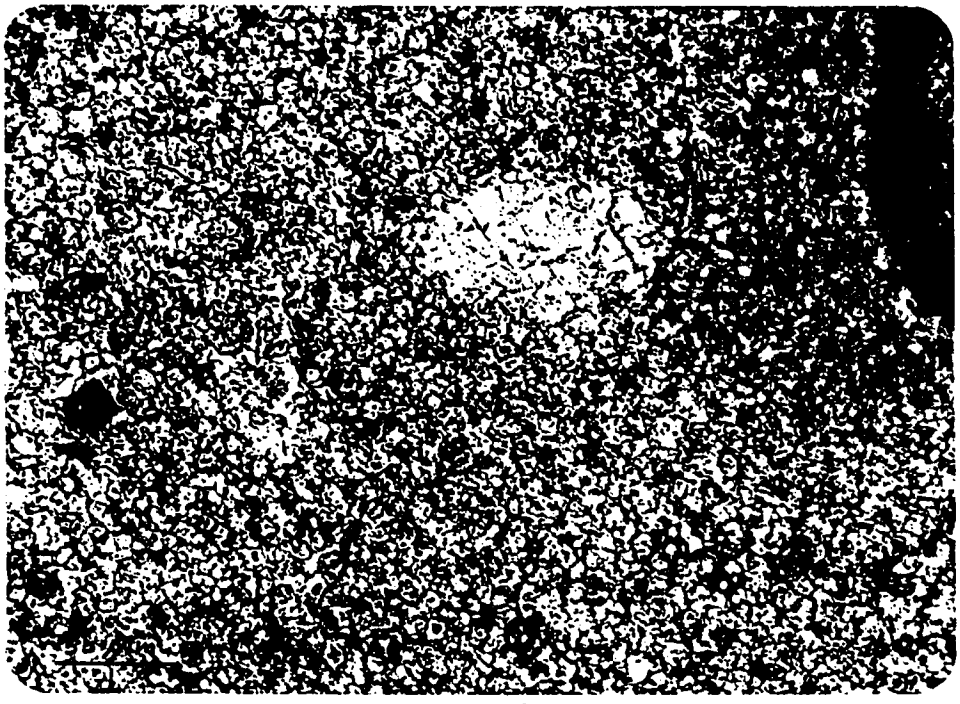

(b)

Plate 25. Centrifugal replacement of calcite

(a) and (b) Gradual replacement of dolomite by calcite. Development of a single large calcite crystal began from the central portion then continued outwards. Transmitted light, cross polarized, scale 50 um, sample 3/69 (15 m).

(a)

(b)

Plate 26. Centripetal replacement of calcite

(a) and (b) gradual replacement of dolomite by calcite. The development of a single large calcite crystal began at the marginal portions to form outline of the crystal, leaving unreplaced pellets inside. Transmitted light, cross polarized scale 125 um, sample number 3/44.3(27 m).

2.7.2 Calcitization mechanism

Calcitization, in contrast to dolomitization, was brought about by seepage of Ca-rich fresh water through the dolomite. Fresh water was available during low sea level, which were accompanied by pluvial periods (Kassler,1973) (Fig.12). Fresh ground water, was probably enriched in calcium by seepage through, and leaching of gypsum from gypsum-rich dolomites in coastal area. The absence of calcite crystals in the upper-most dolomitic beds along with higher concentration of calcite in deeper horizon suggested that calcitizing solutions, came from lower strata.

CHAPTER V

LITHOSTRATIGRAPHY AND DEPOSITIONAL ENVIRONMENTS

1. Lithostratigraphy of dolomitic rocks

The dolomitic rocks include at least five green mudstone layers (each about 1 m thick) separated by white dolomitic beds that include skeletal wackestone/mudstone and both skeletal packstone and pelletal grainstone/packstone. There are at least three discontinuous oolitic grainstone/packstone beds (0.3 m-0.7 m in thickness) developed locally especially near paleoshoals and the shoreline (Fig. 14).

The distribution of dolomitic lithofacies suggests a series of persistent paleoshoals or barriers that appear to have remained intermittently near sea level throughout deposition of the dolomite beds. Thus, the muddy dolomitic lithofacies are separated laterally into two distinct depositional areas. This interpretation is supported by the following observations.

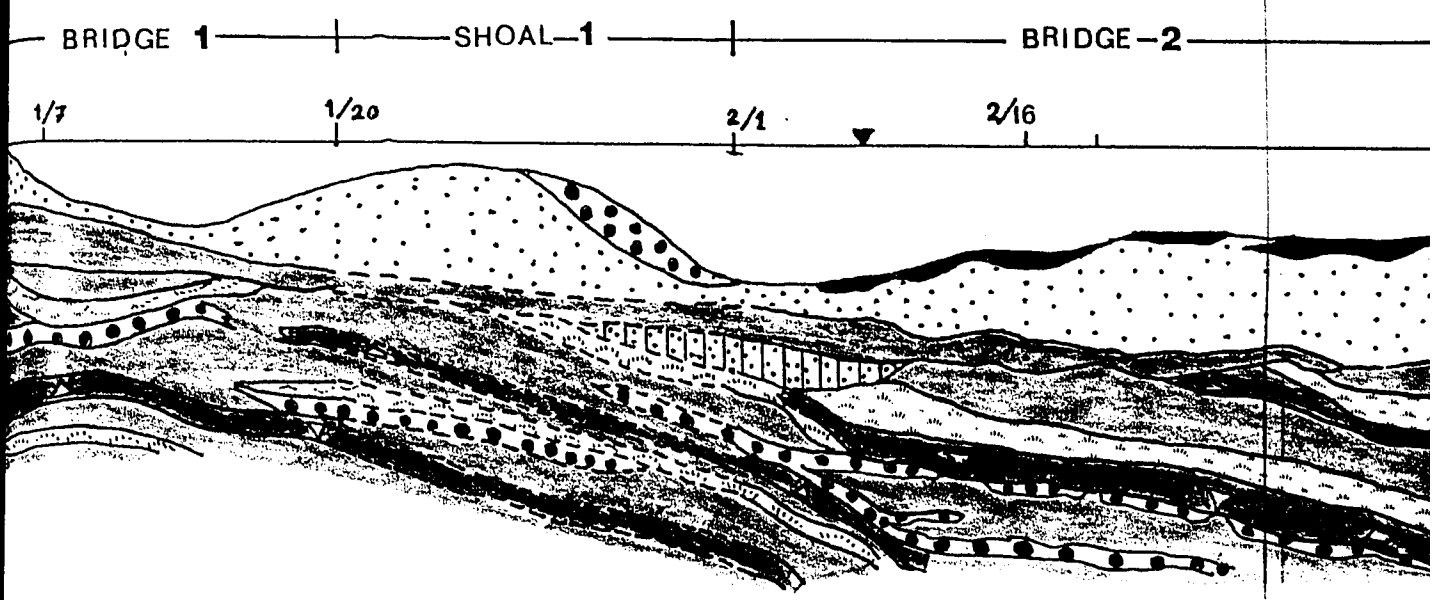

FIG.14 S

NON DOLOMITIC LITHOFACIES

ARAGONITIC SKELETAL SAND AND GRAINSTONE

ARAGONITIC OOLITIC SAND AND GRAINSTONE

QUARTZ SAND

CALCITIC SKELETAL GRAINSTONE

QUARTZ SANDSTONE

DOLOMITIC LITHO

SKELETAL F

OOLITIC GR

PELLETAL C

WHITE SKEL

GREEN MUD

GREEN MUD

BRECCIA

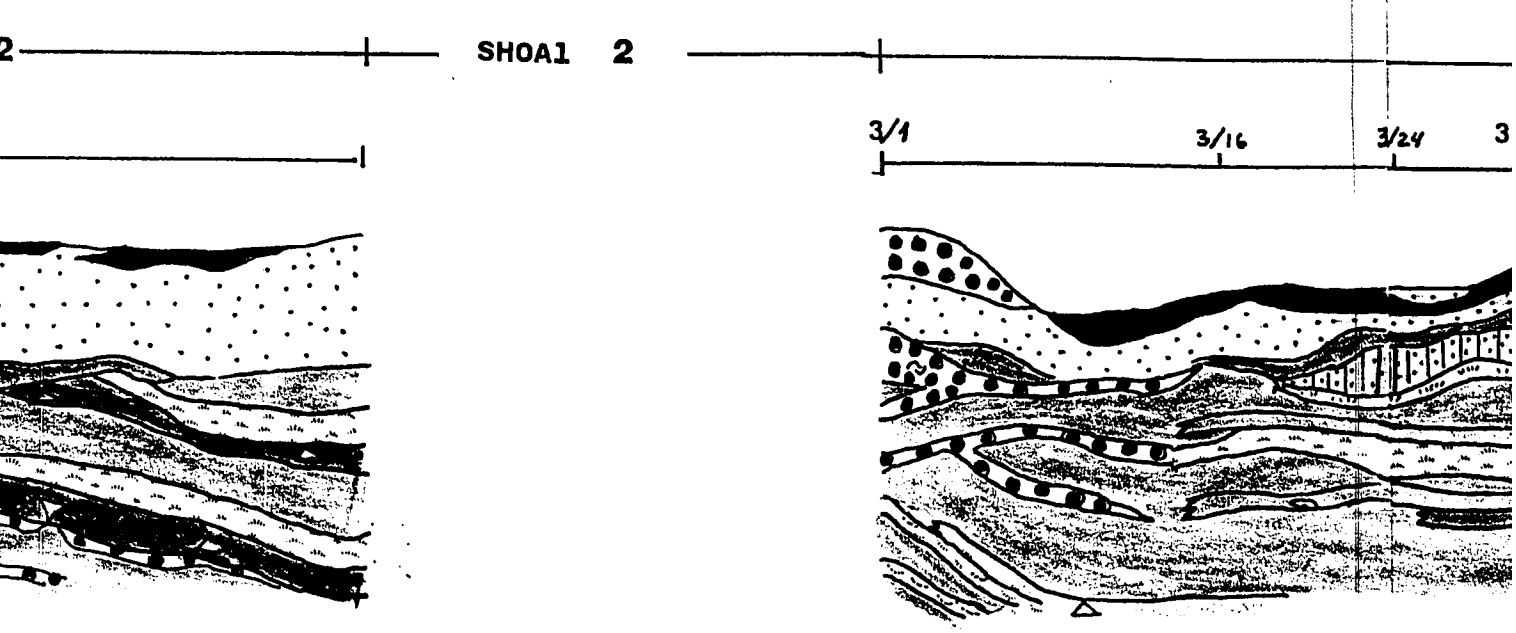

FIG.14 STRATIGRAPHIC CROSS-SECTIOI

LOMITIC LITHOFACIES

SKELETAL PACKSTONE

OOLITIC GRAINSTONE/PACKSTONE

PELLETAL GRAINSTONE/PACKSTONE

WHITE SKELETAL WACKESTONE/MUDSTONE

GREEN MUDSTONE

GREEN MUDSTONE (CALCITE-RICH)

BRECCIA

BRIDGE—3

/24 3/32 3/443 3/69 3/91 3/10

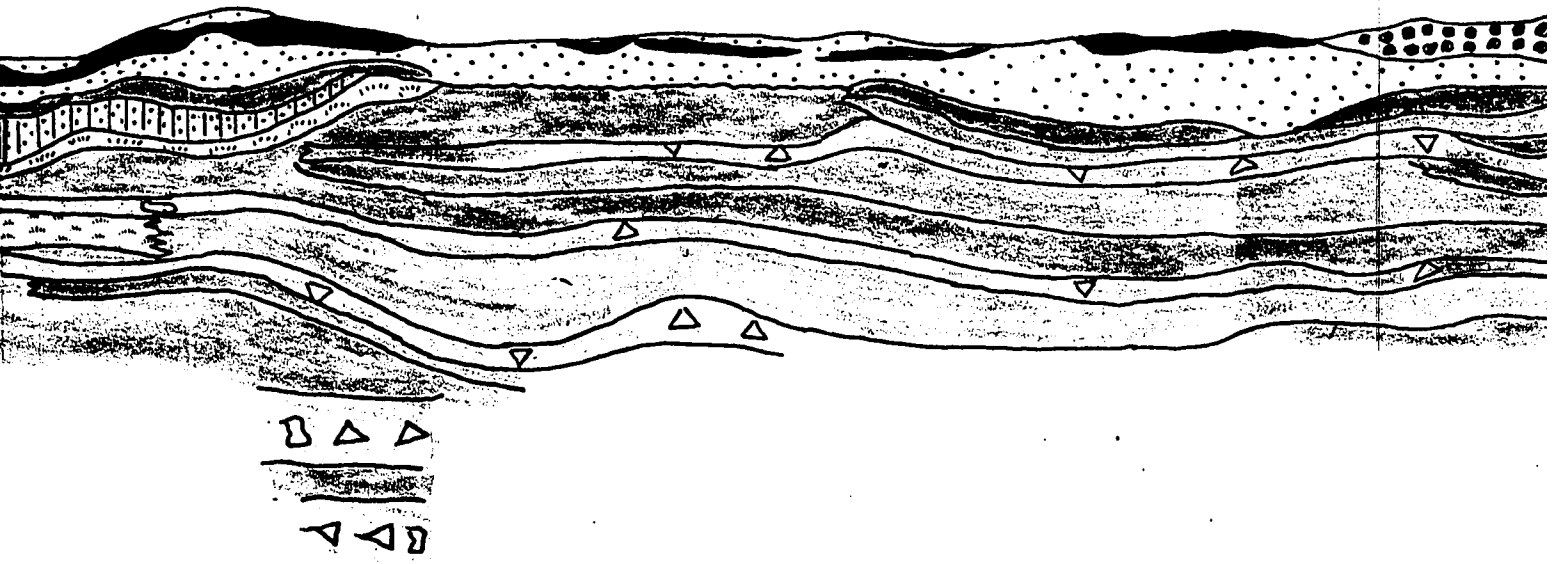

TION

SCALE

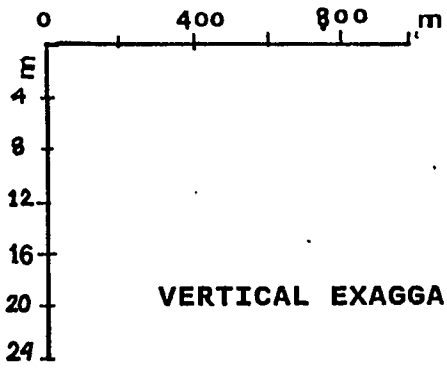

VERTICAL EXAGGARATION = 26X

1- Presence of at least three successive local oolitic beds under shoal 2 (Fig. 14). These beds are interpreted as successive oolitic paleoshoals, deposited in very shallow (2 m or less), agitated sea water.

2- The modern oolitic tidal bars at shoal 2 suggest that this area remains high today.

3- Presence of at least two successive local oolitic beds, which may represent paleoshoals, in the vicinity of shoal 1 (Fig. 14).

4- The green mudstone beds are lenticular between oolite beds (Fig. 14). Moreover, green mudstone layers terminate laterally near the locally developed oolitic layers in the vicinity of the proposed paleoshoals, especially beneath shoal 1 and 2 (Fig. 14).

Another paleoshoal may be present at shoal 3, which is partly shown in Figure 14, where another recent oolitic tidal bar is present. Thus, the cross section (Fig. 14) shows two areas of deposition of low energy muddy sediments sheltered between oolitic shallow water paleoshoals. These areas of muddy sediment appear to represent deposition in two low energy lagoons between the paleoshoals (Fig. 15).

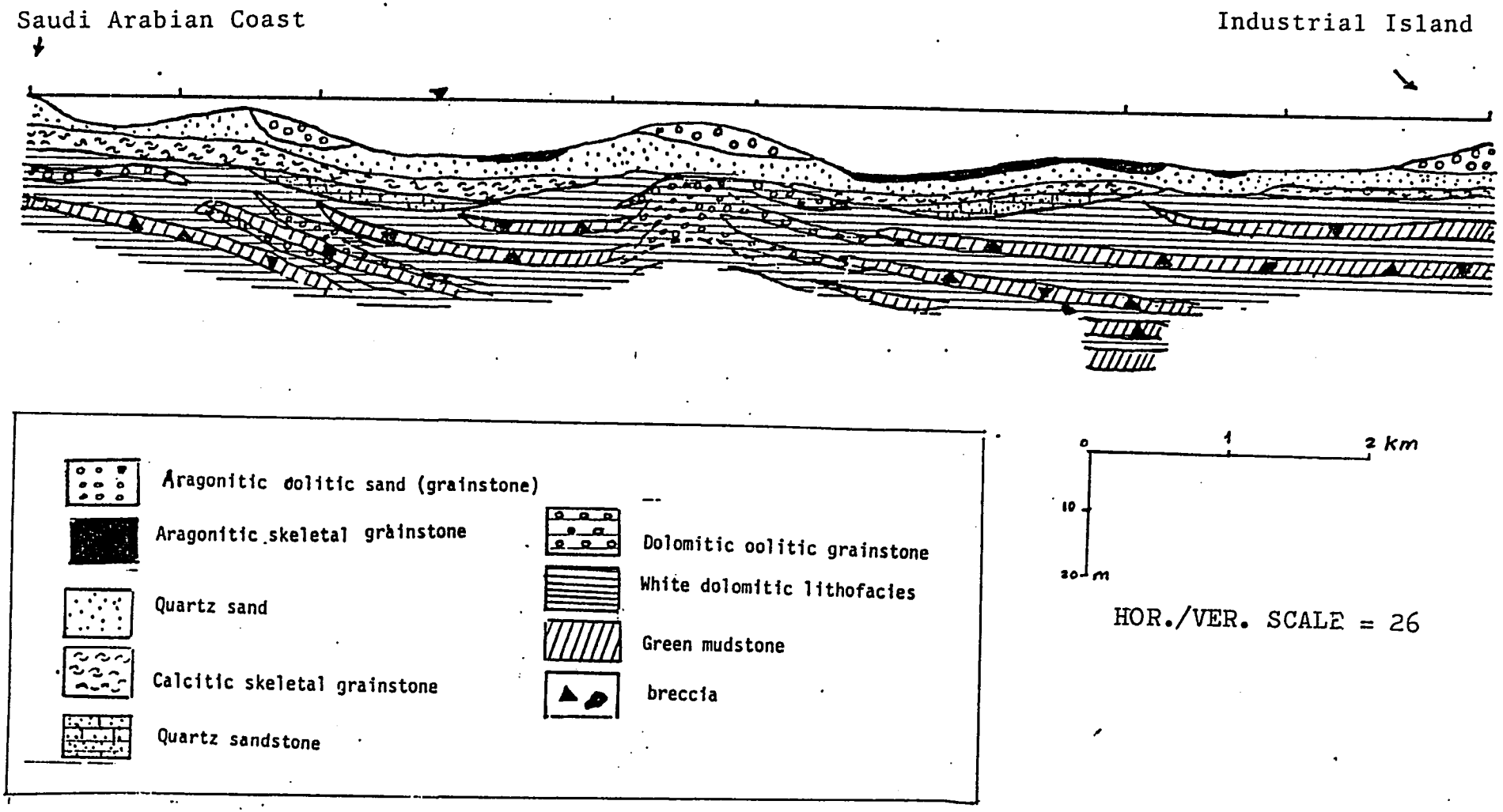

Fig. (15)- Generalized lithofacies cross section
(The same cross section in Fig. 14).

2. Depositional Model for dolomitic layers

Dolomitic rocks appear to represent cyclic, upward shallowing deposition starting generally with subtidal facies, represented by white dolomitic lithofacies, and culminating with extremely shallow to subaerial facies represented by green mudstone with thin breccia horizons. There are at least five upward shallowing cycles in the dolomitic rocks (Fig. 14). Ideal successive upward shallowing cycles, as seen in borehole 3/102, are shown in Figure 16.

A proposed depositional model has been diagrammatically shown in Figure 17. A coastal shallow lagoon was flooded by sea water during relatively high sea level in which a low energy open marine facies of skeletal packstone was deposited. At the same time, oolitic grainstone was deposited in adjoining locally elevated high energy paleoshoals. Later, the water in the lagoon became shallower as result of sediment accumulation, possibly by slight oscillatory lowering of sea level or possibly rising of the sedimentary basin in the study area, resulting in restriction of water circulation. This restriction resulted in the deposition of white skeletal wackestone/mudstone in a subtidal lagoonal environment. This lithofacies lacked

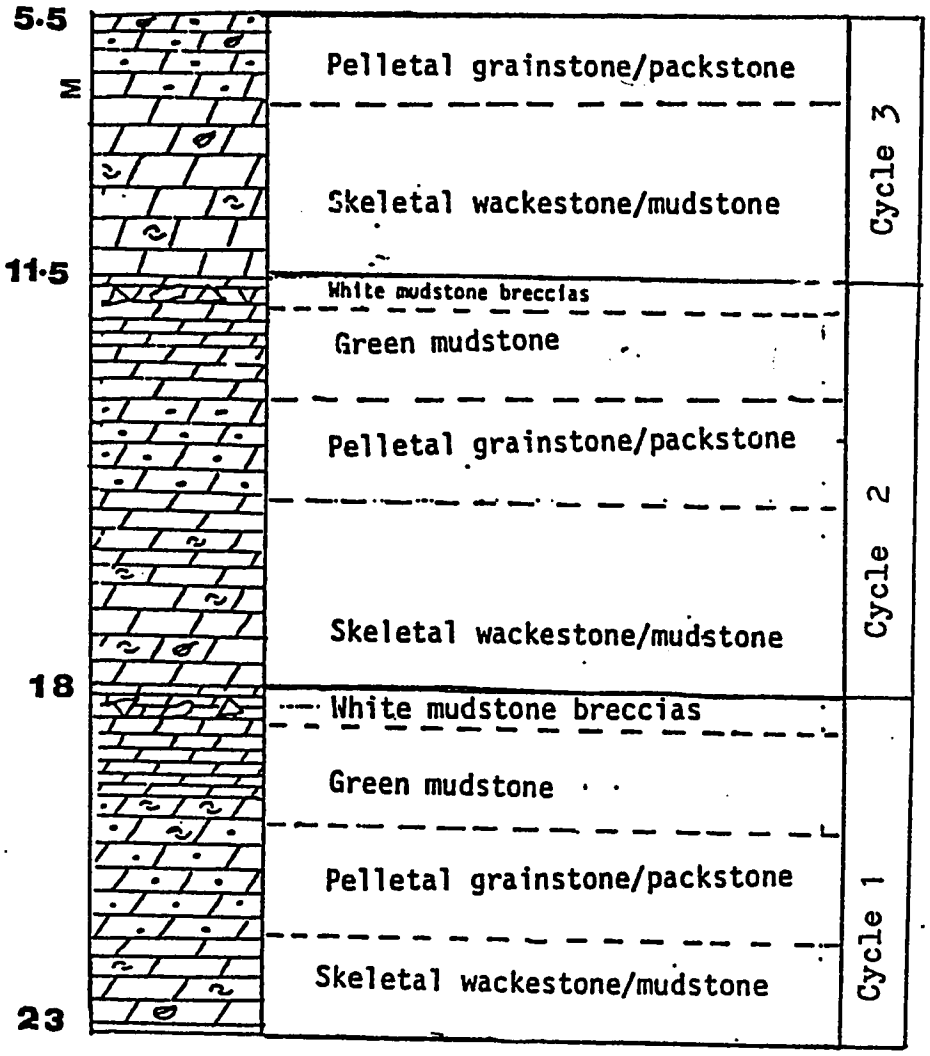

Fig.(16)- Three successive upward shallowing cycles in the dolomitic facies, borehole 3/102.

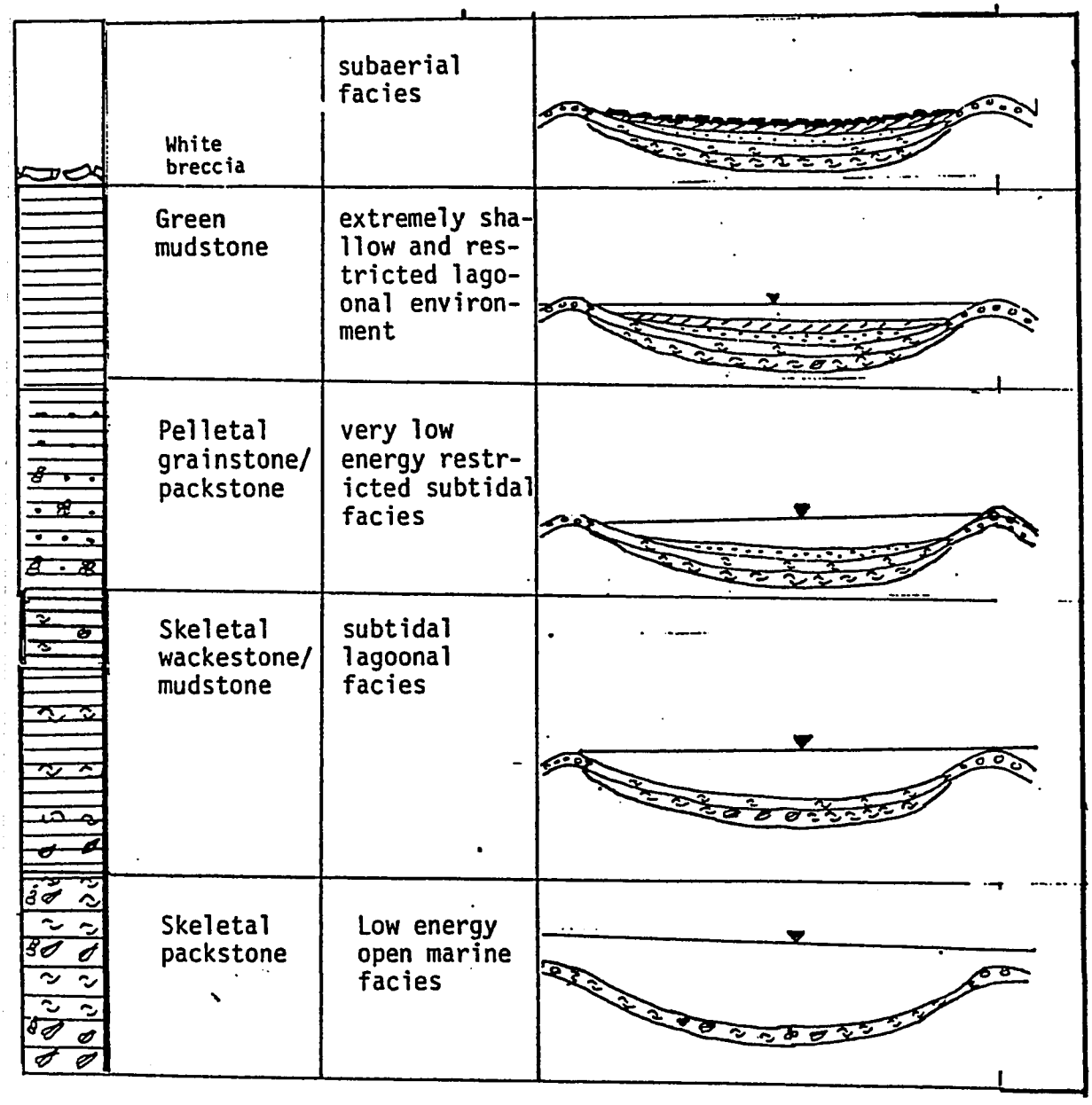

Fig.(17)- Diagram showing proposed idealized depositional model for the dolomitic lithofacies.

primary sedimentary structures due to homogenizing effect of burrowing organisms. As the lagoon shallowed further, circulation was diminished and restriction increased, resulting in deposition of pelletal grainston packstone, which requires a very quiet environment to be preserved. For this reason, both undistorted and distorted pellets are well preserved in the middle of the seaward lagoon between shoals 2 and 3 (Fig. 14), where a quiet, restricted environment prevailed . Continued accumulation of sediments, evaporation and/or possible slight lowering in sea level resulted in an extremely shallow and restricted environment with very limited water cirulation. Green mudstone, which lacks fossils, was deposited in this environment. Such conditions probably resulted in high salinity and a reducing environment causing the absence of fauna. The green color probably resulted from th presence of illite (Ehlers and Blatt, 1980, p. 287) and perhaps reduced iron. The slight increase in percentage of iron in the green mudstone horizons (Appendix D) may support the second possiblity.

Authigenic palygorskite in the green mudstone suggests an arid to semi-arid climate and formation in closed shallow basin (Weaver and Beck, 1977).

Several thin white mudstone breccia horizons, included in the green mudstone, represent periods of brief subaerial exposure and dessication (Fig. 8 in Shinn, 1984). The mud fragments were not well indurated and many were deformed to irregular and wispy fragments when rewetted.

A new rise in sea level, associated with possible rising of oolite paleoshoals, started each new depositional cycle. Not all lithofacies of the idealized cycle were present everywhere (Fig. 17). For example, no skeletal packstone was deposited in most of the depositional cycles of the seawar lagoon, and pelletal grainstone/packstone is not found in the shoreward lagoon. Skeletal packstone may also be deposited locally associated with oolitic shoals.

3. Lithostratigraphy of non-dolomitic layers

A discontinuous subhorizontal layer of quartz sandstone lies directly over the dolomitic lithofacies . The maximum thickness of this layer is 3 m. It is cemented by either microcrystalline calcite or dolomite. Dolomite-cemented quartz sandstone appeared only in borehole 3/44.3.

There is a calcitic skeletal grainstone layer overlying the sandstone. This layer is subhorizontal and continuous along the line of section from the shoreline to near

shoal 2, beyond which it becomes discontinuous (Fig. 14). Average thickness of this layer is 2.5 m and it thickens landwards to about 6 meters. The lower part of this layer includes some oolitic grains.

A thick, uncemented quartz sand sheet that directly overlies directly over the calcitic skeletal grainstone. It reaches 7 m in thickness and thins shoreward. This layer blankets all of the underlying rocks.

The surface sediments consist of discontinuouos aragonitic skeletal and oolitic sand. Several oolitic tidal sand bars are present in this area (Fig. 18). These bars, which attain maximum thickness of 4 m, locally overly the quartz sand, especially in shoals 2 and 3. Shoal 1 is mapped as an oolitic tidal sand bar by Loreau and Purser (1973) (Fig. 18). The oolitic sand includes some thin cemented beds (20 cm thick), especially in the upper meter. The aragonitic skeletal sand occurs in scattered patches up to 1.5 m thick. It contains some weakly lithified bands of skeletal grainstone interbedded with quartz sand.

4. Depositional environment of non-dolomitic layers

The quartz sandstone layer, which lies directly over dolomitic layers, represents a first episode of sand dune migration (Fig. 19).

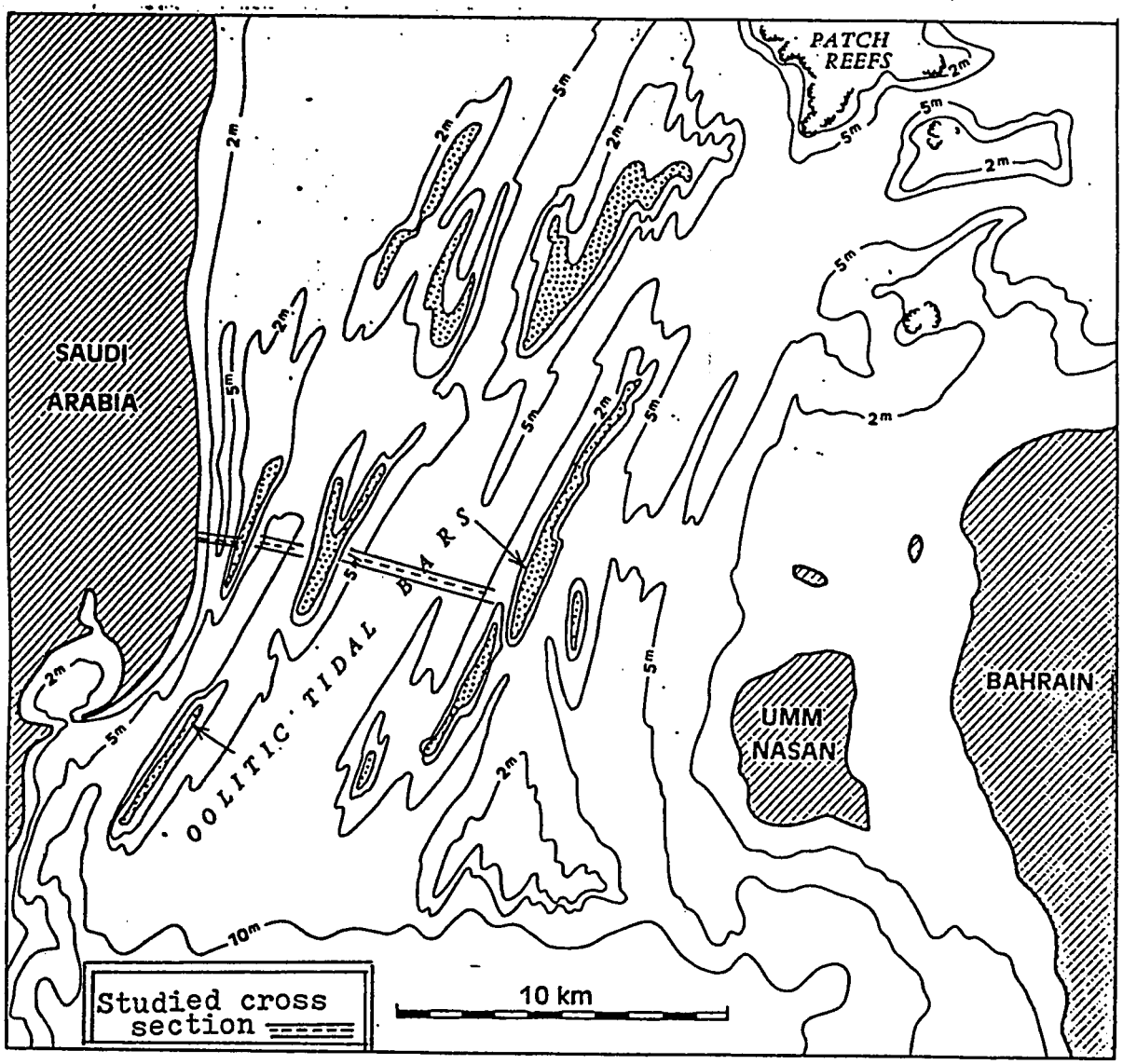

Fig.(18)- Map showing distribution of oolitic tidal bars between Bahrain island and coastal Saudi Arabia (After Loreau & Purser, 1973,Fig.7).

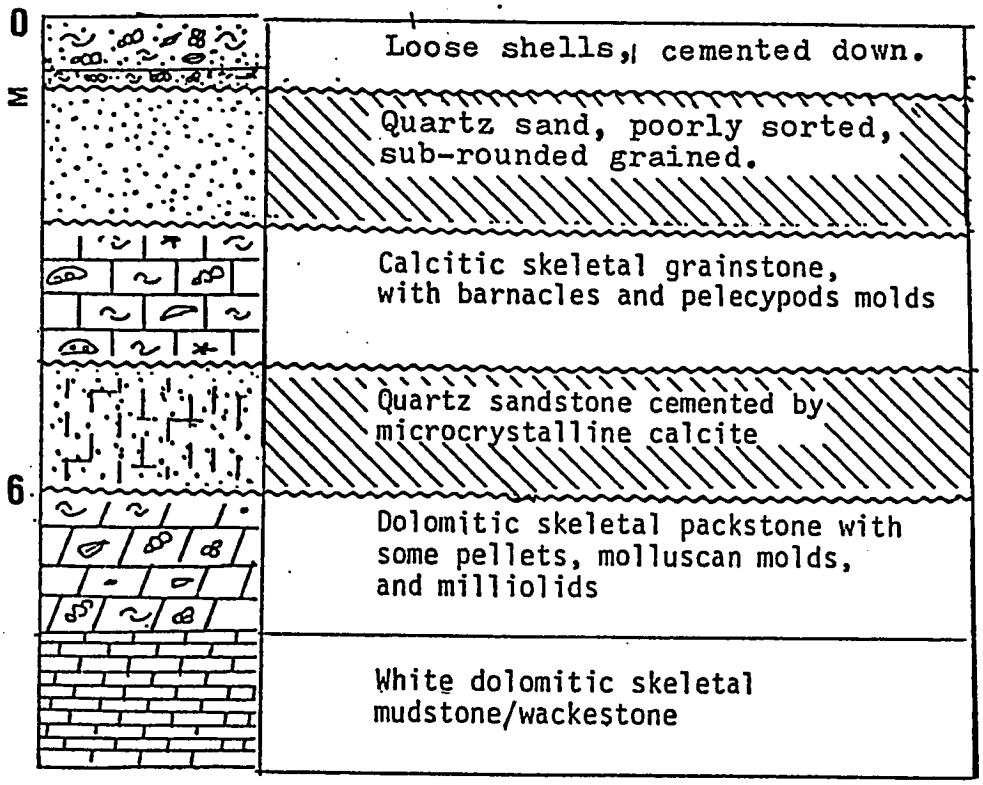

Fig. (19)- Stratigraphy of non-dolomitic lithofacies showing the two major subaerial exposures in the study area (Borehole # 3/32).

The calcitic skeletal grainstone lies directly over the quartz sandstone . This layer, which was originally aragonitic, was deposited in an open marine, high energy environment, as indicated by barnacles and oolitic grains. The calcium carbonate derived from leached aragonitic shells provided the cement for the underlying quartz sand.

There is a thick quartz sand sheet blanketing all the underlying rocks. This sheet is considered to represent aeolian sand dunes .

Aragonitic skeletal and oolitic sands, overlying quartz sand, represent present day sediments, deposited in a subtidal, high energy environment. Present water depths range from 2 to 10 m (Fig. 14).

5. *History of sea level changes in the study area*

In this discussion, I have related depositional facies and diagenetic changes to the sea level profile interpreted by Kassler (1973) (Fig. 20). My interpretations, (Fig. 19, 21, 22), is added to Kassler's Figure (Fig. 20).

All dolomitic lithofacies suggested a shallow water origin and were probably deposited at sea level slightly lower than that of today with several brief intermittent periods of subaerial exposure (Fig. 21, 22). These periods

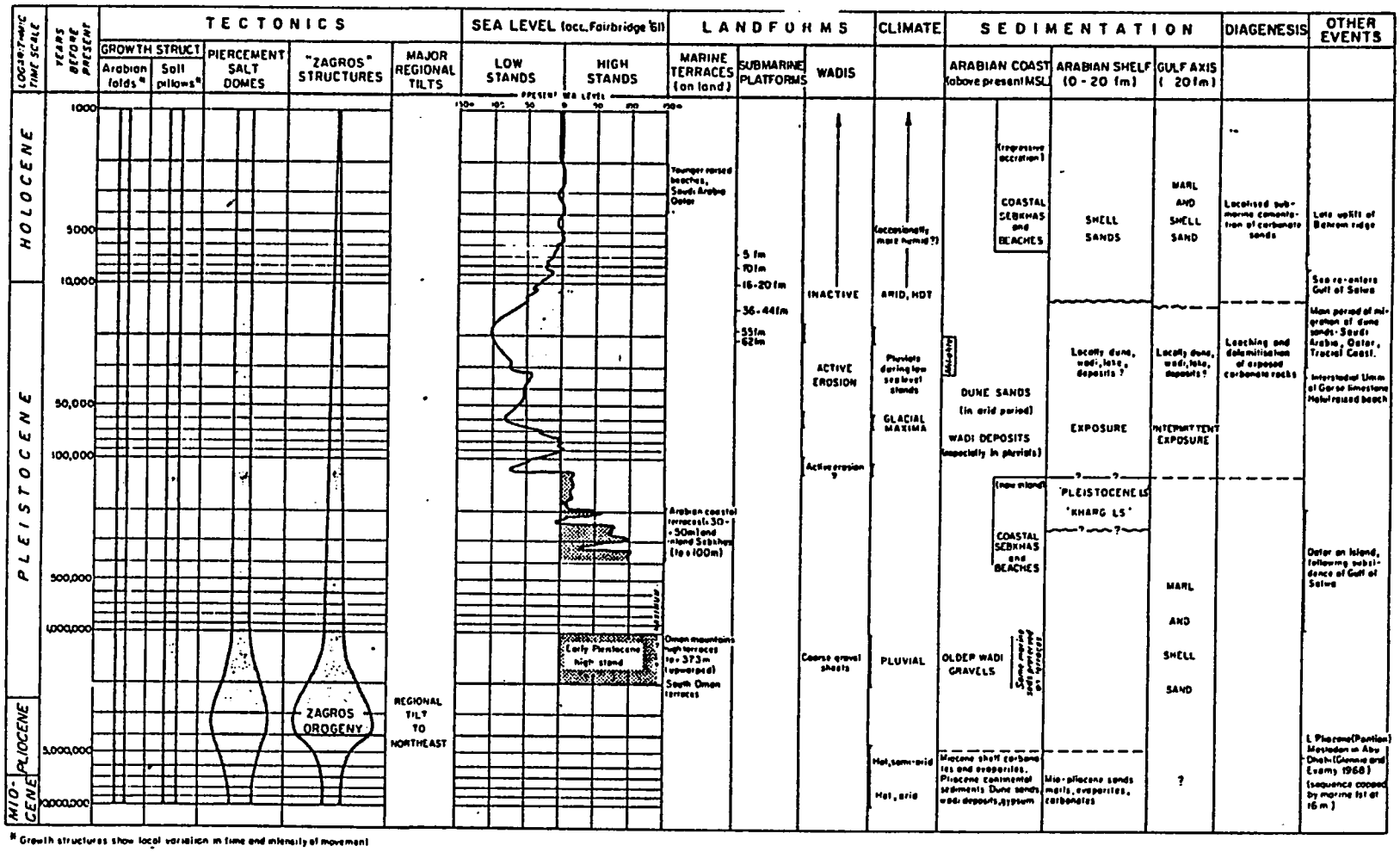

Fig.(20)- Generalized late Tertiary and Quaternary history of the Arabian Gulf and the Arabian coastal area (logarithmic time scale) (From Purser,1973.Fig.3).

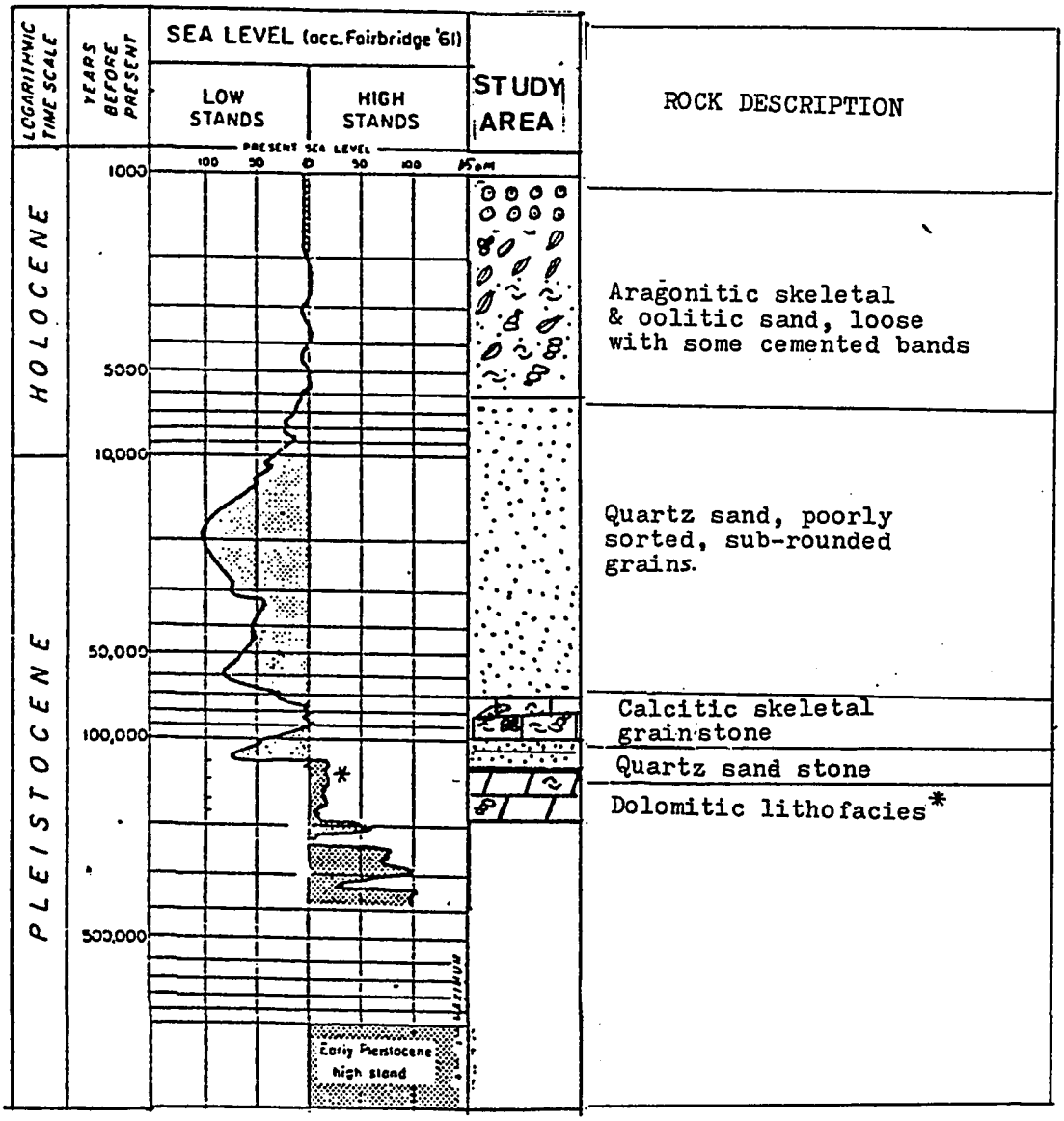

* Dolomitic lithofacies suggest a lower sea level stand than represented here (see fig. 22)

Fig. (21)- Relationship of stratigraphy in the study area to Holocene-Pleistocene sea level changes in the Arabian Gulf.

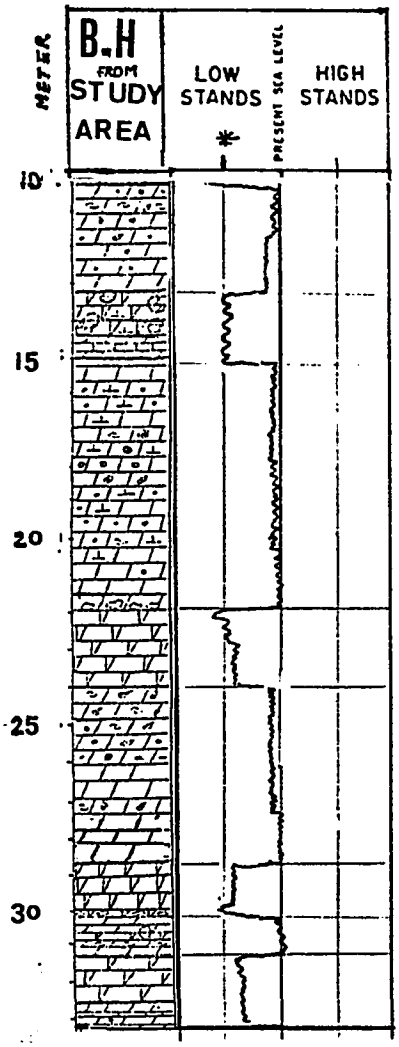

Fig.(22) - Sea level changes in dolomitic interval . The dolomitic breccia horizons represent only minor oscillations in sea level .

of subaerial exposure may represent minor lowering in sea level. As many as five minor oscillations in sea level were are indicated by th cyclical repetition of lithofacies. These depositional sequences were considered to represent sedimentation before the first Pleistocene regression, beginning at about 110,000 y.b.p. (Fig. 21).

Dolomitization probably occurred during and perhaps shortly after the time of deposition of dolomitized rocks due to the availability of high-Mg brines from the coastal sabkhas (150,000-110,000 y.b.p) (Kassler, 1973) (Fig. 20). The heavy brine refluxed through porous muddy sediments accumulating in the Gulf of Salwa.

The rock sequence above the dolomitic layers contains two quartz sand and sandstone layers separated by calcite skeletal grainstone. The lower quartz sandstone layer represents deposition of aeolian sand during the low stand of sea level, which corresponds to the brief Pleistocene regression (110,000-90,000 y.b.p) (Fig.21). In this period, the sea level was 70 m below present sea level (Kassler, 1973) and resulted in complete exposure of large areas of the Gulf, including the study area.

Calcitic skeletal grainstone, originally aragonitic, was deposited during the minor transgression between 90,000 and

70,000 y.b.p. (Fig. 21). This high sea level period was followed by the major late-Pleistocene regression (80,000-6000 y.b.p), that emptied the Gulf completely. During this subaerial period, aragonitic shells in the calcitic skeletal grainstone were leached by fresh water dissolution. Fresh water was available during several pluvial periods (Fig. 20). Cement in the underlying quartz sandstone was derived from these solutions.

The upper quartz sand sheet represents the main period of dune migration during major lowering of sea level that emptied the Arabian Gulf to -120 m below present sea level (Sarathein, 1972; Kassler, 1973). Thus, between 70,000 and 17,000 y.b.p., continental and arid conditions existed over most of the Arabian Gulf (Fig. 21).

Finally, the quartz sand sheet was followed by transgressive aragonitic skeletal and oolitic sand after the Holocene rise (Flandrian Transgression) to present sea level. This transgressive sea reached the -18 m level near Bahrain about 8,000 y.b.p. and entered the Gulf of Salwa to isolate the island of Bahrain at about -7.2 m level 6000 years ago (Doornkamp et.al, 1980). This sea level rise limited further migration of Saudi Arabian quartz sand and led to the initiation of extensive recent marine deposits, including aragonitic skeletal and oolitic sand.

CHAPTER VI

CONCLUSIONS AND RECOMMENDATIONS

1. Conclusions

- Pleistocene-Holocene sediment and rocks under King Fahd Causeway between Saudi Arabia and Bahrain consist of two mineralogical units:

  (1) An upper non-dolomitic interval, three to nine meters thick, of interbedded quartz sandstone, calcitic skeletal grainstone, quartz sand, and aragonitic skeletal and oolitic sand and grainstone.

  (2) A lower dolomite interval, as much as 40m thick, which comprises several shallowing upward cycles consisting of, from top to base:

  (a) Green mudstone with thin white mudstone breccia horizons.
  (b) Pelletal grainstone/packstone
  (c) Skeletal wackestone
  (d) Skeletal packstone

- These lithofacies represent upward shallowing cycles, which start with shallow open marine subtidal environment, shallowing progressively to extremely

shallow restricted lagoonal environment, with brief periods of subaerial expusure.

- The dolomite lithofacies appear to represent deposition in two shallow lagoons between recurring oolitic paleoshoals.

- Sediments of dolomite interval were deposited during late Pleistocene when sea level was lower than today (before 110,000 y.b.p).

- Dolomitization began soon after deposition.

- Dolomite was subsequently calcitized by calcium-rich fresh water.

- Discontinuous quartz sand was deposited during the subsequent brief low stand of sea level (110,000 y.b.p).

- Skeletal grainstone was deposited during later transgression (90,000 - 75,000 y.b.p).

- Next, entire Gulf was emptied during the major late Pleistocene regression. Rainfall during late Pleistocene pluvials supplied freshwater which caused:

  (1) Leaching of the aragonitic constituents from skeletal grainstone and the precipitation of calcite cement.

  (2) Supplying carbonate cement for underlying sand.

  (3) Supplying fresh water for calcitization of deeper dolomite horizon.

- A blanket of dune sand accumulated in coastal Arabia, including the studied area, during an arid period.

- Aragonitic oolitic and skeletal sand (grainstone) were deposited durin the Flandrian transgression, when the Gulf of Salwa was flooded (6000 y.b.p).

2. Recommendations for further studies

(a) Detailed study of diagenetic changes in the rock with depth.

(b) Completing the study by matching the studied sediments with the Bahrain side sediments.

(c) Clay mineralogy studies and relating that to paleoclimate.

(d) Carrying out oxygen isotope study and relating that to sea level changes.

APPENDICES

APPENDIX A

GEOLOGICAL PROFILES FOR THE STUDIED BOREHOLES

(Location map in Figure 5)

EXPLANATION

MINERALS


Dolomite


Calcite


Calcitic dolomite


Halite


Quartz sand


Clay minerals


Gypsum

TEXTURES


oolite


Skeletal grainstone/packstone


Dolomitic skeletal wackestone


Dolomitic mudstone


Pelletal grainstone/packstone


Molluscs-Bivalves


Gastropods


Benthonic foram.


Barnacles


Undefined fossil


Echinoids

Legend for the textural and mineralogical symbols, which were used in this study.

Qualitative description of borehole # 1/1

LOG	COLOR	ROCK DESCRIPTION	MINERAL CONT (XRD)	TEXTURE (DUNHAM 62)	MAIN FOSSILS TYPES: FOSSIL CONTENT	PELECYPODS	GASTROPODS	BENTH. F
				M W P G	L M H	L M H	L M H	L M
	Grey to light grey	Loose, skeletal, quartz sand mainly molluscan shells. Loose, fine to med. quartz sand with about 10% quartz silt.						
	Light grey	Loose shelly quartz sand with about 10-20% fine calcite (clay & silt size).						
	Milky white	Calcitic skeletal grainst--one, mainly molluscan molds and barnacles with some benthonic forams (milliolid & peneroplids). It is oolit--ic in the lower part.						
	Pale yellow	Dolomitic wackestone/mud--stone, slightly skeletal. Dolomitic skeletal grainst--one/packstone, mainly moll--uscan molds and forams.						
	Pale yellow to light green--ish white	Dolomitic wackestone/mud--stone, with scattered skeletal molds (mull. & fora--minefera)						
	Creamy white	Dolomitic skeoolitic grain--stone with some skeletal molds.						
	Pale yellow	Dolomitic mudstone, fossils are rare.						
	Pale green to grey	Dolomitic green mudstone with some gravel size white rock fragment.						
	Grey	Dolomitic oolitic grainsto:						
	Off-white	Dolomitic mudstone, slight--ly skeletal.						
	Pale yellow	Dolomitic skeletal grainsto--one/packstone, maily pelecypods.						
	Off-white	Dolomitic wackestone/mudst--one						

* Compared to the total fossil content

Figure A1 . Geological profile of borehole number 1/

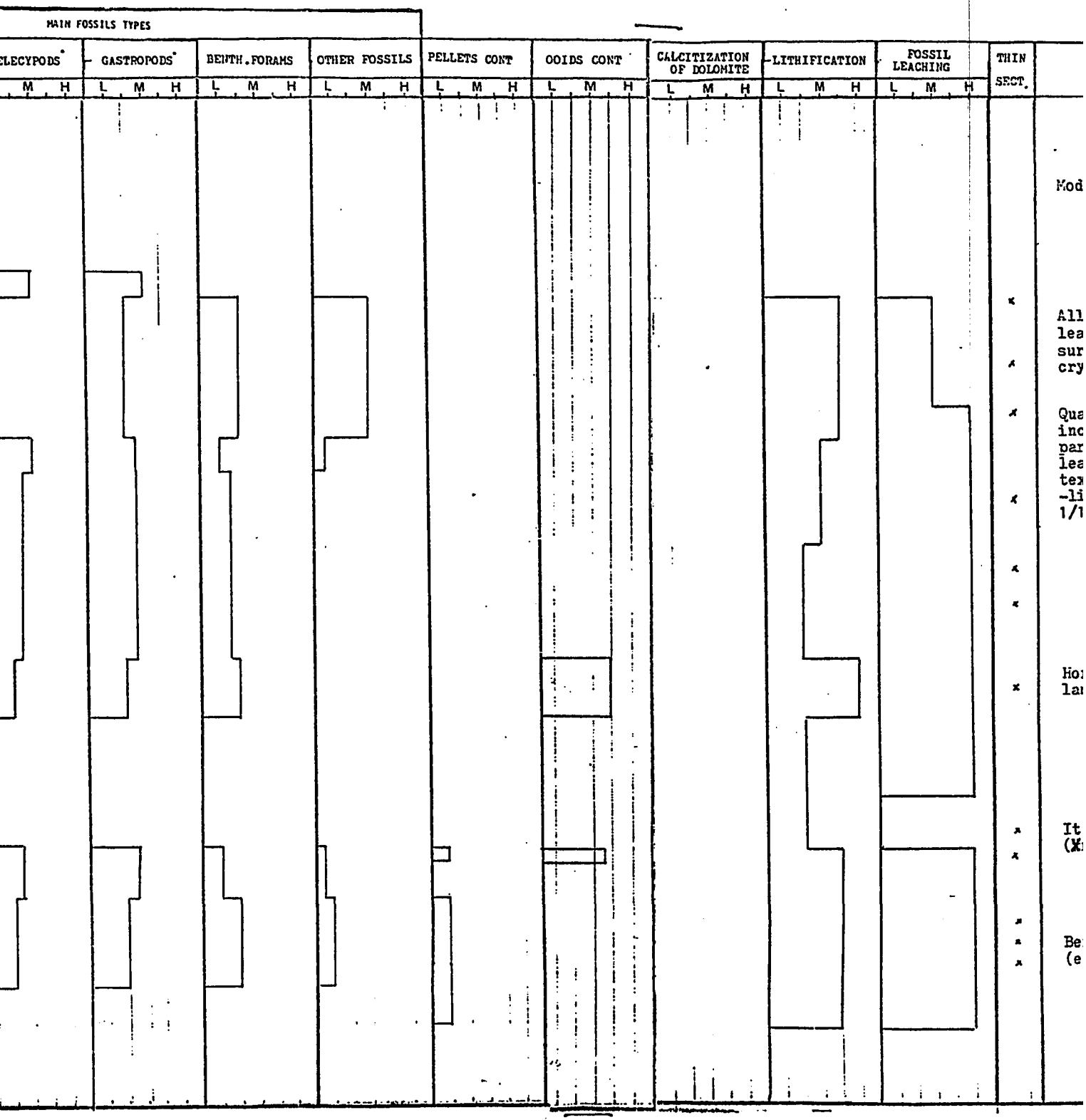

f borehole number 1/1 .

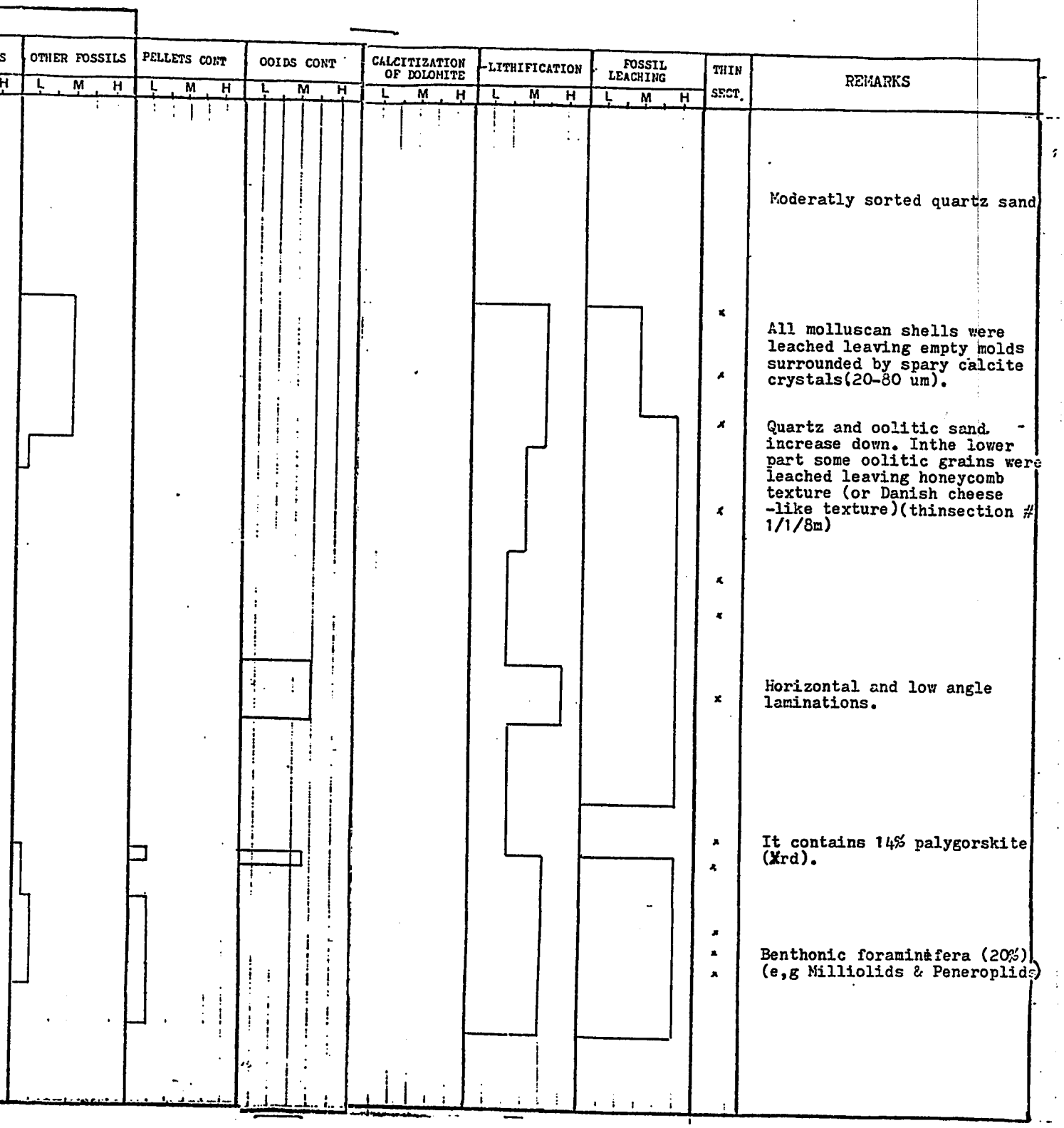

S	OTHER FOSSILS	PELLETS CONT	OOIDS CONT	CALCITIZATION OF DOLOMITE	LITHIFICATION	FOSSIL LEACHING	THIN SECT.	REMARKS
H	L M H	L M H	L M H	L M H	L M H	L M H		
								Moderatly sorted quartz sand
							x	All molluscan shells were leached leaving empty molds surrounded by spary calcite crystals(20-80 um).
							x	Quartz and oolitic sand. - increase down. Inthe lower part some oolitic grains were leached leaving honeycomb texture (or Danish cheese -like texture)(thinsection # 1/1/8m)
							x	
							x	
							x	Horizontal and low angle laminations.
							x	It contains 14% palygorskite (Xrd).
							x	
							x	Benthonic foraminifera (20%) (e,g Milliolids & Peneroplids)
							x	

BORE 1/7

LOG	COLOR	ROCK DESCRIPTION
	Brown	Quartz sand, poorly sorted, sub-rounded
	Yellowish white	Calcitic skeletal grainstone, with 10-20 % sub-rounded quartz sand. Fossils are mainly molluscan (gast. & pelecy.), benthonic forams and barnacles, with scattered oolitic grains increase down. There is 15 cm long borrower with 2cm in diameter.
	Yellowish white	Dolomitic mudstone, containing 10 cm of green mudstone (between 7.3 & 7.4)
	Pale yellow	Dolomitic skeletal packstone, mainly molluscan molds (casts), with some oolitic grains scattered in the lower part.
	Pale yellowish white	Dolomitic oolitic packstone, becomes pe -lletal in the lower part (Oolite ≈ 500 μm pellet ≈ 150 μm)
	Pale yellow	Dol. mudstone, slightly skeletal.
	Pale green	Dol. green mudstone, with at least 10% clay minerals (mainly palygorskite WIth some illite). There is a thin band of white mudstone fragments in green muds. -stone groundmass.
	Off-white	
	Light grey	Dol. skeletal packstone, mainly mollusc -an molds and benthonic forams.
	Light grey	Dol. skeletal wackestone, with some moll -uscan molds.

Figure A2 . Geological profile of borehole number 1/7.

BORE 1/20

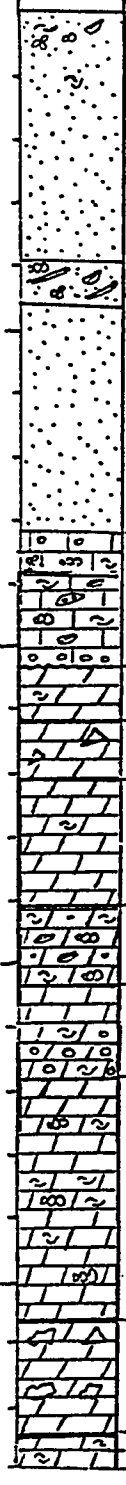

COLOR	ROCK DESCRIPTION
Light grey	Quarts sand, poorly sorted with at least 20 % quartz silt & clay, skeletal in the upper 20cm
Light grey	Loose shells, mainly mollusca.
Brown	Quartz sand, poorly sorted, sub-rounded.
Creamy white	Calcitic skeletal grainstone, mainly molluscan molds and barnacles. There are poorly develope -ed oolitic grains in the upper and lower part
Pale yellow	Dolomitic mudstone, slightly skeletal.
Pale green/grey	Dol. green/grey mudstone with gravel size white mudstone fragments.
Off-white	Dolomitic mudstone, slightly skeletal.
Off-white	Dolomitic skeletal packstone, mainly gastropod with some pellets.
Greyish white to off-white	Dolomitic oolitic packstone, with some skeletal molds(mainly mollusca).
Off-white	Dolomitic skeletal wackestone with thin band. of skeletal packstone at 18.5 m.
Greenish grey	Dolomitic green mudstone with some white mud- -stone fragments(.5 cm- 3 cm).
Off-white	Dolomitic wackestone/mudstone, slightly skeletal

Figure A3 . Geological profile of borehole number 1/20 .

BORE 2/16

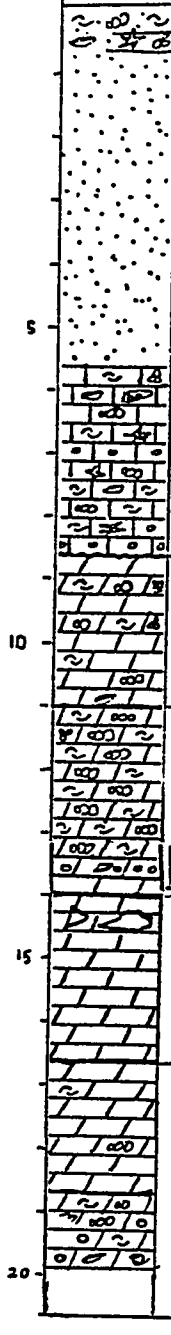

LOG	COLOR	ROCK DESCRIPTION
	Brown	Loose, gravel and sand size shells, mainly mollusca & benthonic forams. There is a 30 cm aragonitic skeletal grainstone band.
	Yellow-pale brown	Quartz sand, poorly to mod. sorted, sub-rounded. No fossils.
	Pale yellow to yellowish white	Calcitic skeletal grainstone, mainly molluscan molds, benthonic forams & barnacles, with 10-20% coarse quartz sand. There is ocasional thin oolitic bands especially in the lower part.
	Off-white	Dolomitic skeletal wackestone, with some skeletal packstone bands.
	Off-white to geeyish white	Dolomitic skeletal packstone, mainly molluscan molds & benthonic forams. Thin oolitic band in the base.
	Pale green & off-white	Dolomitic green mudstone with off-white dolomitic mudstone fragments in the upper parts(gravel size).
	Off-white with some creamy white spots.	Dolomitic skeletal wackestone (moll.) It shows some mottling in colors, creamy white spots in off-white ground -mass.
	Off-white	Dolomitic skeletal packstone, mainly molluscan molds, abandance of solusion cavities (.5cm), with some oolitic grains in the base.

Figure A5 . Geological profile of borehole number 2/16 .

Qualitative description of borehole # 3/1

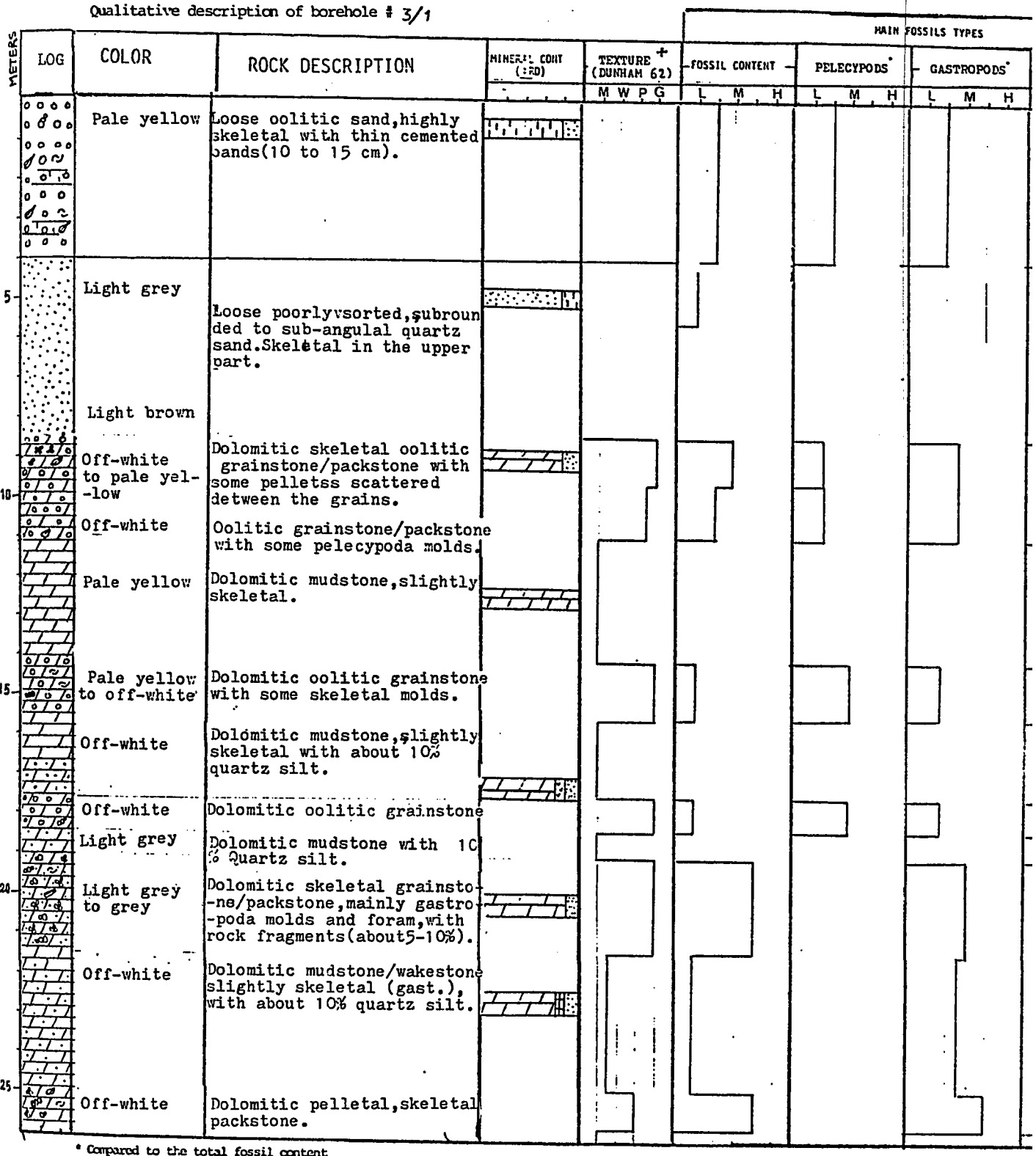

* Compared to the total fossil content
+ See Chapter III , Introduction .

Figure A6 . Geological profile of borehole number 3/1 .

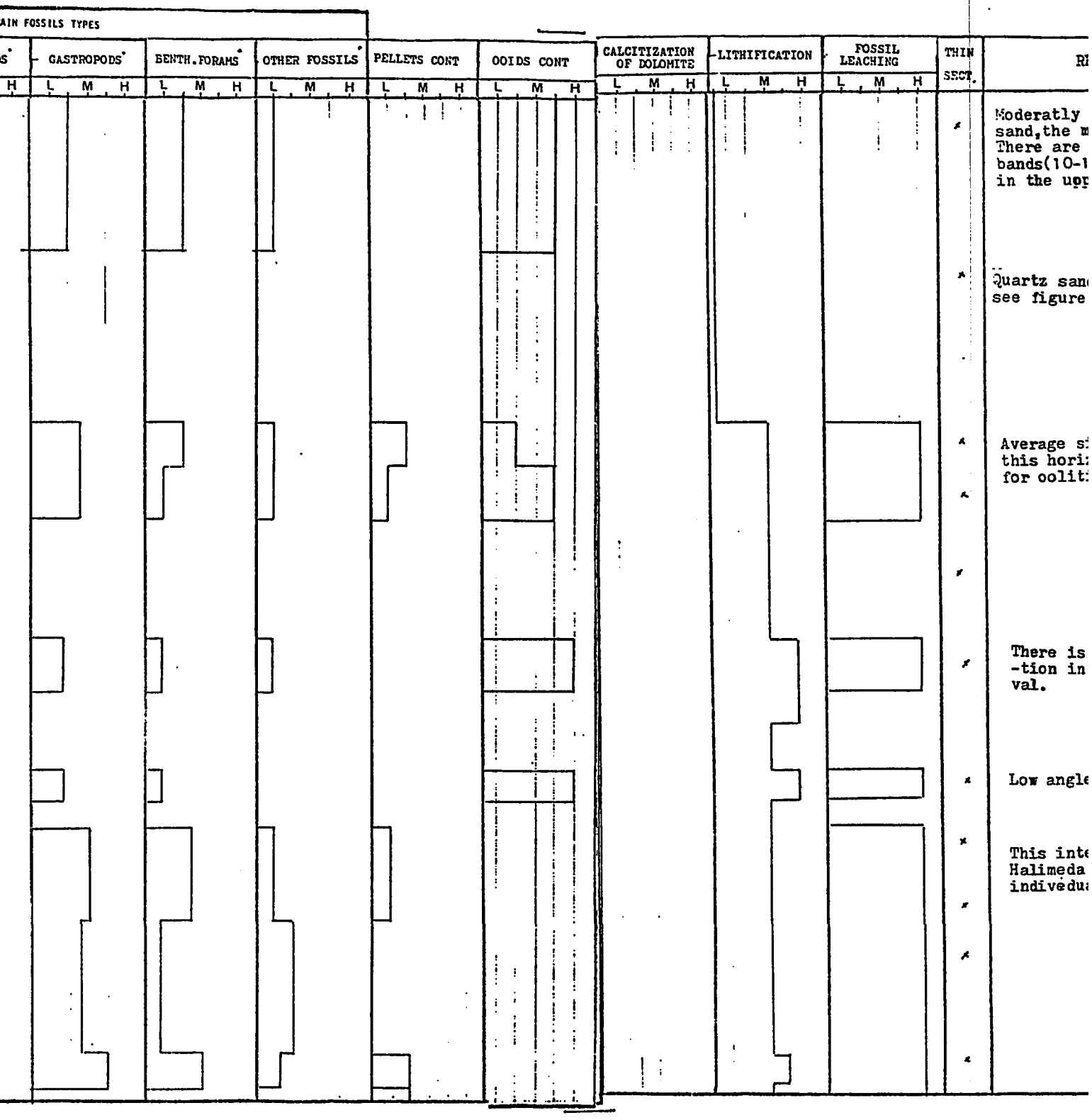
AIN FOSSILS TYPES
GASTROPODS
BENTH.FORAMS
OTHER FOSSILS
PELLETS CONT
OOIDS CONT
CALCITIZATION OF DOLOMITE
LITHIFICATION
FOSSIL LEACHING
THIN SECT.
L M H
Moderatly sand,the m There are bands(10-1 in the upp
Quartz san see figure
Average si this hori: for oolit:
There is -tion in val.
Low angle
This inte Halimeda indivedua

ıber 3/1 .

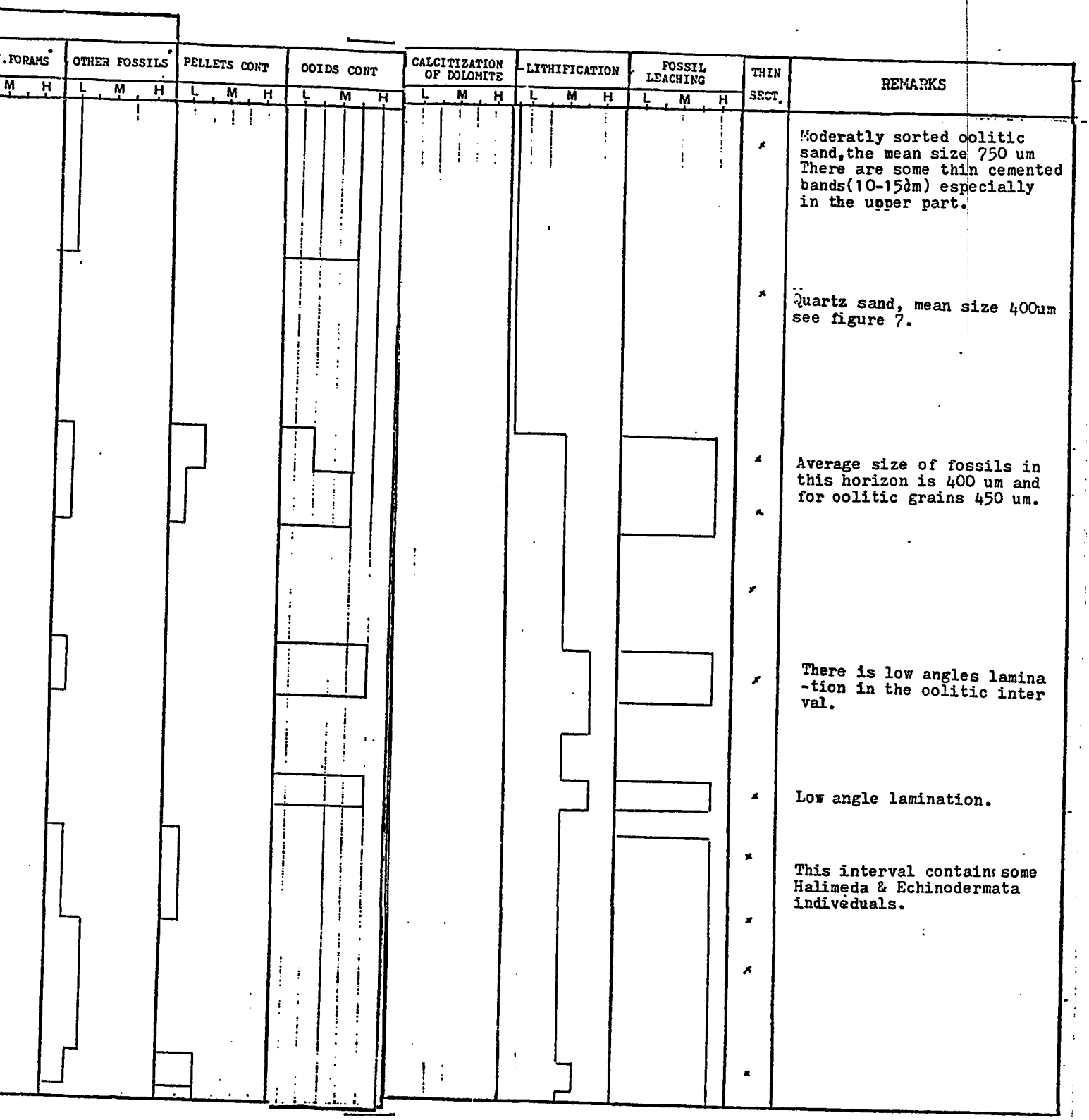

.FORAMS L M H	OTHER FOSSILS L M H	PELLETS CONT L M H	OOIDS CONT L M H	CALCITIZATION OF DOLOMITE L M H	LITHIFICATION L M H	FOSSIL LEACHING L M H	THIN SECT.	REMARKS
							x	Moderatly sorted oolitic sand, the mean size 750 um There are some thin cemented bands(10-15cm) especially in the upper part.
							x	Quartz sand, mean size 400um see figure 7.
							x	Average size of fossils in this horizon is 400 um and for oolitic grains 450 um.
							x	
							x	There is low angles lamina -tion in the oolitic inter val.
							x	Low angle lamination.
							x	This interval contains some Halimeda & Echinodermata indivéduals.
							x	
							x	
							x	

BORE 3/32

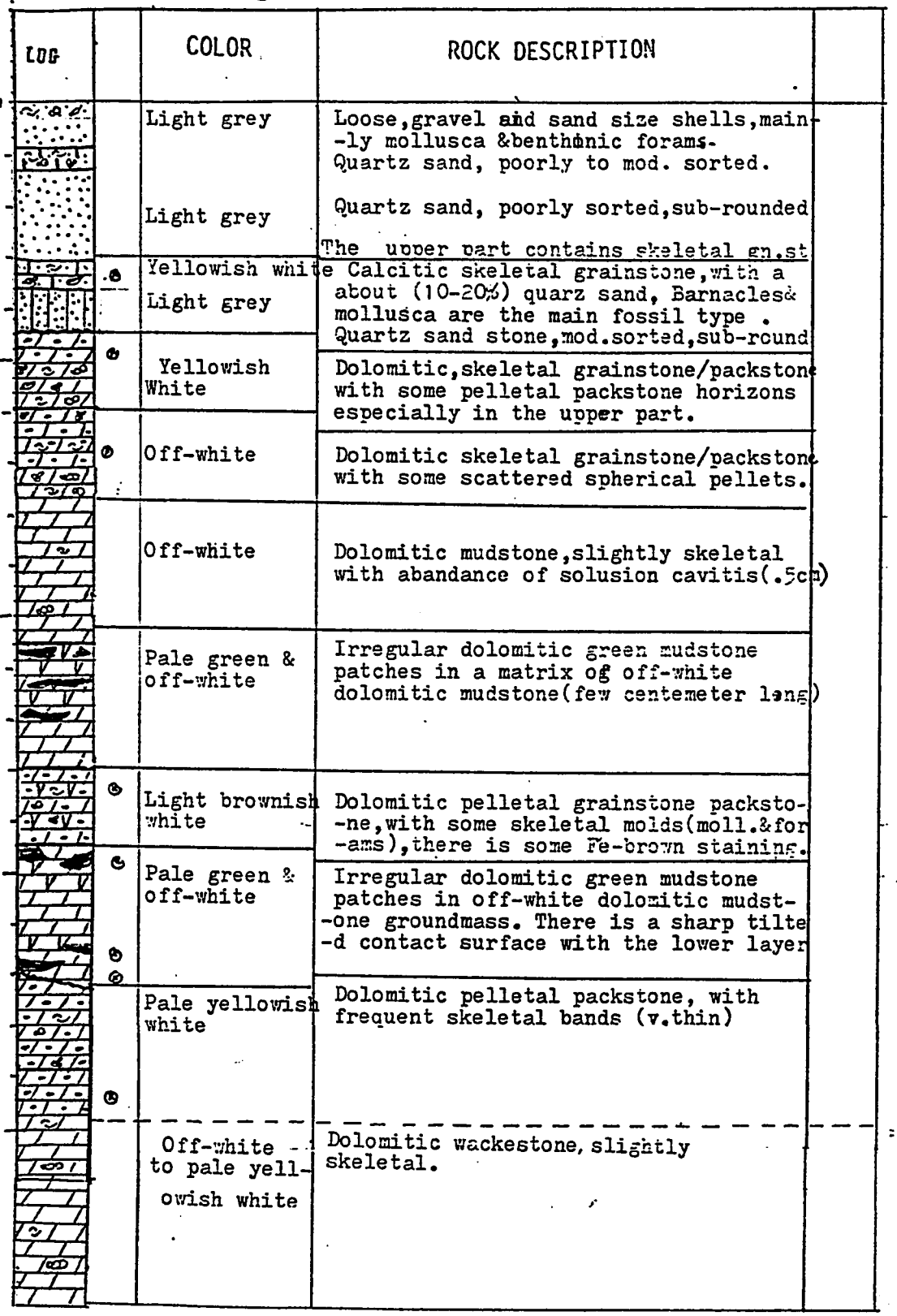

Figure A7 . Geological profile of borehole number 3/32 .

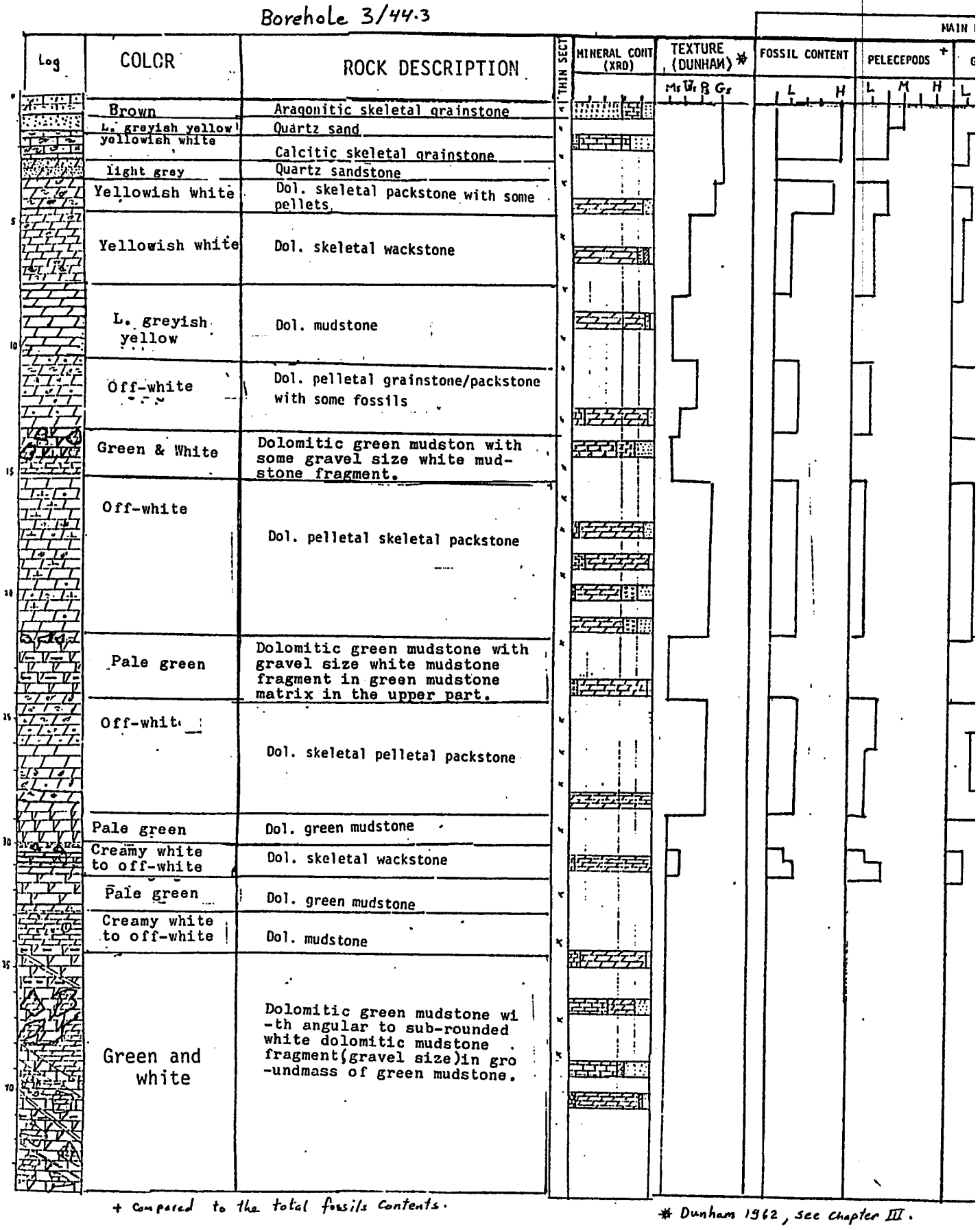

Figure A8 . Geological profile of borehole number 3/44.3 .

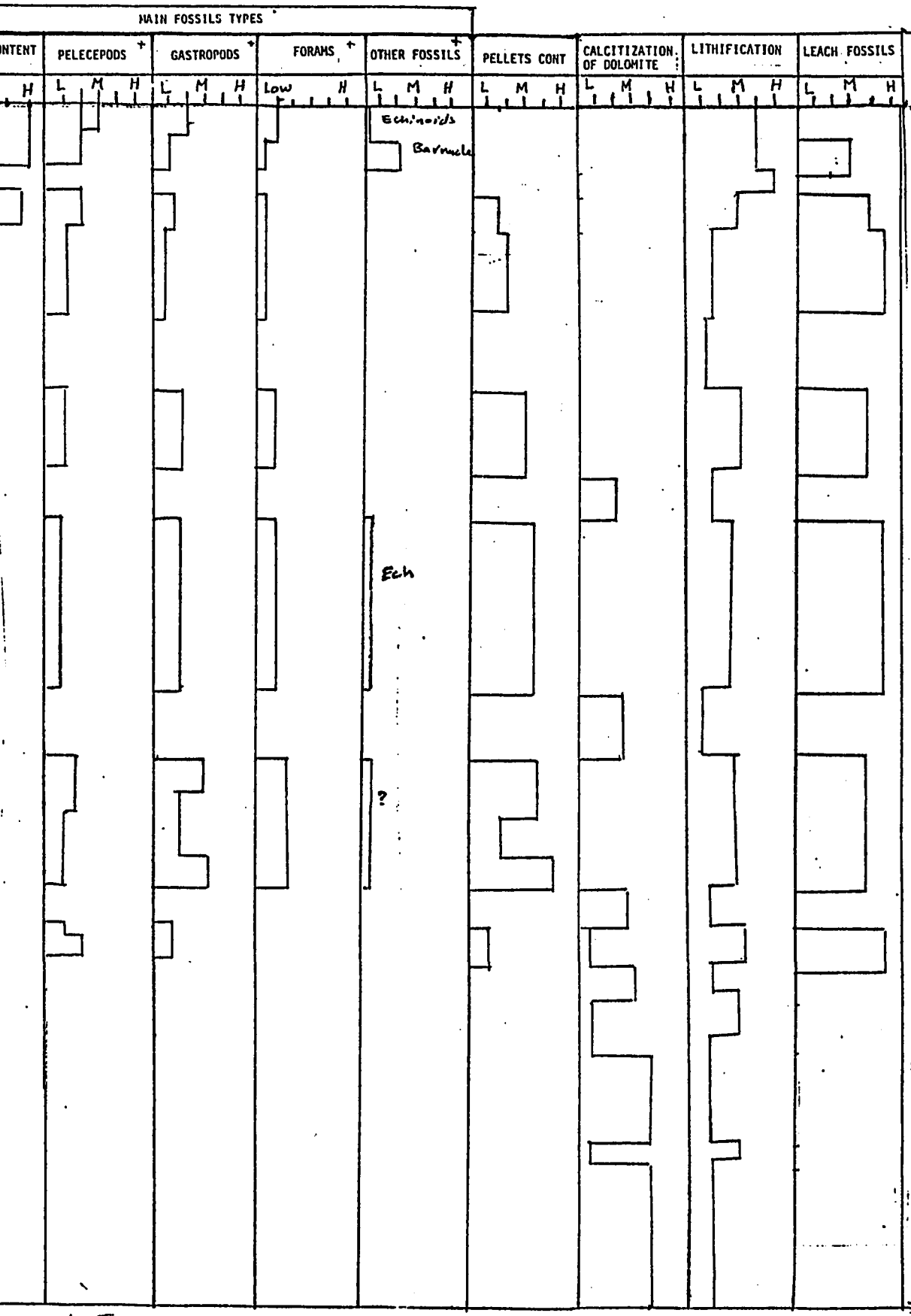

REMARKS

0.5–1.5 m
Poorly sorted, sub
to sub-rounded qu
No structural fea
clear.

13 m – 15 m
Scattered Fe-sta

In this horizon,
at least 3 brecc
Each band contai
to sub-angular wh
-tic mudstone in
stone matrix.

24-24.5 m
There is a brecc
in the upper par

37 – 44 m
There are at lea
paralleled 40-50°
in the core fill
green mudstone.
In all the dolom
mudstone horizon
small amount of
-ls .The fibrous
-ure could be ss
photographs, but
-icult to detect
of clay minerals
XRD procedure.

See Chapter III.

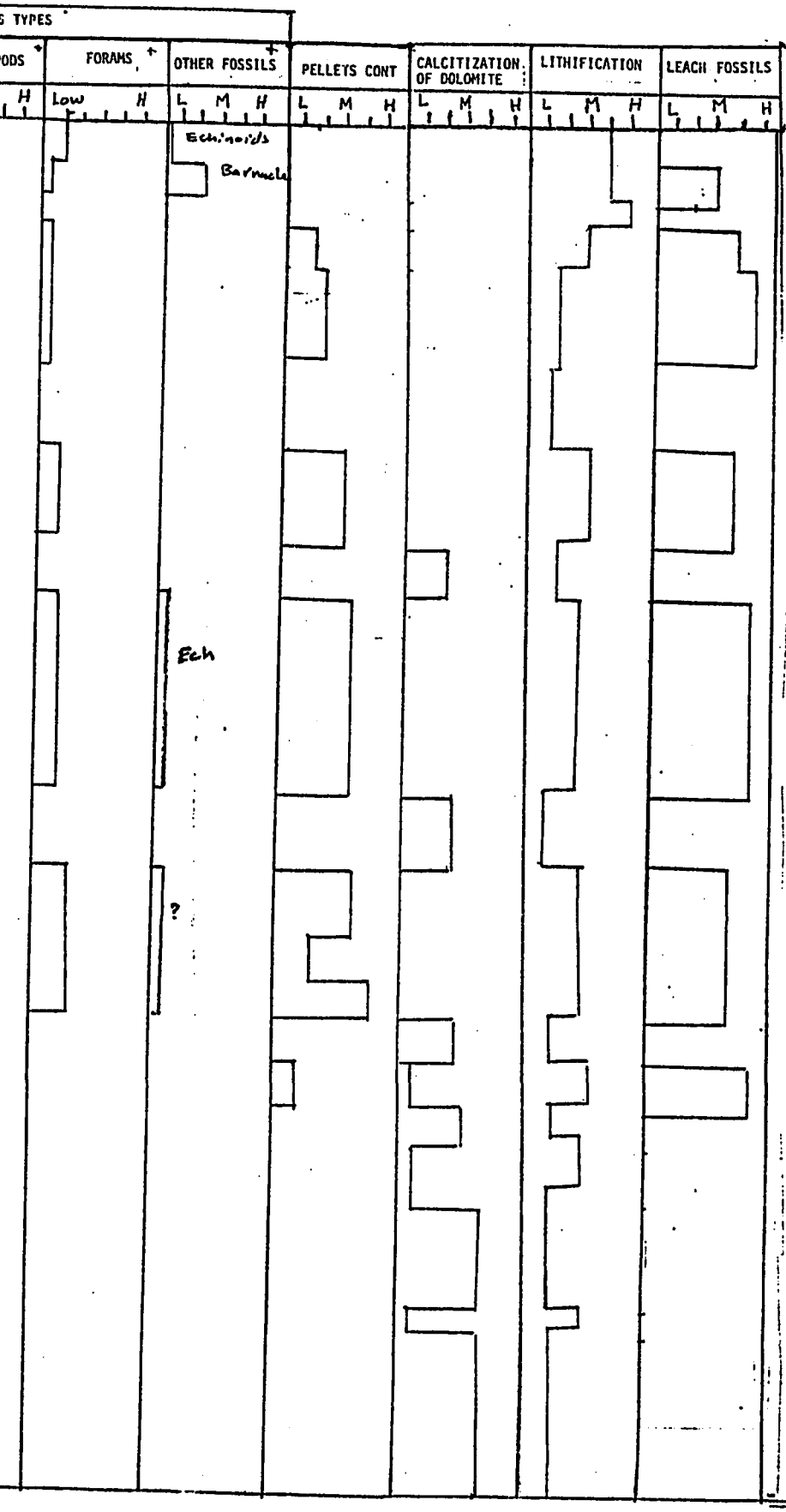

REMARKS

0.5–1.5 m
Poorly sorted, sub-angular to sub-rounded quartz sand. No structural features are clear.

13 m–15 m
Scattered Fe-staining, brown

In this horizon, there are at least 3 breccia bands Each band contains angular to sub-angular white dolomi-tic mudstone in green mud-stone matrix.

24–24.5 m
There is a breccia horizon in the upper part.

37 – 44 m
There are at least 3 paralleled 40-50° fractures in the core filled with green mudstone.
In all the dolomitic green mudstone horizons, there is small amount of clay minera-ls .The fibrous clay textu-ure could be seen in SEM photographs, but it is diff-icult to detect the type of clay minerals by normal XRD procedure.

BORE 3/91

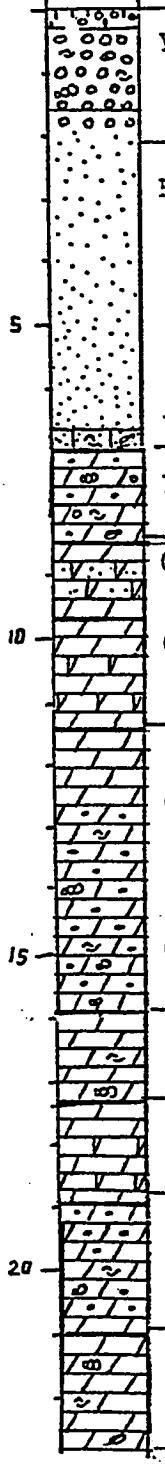

LOG	COLOR	ROCK DESCRIPTION
	Yellowish white	Aragonitic oolitic sand, skeletal, highly polished, mod. sorted sand .There are some thin cemented bands in upper part.
	Brown	Poorly sorted quartz sand, sub-rounded to sub-angular grains.
	Yellowish brown	Calcitic skeletal grainstone,with qz.
	Yellowish white	Dolomitic, skeletal, pelletal grainstone mainly spherical pellets And moll. molds
	Olive green Greenish yellow	Dolomitic green mudstone with (≃10%) calcite crystals (300-400 um) XRD analysis show small percent of clay minerals mainly palygorskite and illite (according to SEM photographs).
	Off-white	Dolomitic mudstone slightly skeletal
	Off-white	Dolomitic pelletal packstone, with some molluscan molds & benthonic foraminefri-ds.
	Off-white	Dolomitic wackestone/mudstone slightly skeletal(mainly molluscan molds).
	Pale green	Dolomitic green mudstone with at least 10% calcite crystals (300 um).
	Off-white	Dolomitic pelletal grainstone/packstone with some rode- like pellets (200um) There is some intraclastic grains.
	Off-white	Dolomitic wackestone/mudstone,slightly skeletal.

Figure A9 . Geological profile of borehole number 3/91 .

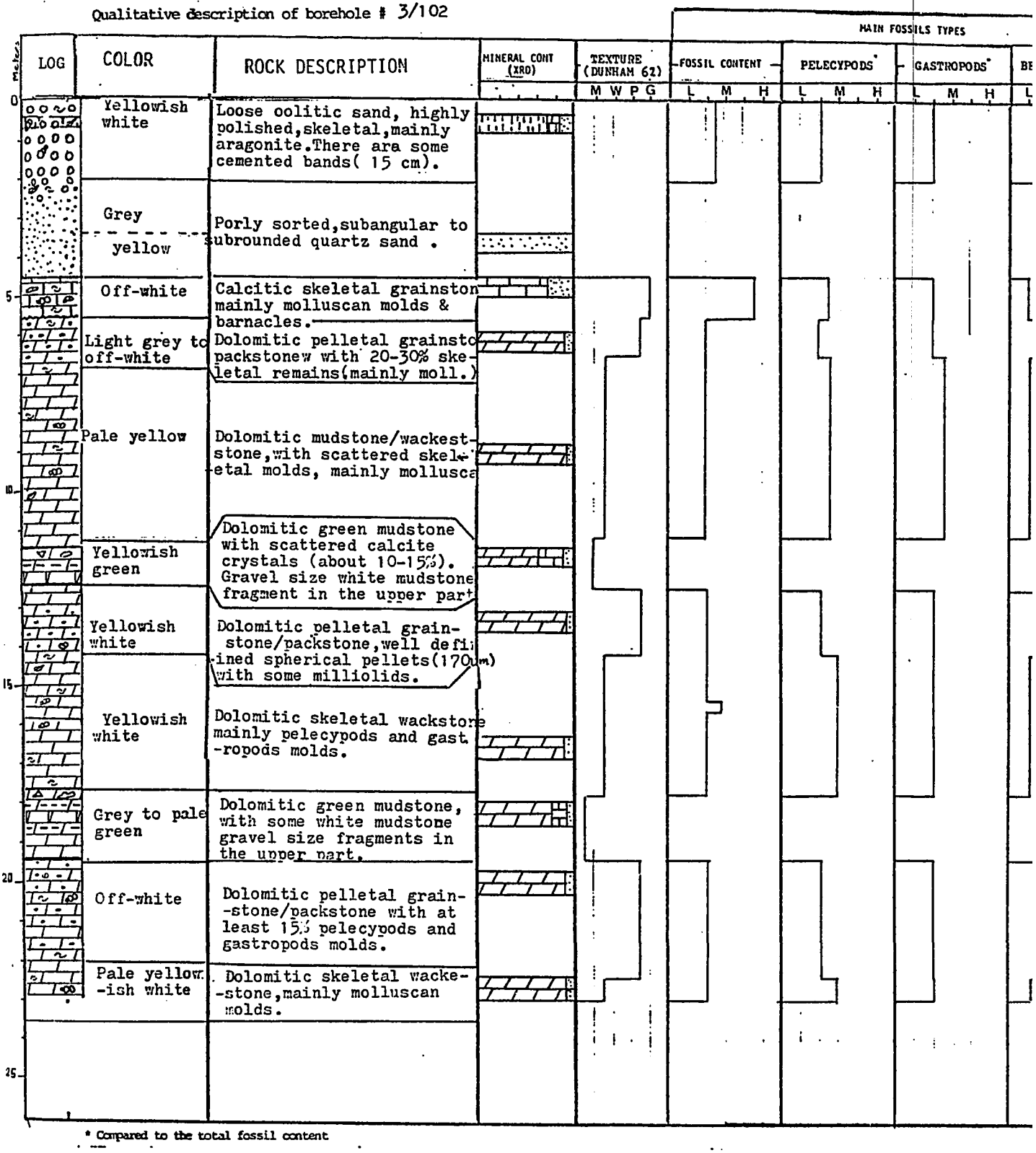

Figure A10 . Geological profile of borehole number 3/102 .

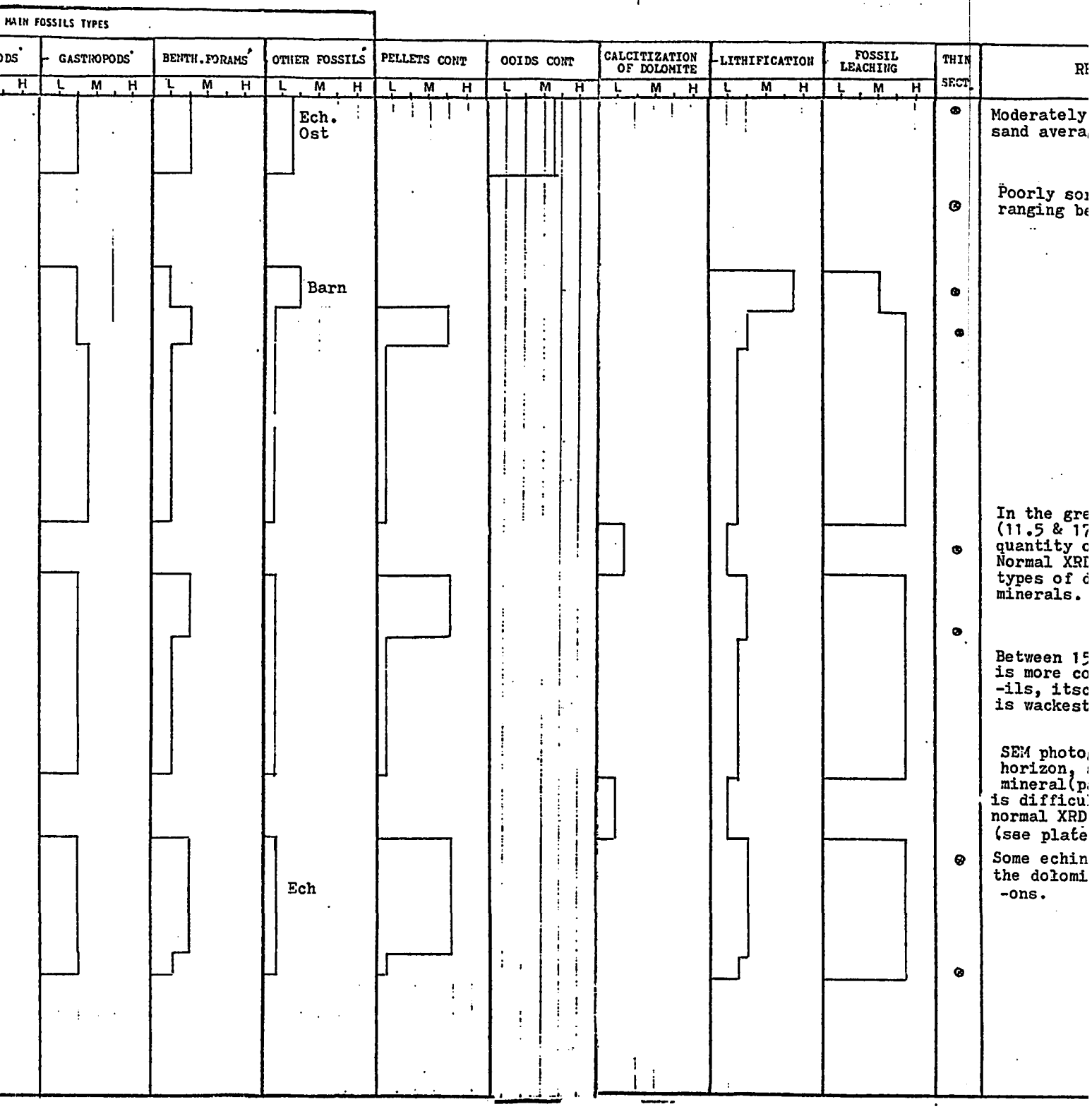

Moderately
sand avera

Poorly so
ranging be

In the gre
(11.5 & 17
quantity c
Normal XRI
types of c
minerals.

Between 15
is more co
-ils, itsc
is wackest

SEM photo
horizon,
mineral(p
is difficu
normal XRD
(see plate

Some echin
the dolomi
-ons.

ber 3/102 .

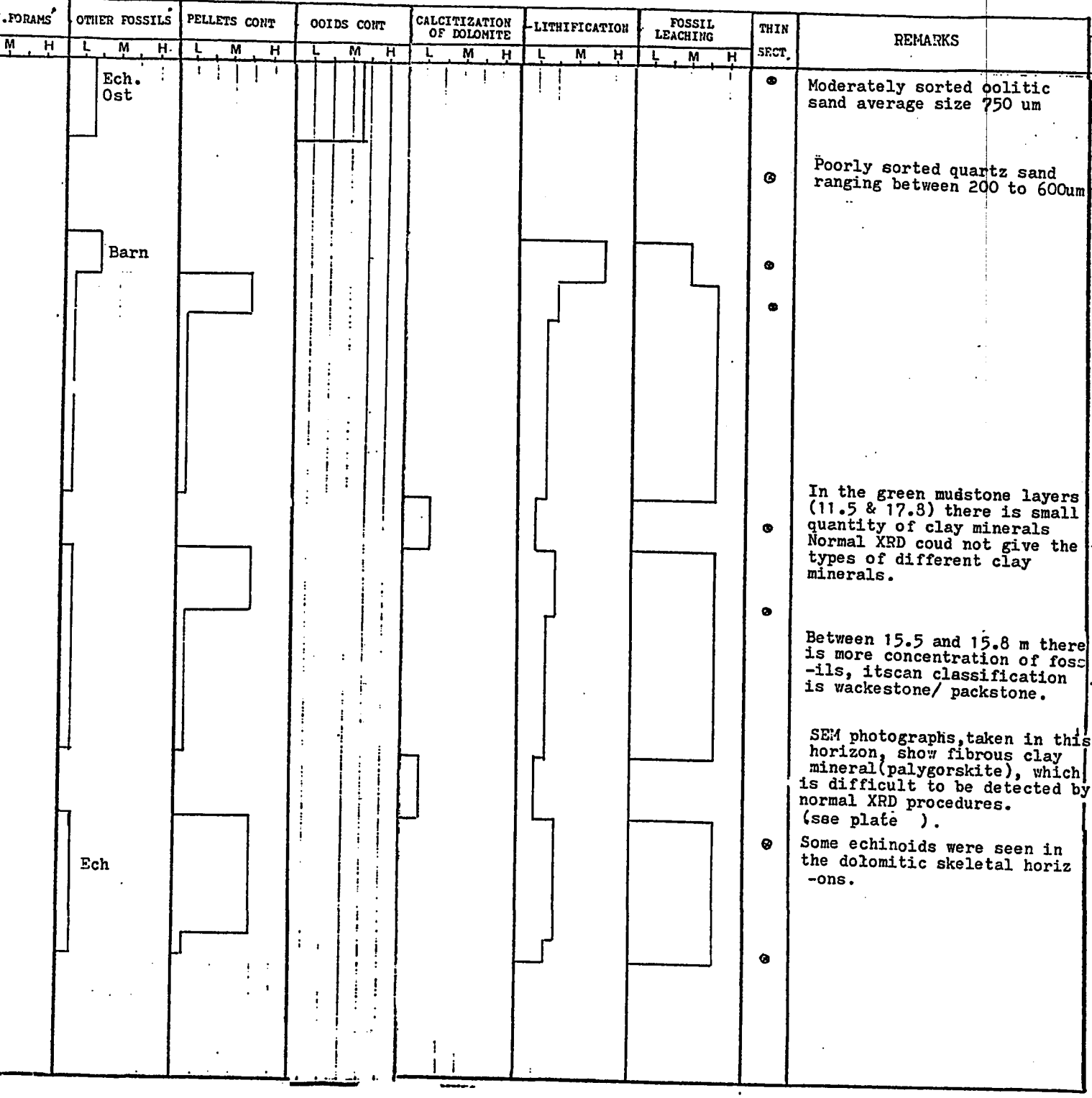
.FORAMS
M H
OTHER FOSSILS
L M H
PELLETS CONT
L M H
OOIDS CONT
L M H
CALCITIZATION OF DOLOMITE
L M H
LITHIFICATION
L M H
FOSSIL LEACHING
L M H
THIN SECT.
REMARKS
Ech.
Ost
Barn
Ech
Moderately sorted oolitic sand average size 750 um
Poorly sorted quartz sand ranging between 200 to 600um
In the green mudstone layers (11.5 & 17.8) there is small quantity of clay minerals Normal XRD coud not give the types of different clay minerals.
Between 15.5 and 15.8 m there is more concentration of foss -ils, itscan classification is wackestone/ packstone.
SEM photographs,taken in this horizon, show fibrous clay mineral(palygorskite), which is difficult to be detected by normal XRD procedures. (sse plate).
Some echinoids were seen in the dolomitic skeletal horiz -ons.

APPENDIX B

EXAMPLES OF XRD DIFFRACTOGRAMS.

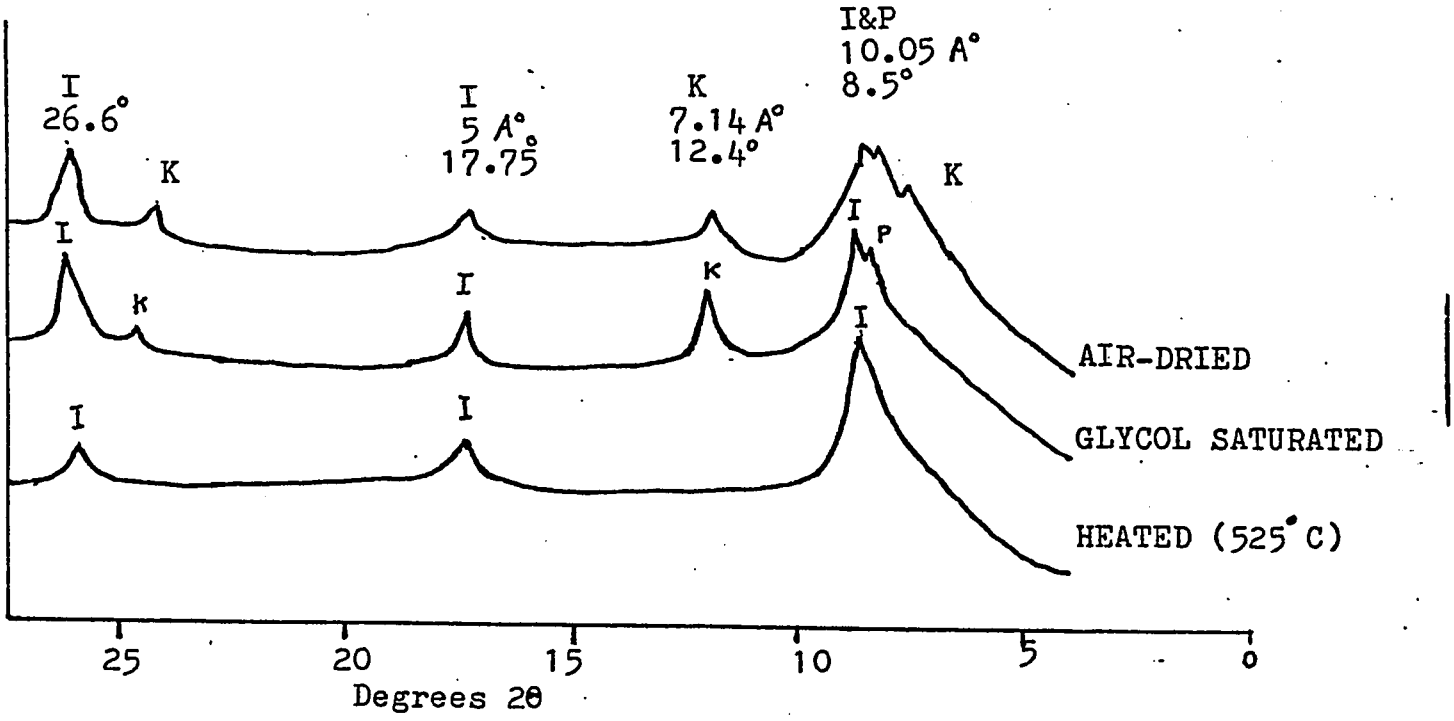

Figure B/ . X-ray diffractograms of air dried, glycol saturated, and heated (525° C) clay fraction of sample No. 3/16 (9m).

I= Illite K= Kaolinite P=Palygorskite

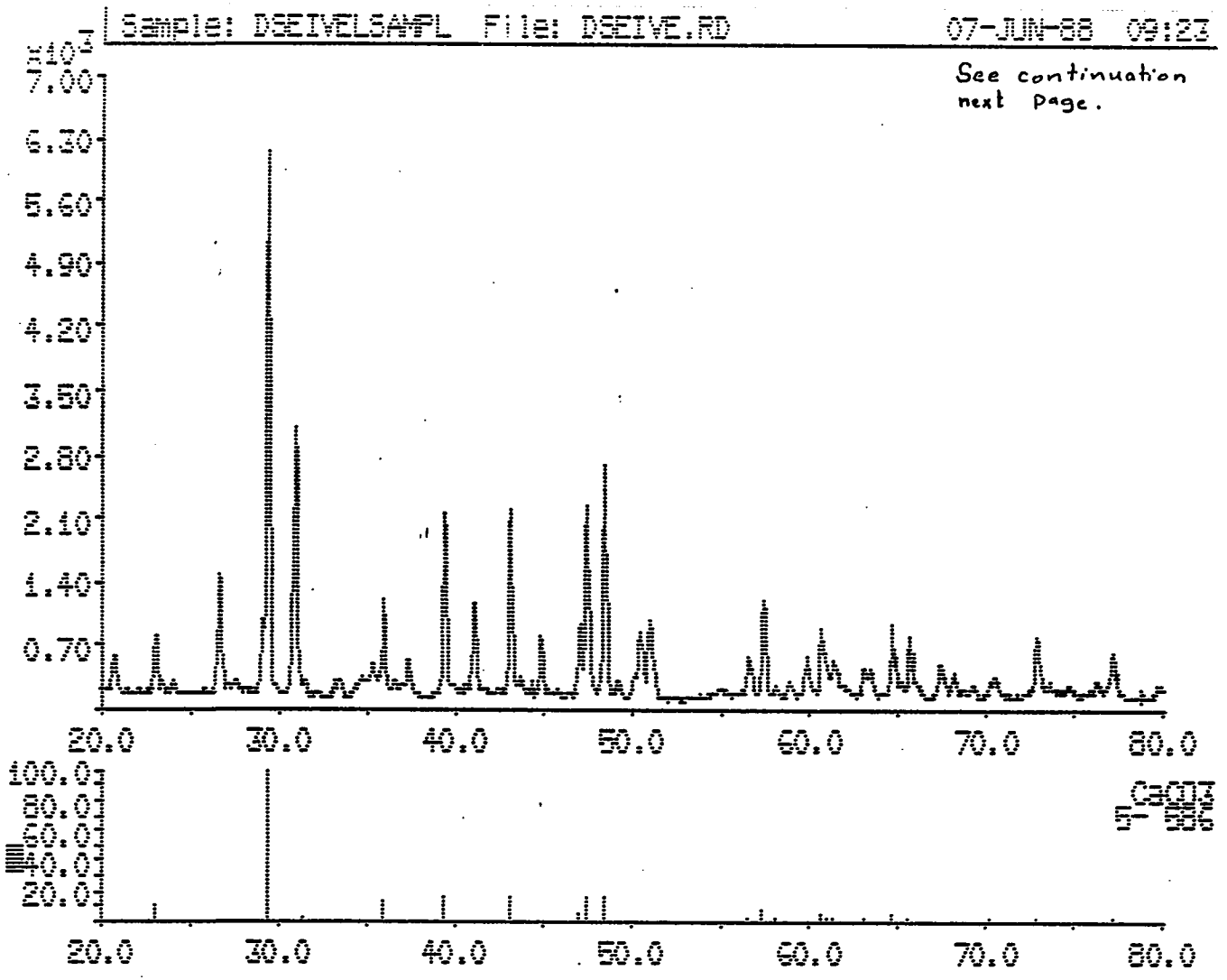

Figure B2.1. X-Ray diffractogram for rock sample No.3/44.3(42m). It continues next page .

Continued from the previous page.

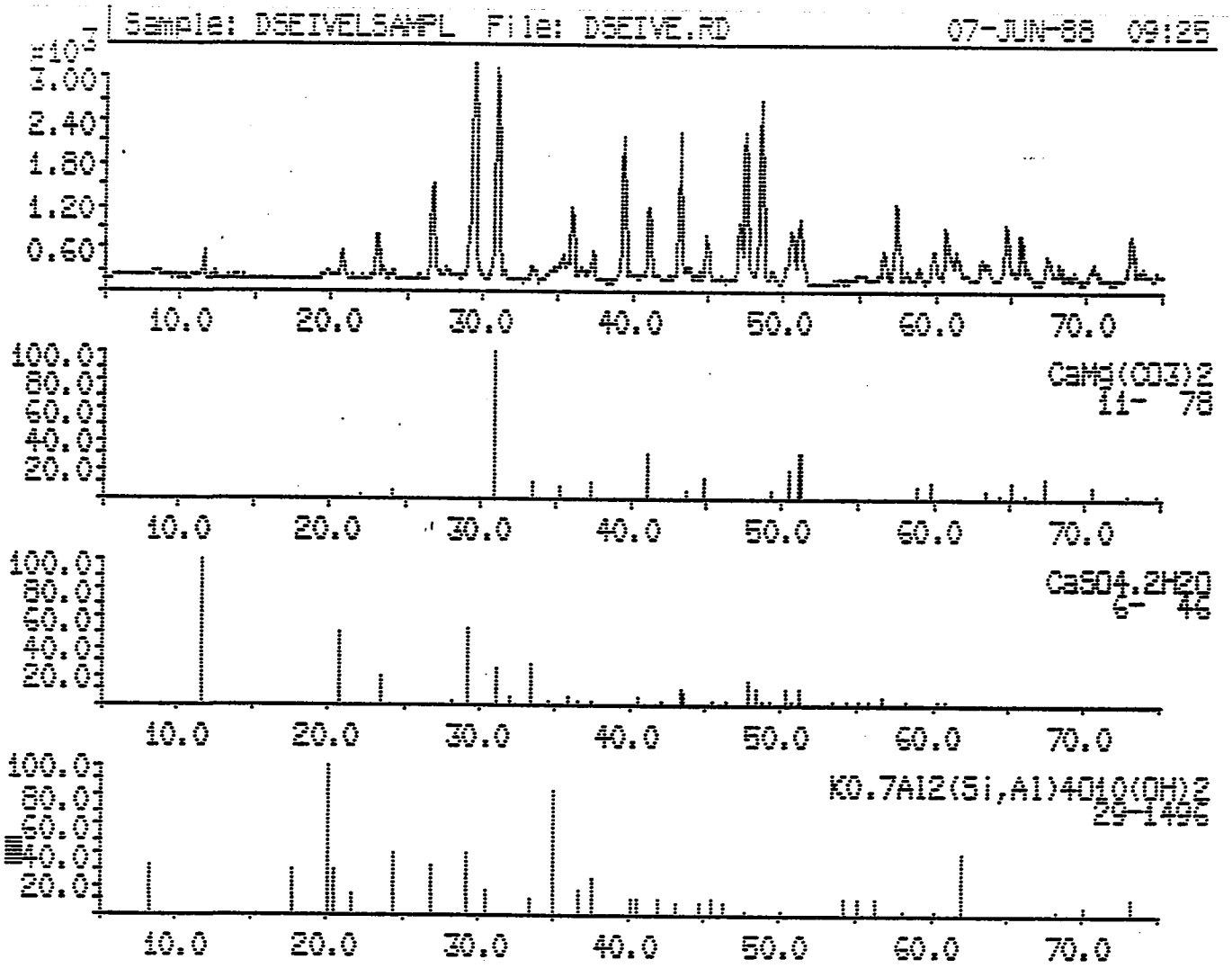

Figure B2.2. X-Ray diffractogram for rock sample No 3/44.3(42m). (continuation of the previous page)

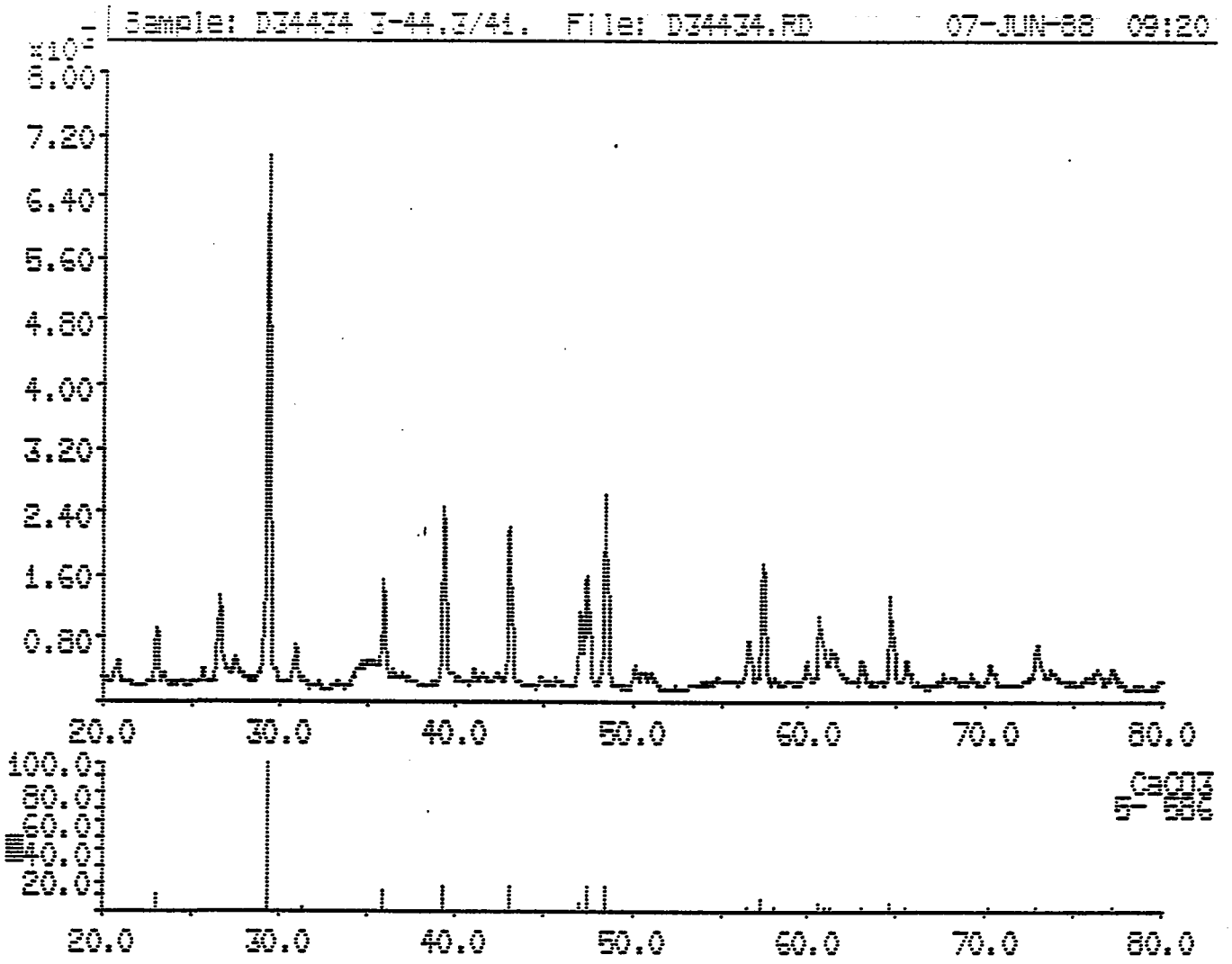

Figure B3.1. X-Ray diffractogram for rock sample No 3/44.3(41m)
It continues next page .

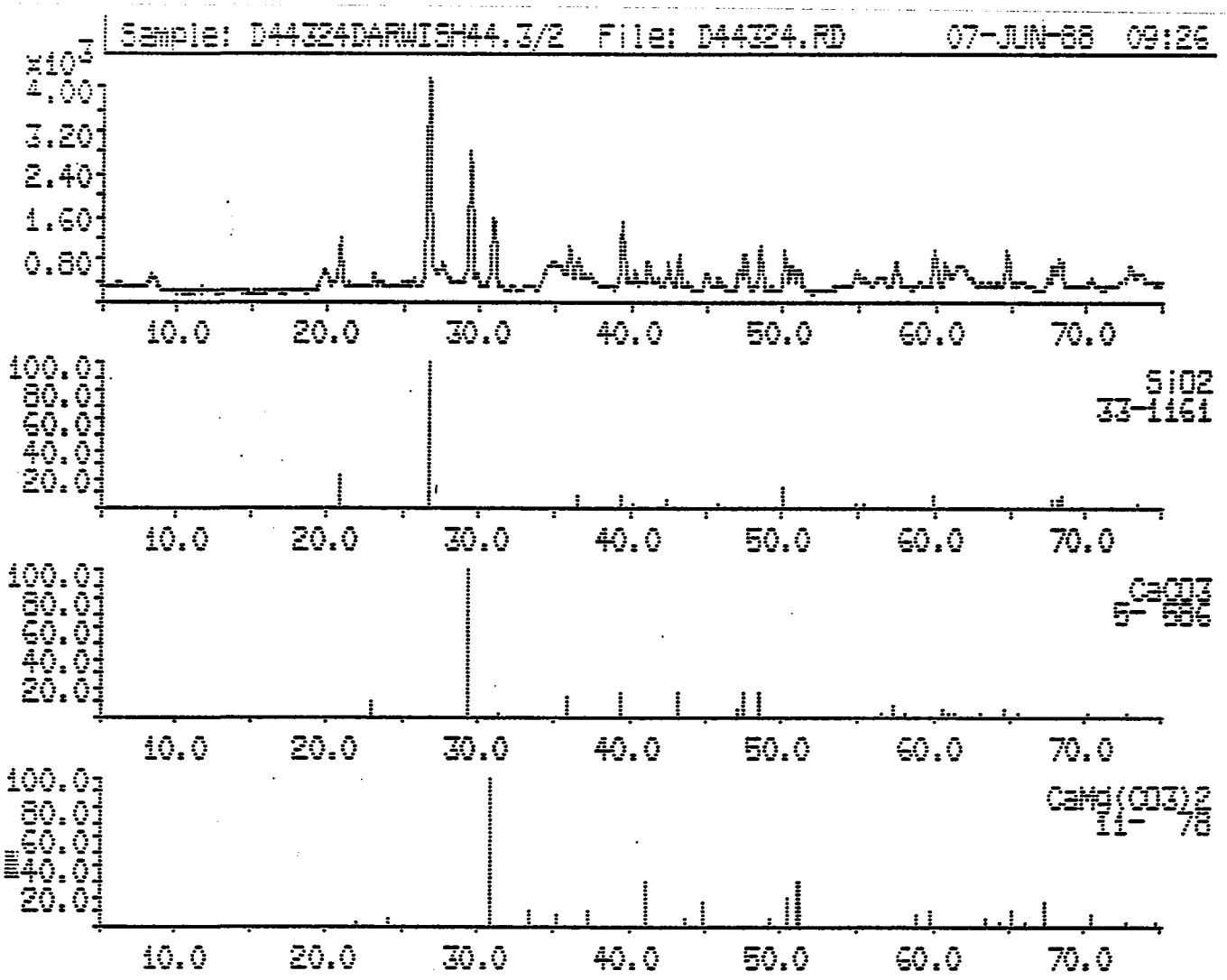

Figure B4.1. X-Ray diffractogram for rock sample No 3/44.3(24m)
It continues next page .

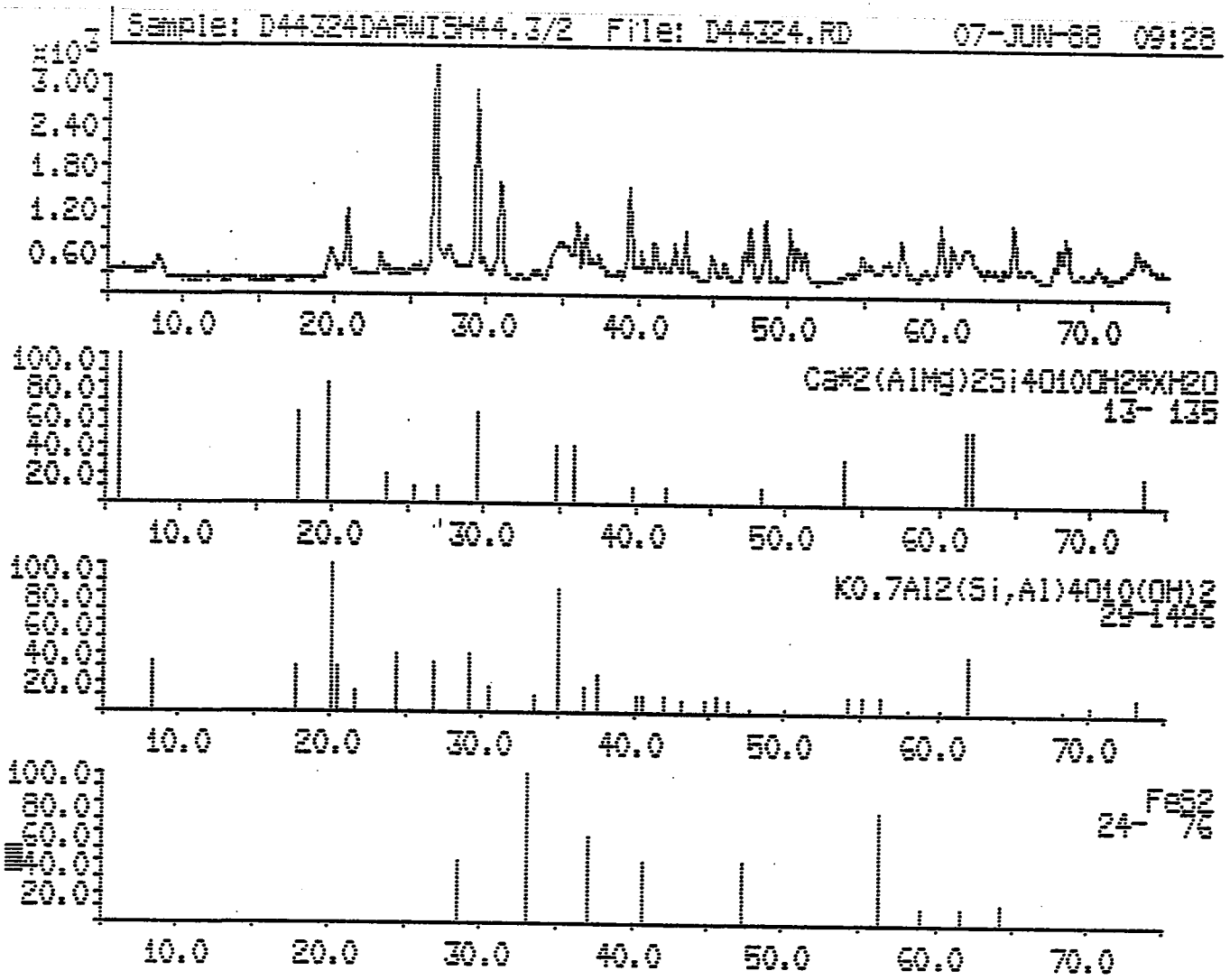

Figure B4.2. X-Ray diffractogram for rock sample No. 3/44.3(24m) (continuation of the previous page).

Examples of Semi-quantitative mineral analysis by XRD technique.

Some examples of semi-quantitative XRD mineral analysis for rock samples are given in the next pages. The weight fraction , printed on diffractograms, is calculated by comparing the intensity of the most intense peak of that phase with the standard. The intensities of the diffraction peaks are mainly governed by the amount of material, however lot of other factors also play an important role . Thus, it should be noted that the X-ray Diffraction technique is not powerful technique for quantitative analysis. Thus the weight fraction is only approximate. I shoud also mention here that any amorphous compound would not be detected by X-Ray Diffraction.

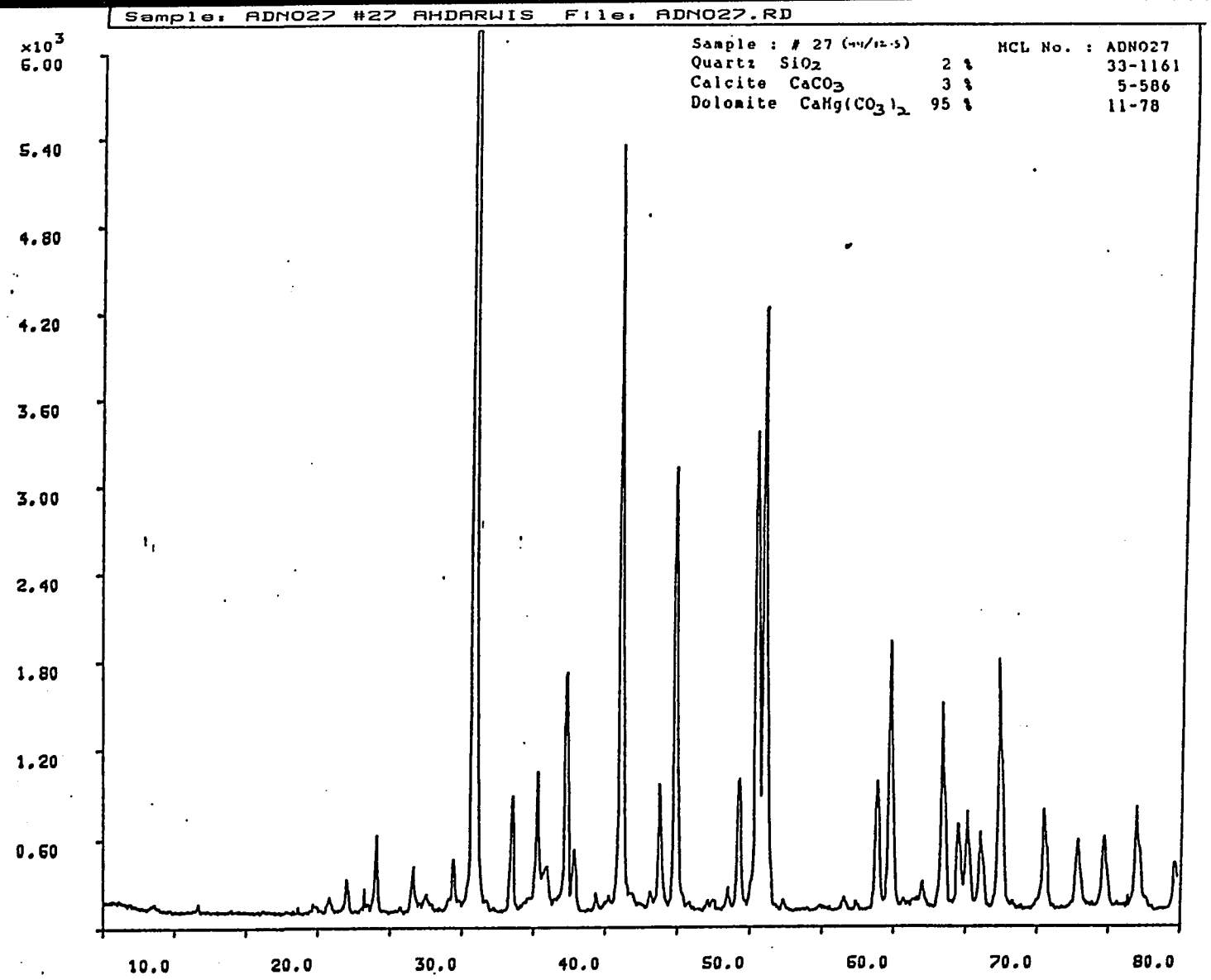

Figure B5. X-Ray diffractogram for rock sample No.3/44.3(12.5m), with semi-quantitative analysis in the upper part.

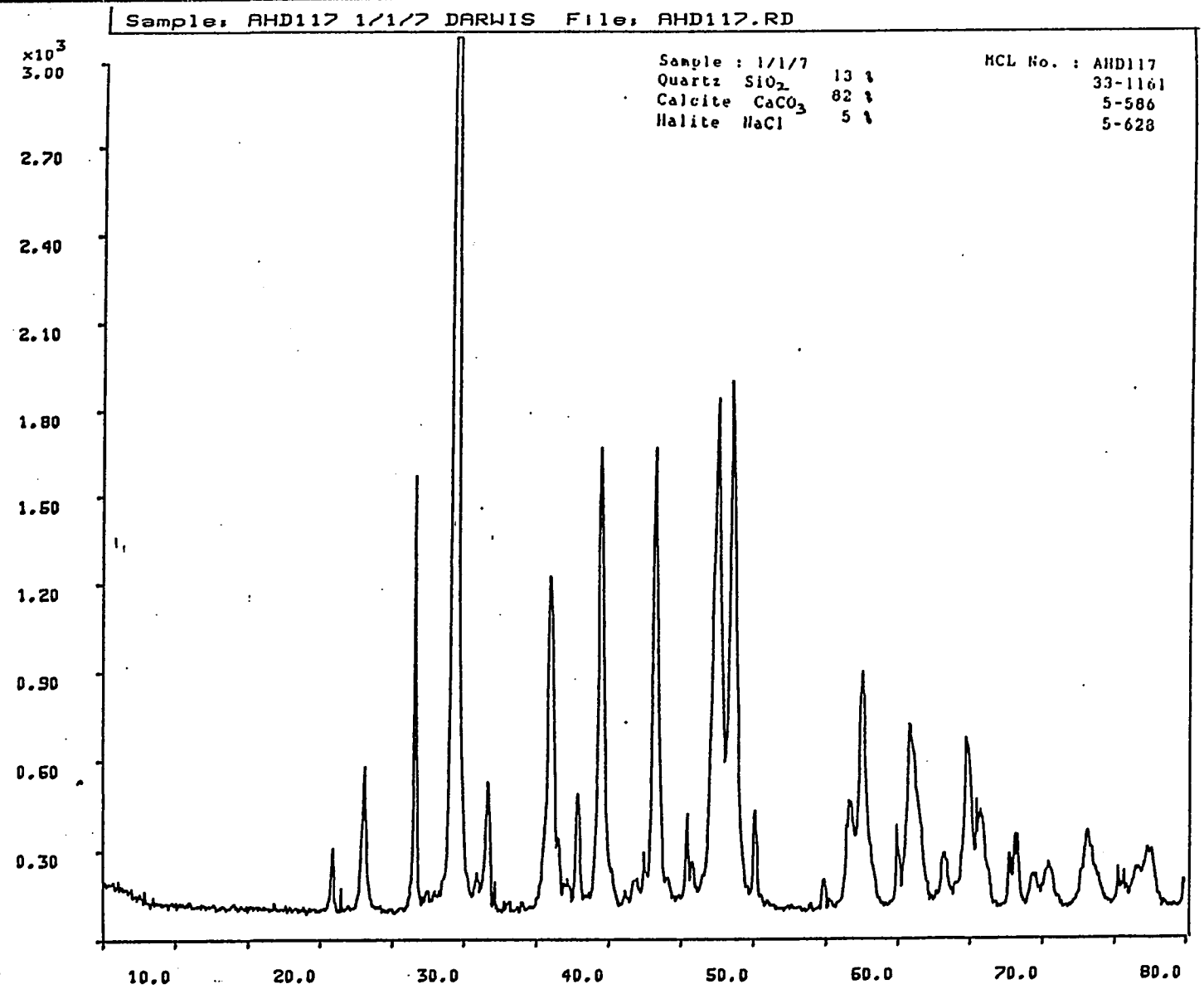

Figure B6 . X-Ray diffractogram for rock sample No. 1/1(7m), with semi-quantitative analysis in the upper part.

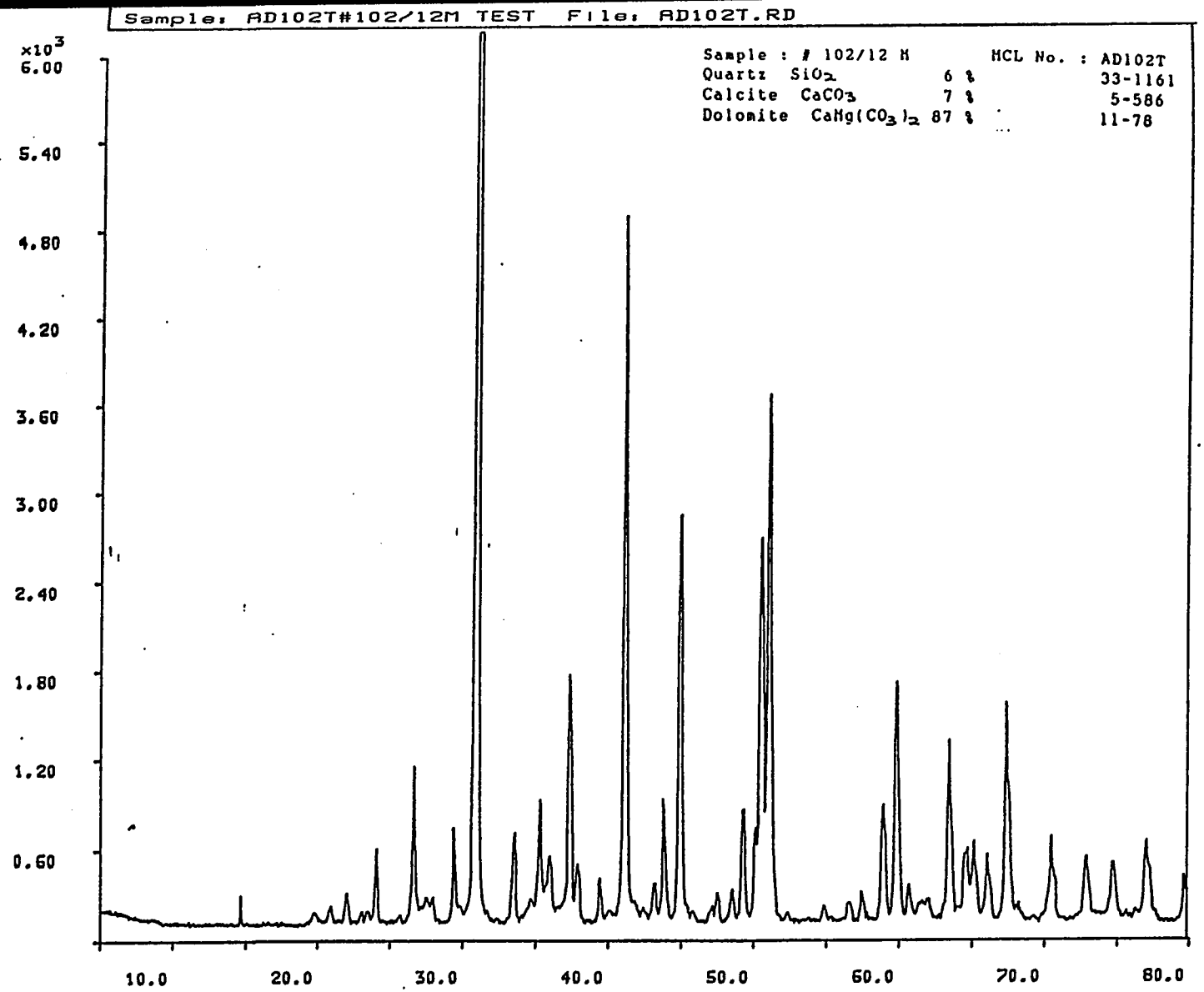

Figure B7 . X-Ray diffractogram for rock sample No.3/102(12m), with semi-quantitative analysis in the upper part.

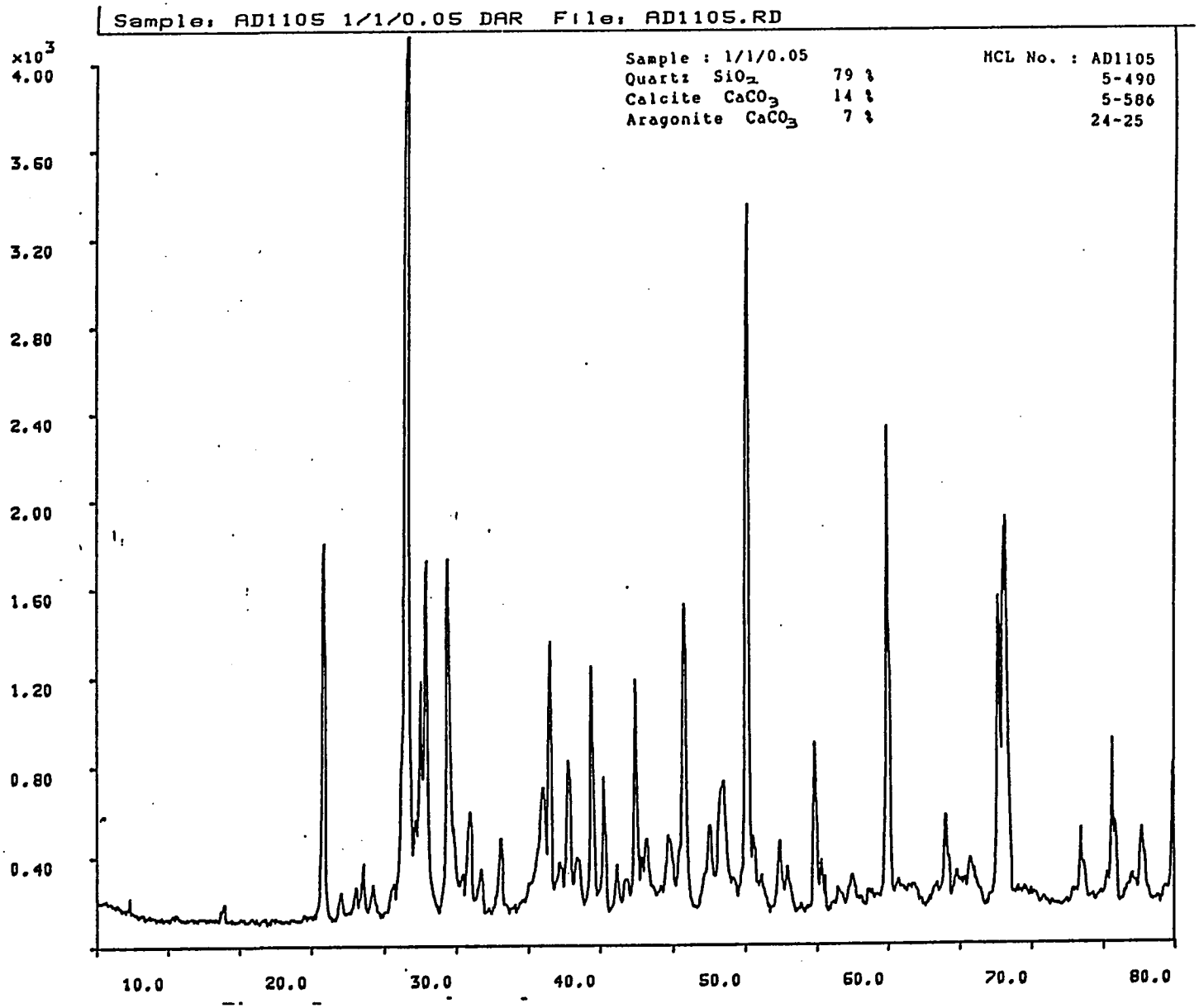

Figure B8 . X-Ray diffractogram for rock sample No.1/1(.05m), with semi-quantitative analysis in the upper part.

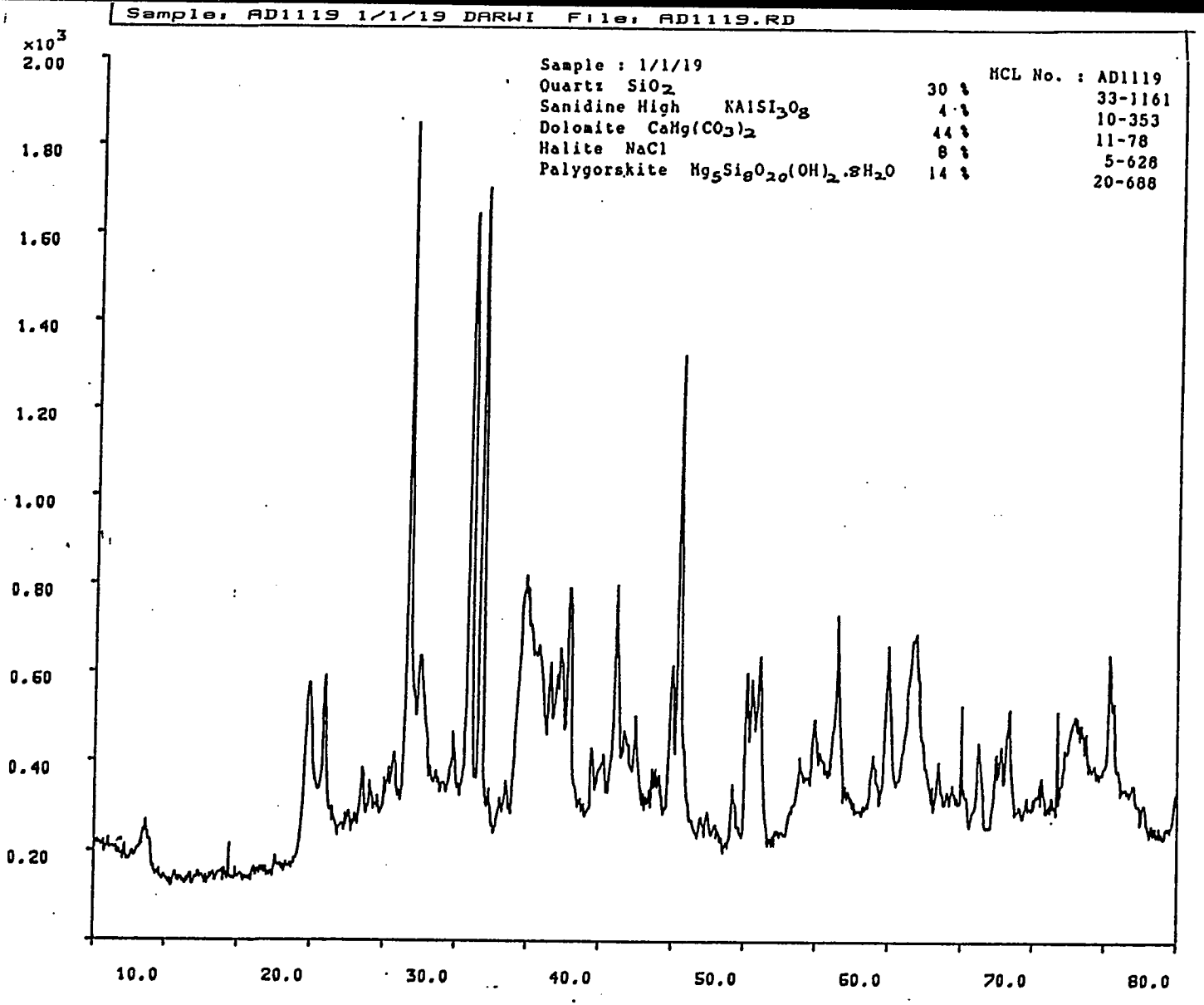

Figure B9 . X-Ray diffractogram for rock sample No. 1/1(19m), with semi-quantitative analysis in the upper part.

APPENDIX C

EXAMPLES OF SEM COMPOSITIONAL DATA BY ENERGY DISPERSIVE XRF ANALYSIS (XRF SPOT ANALYSIS).

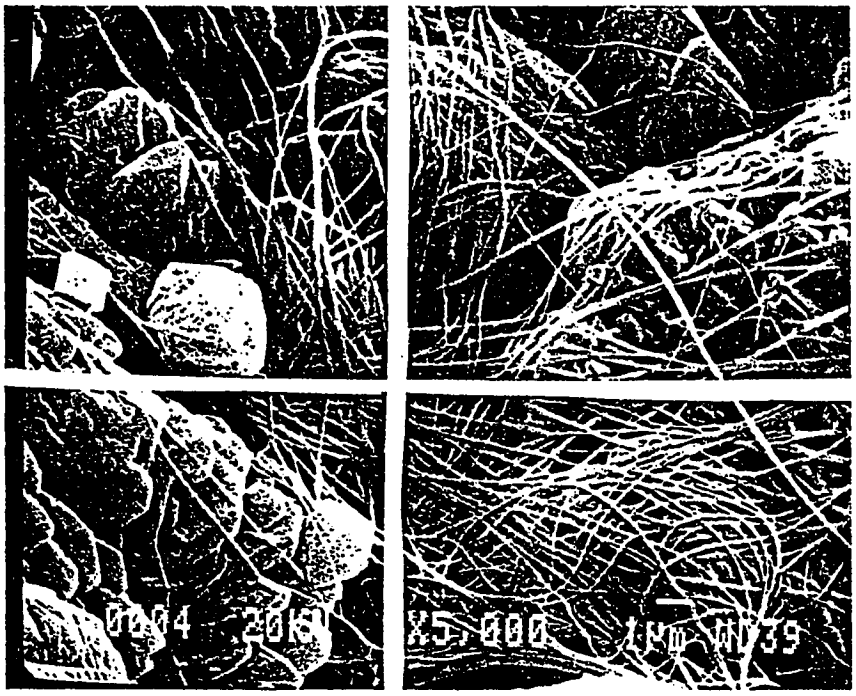

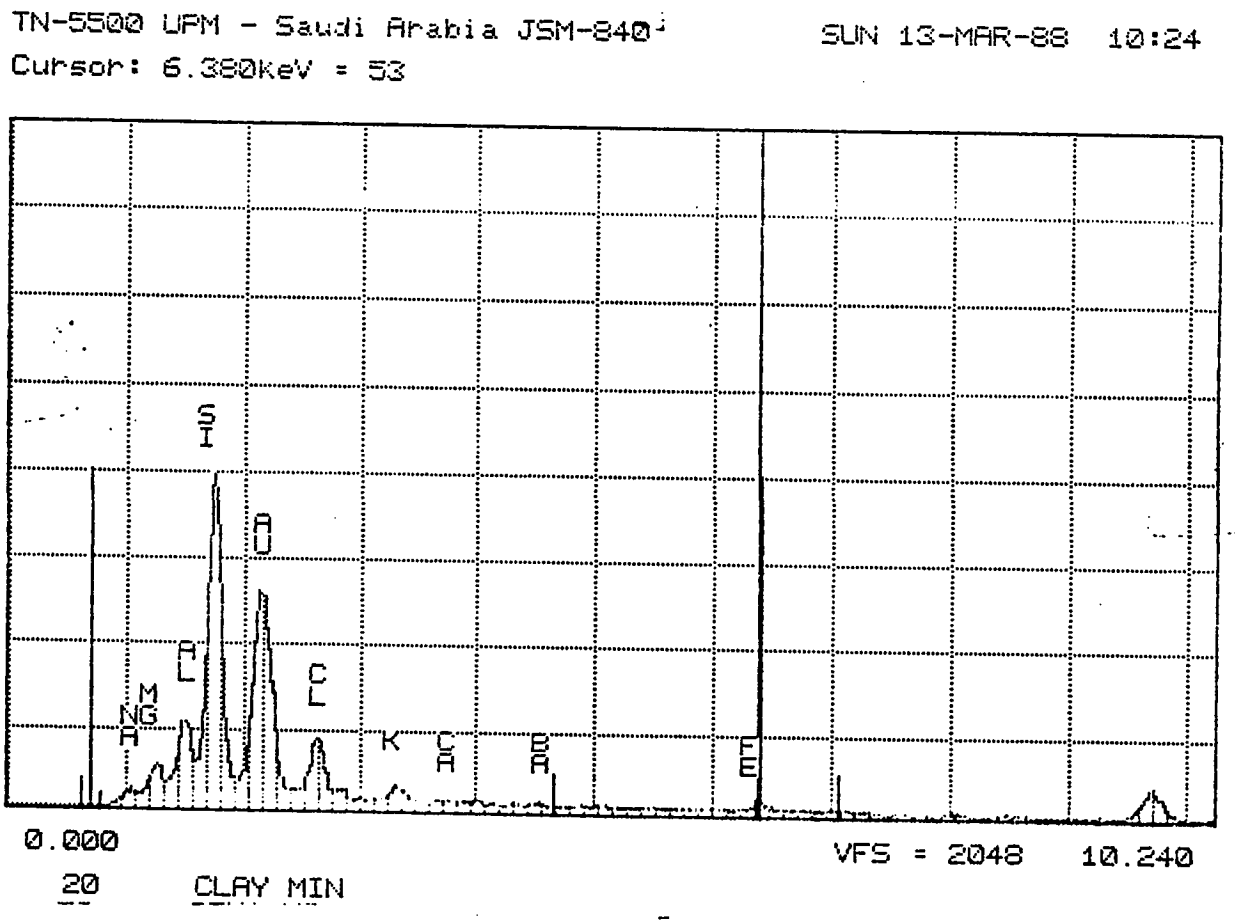

Figure C1. SEM compositional data by energy dispersive XRF analysis. Spot analysis for dolomitic green mudstone showing palygorskite elements, sample 3/102(18m).

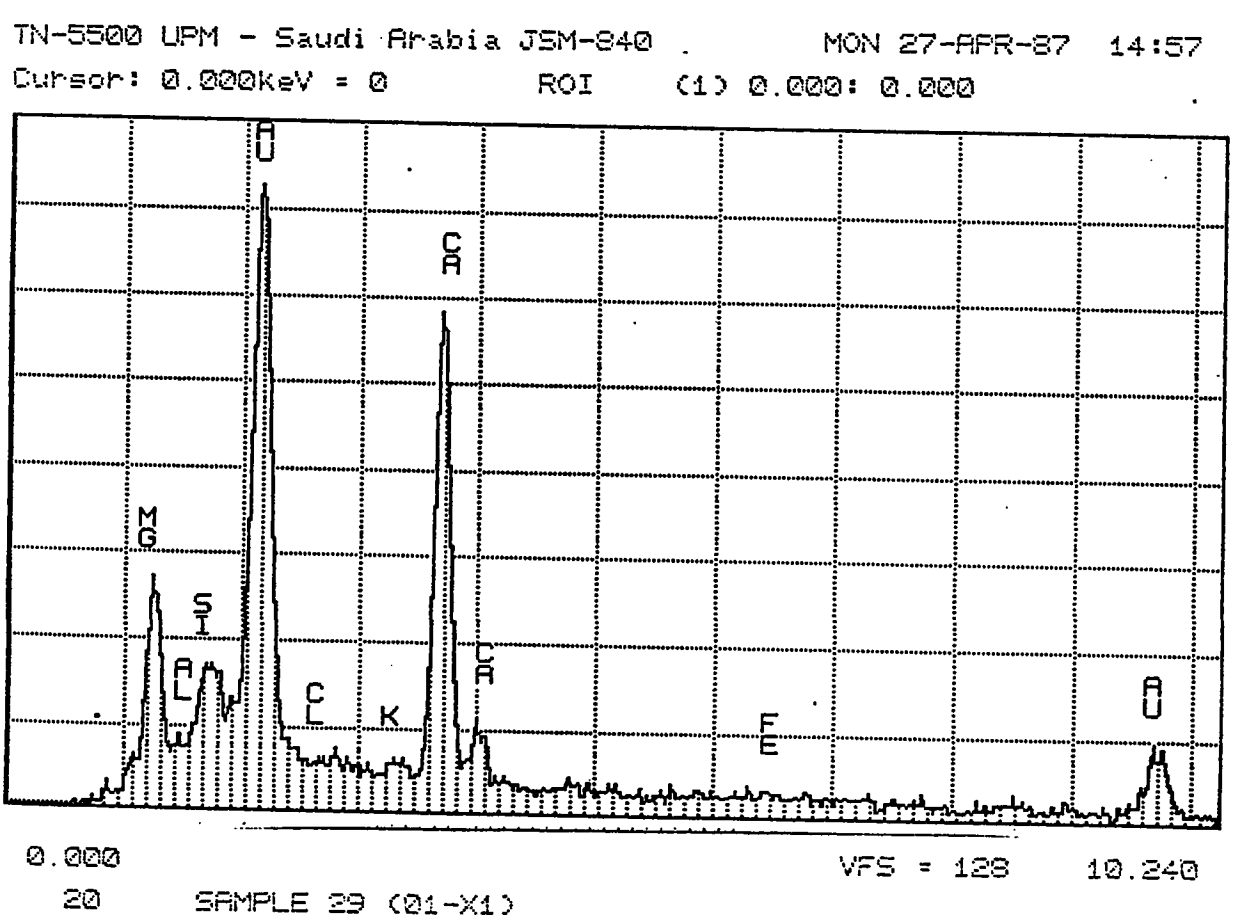

Figure C2. XRF spot analysis for dolomitic oolitic grainstone, sample No. 1/1 (15m).

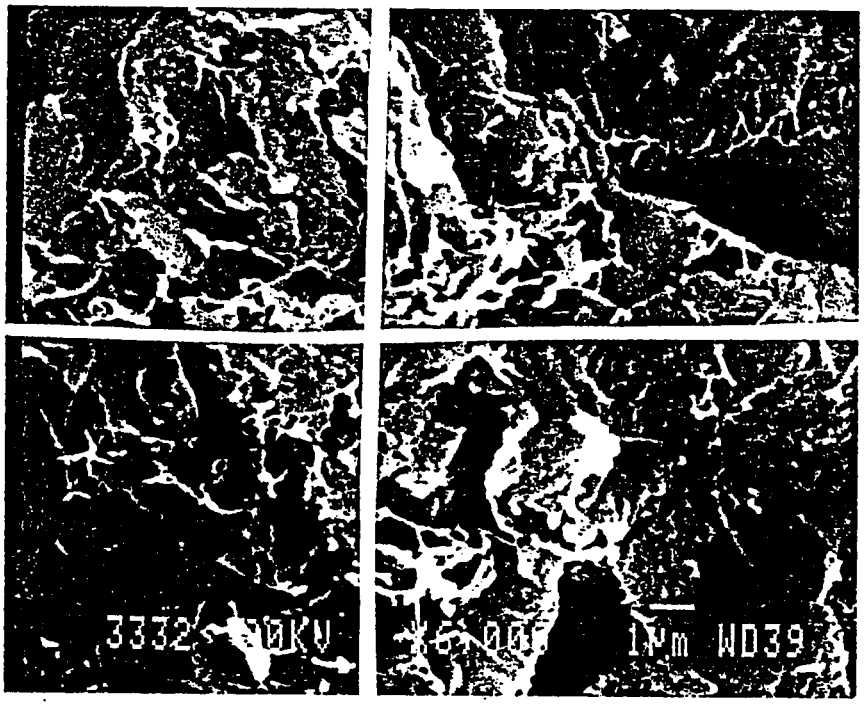

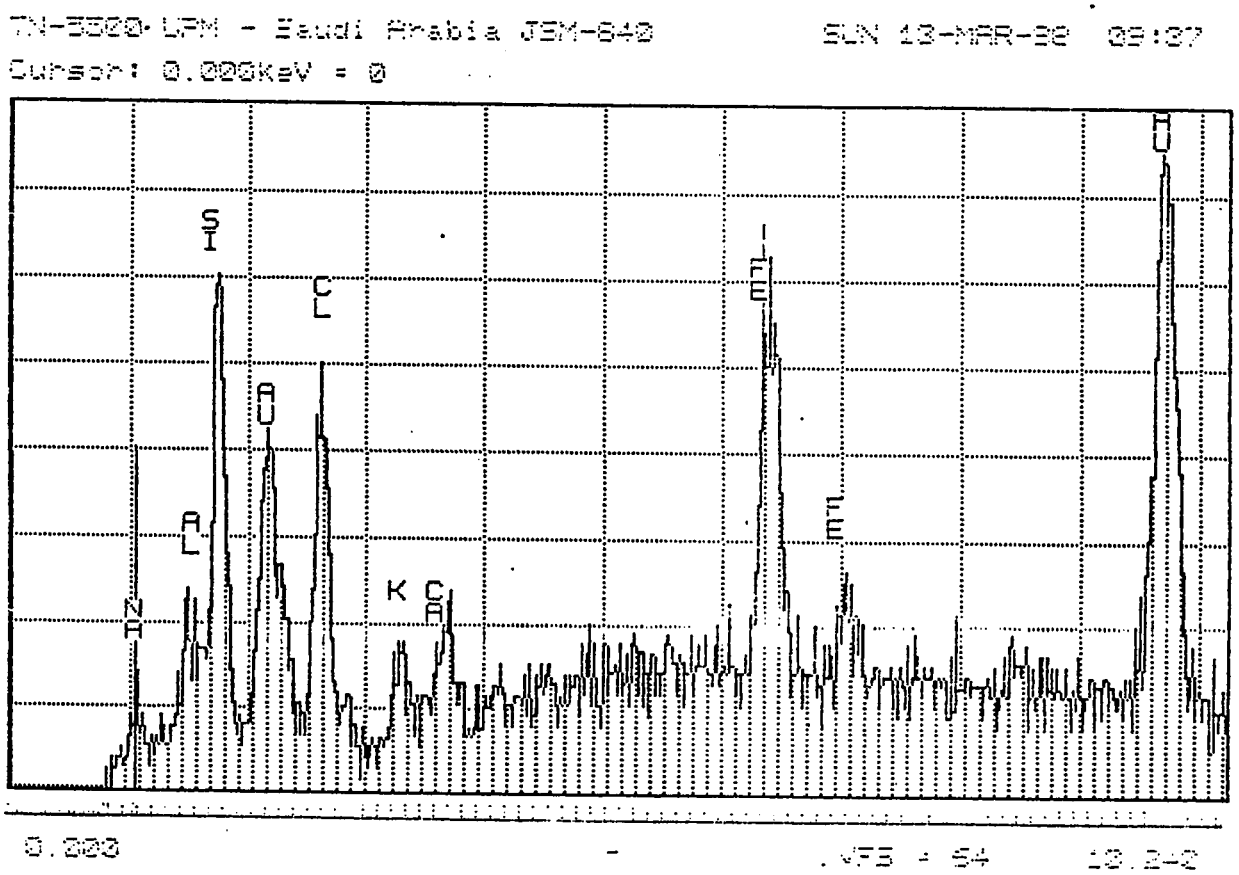

Figure C3. SEM compositional data by energy despersive XRF analysis. Spot analysis for dolomitic green mudstone sample showing illite elements, sample No. 3/32(15m).

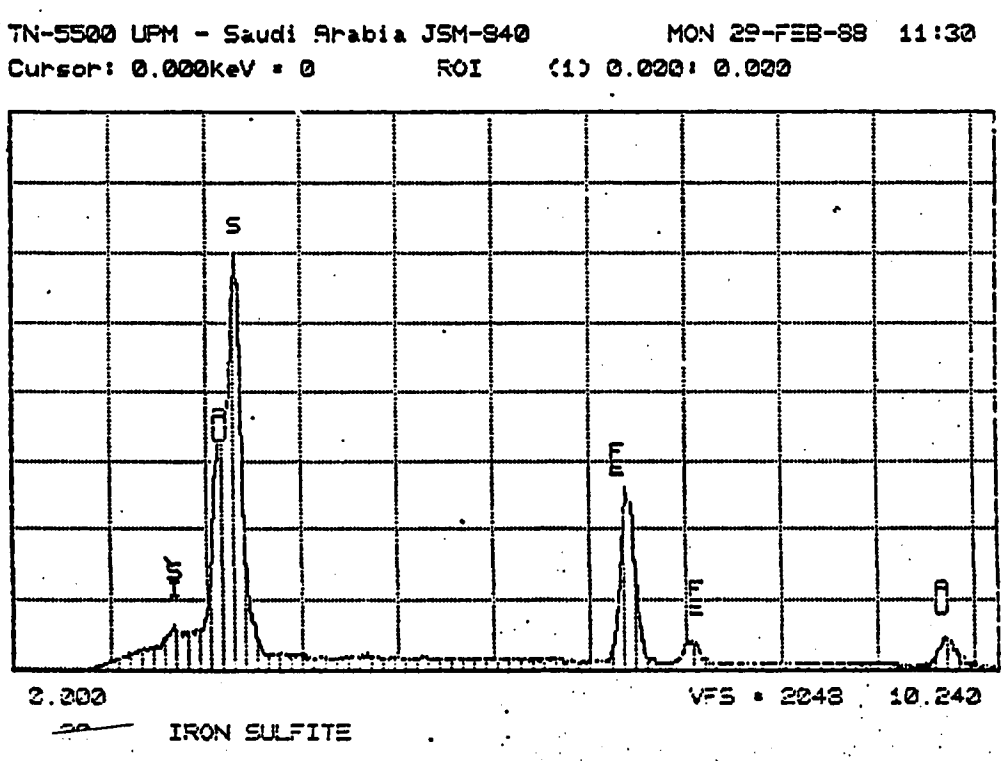

Fig. C4-SEM compositional data by energy dispersive XRF analysis. Spot analysis for pyrite crystal in dolomite groundmass, borehole 3/32 (12m).

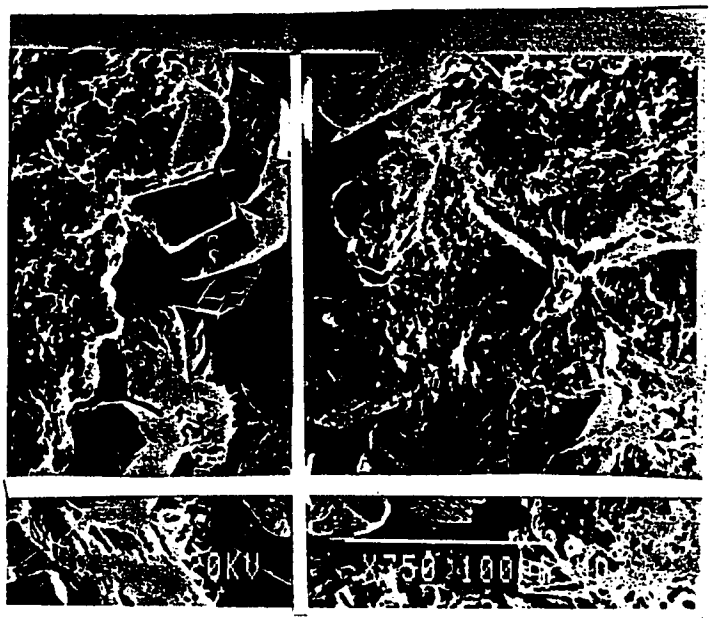

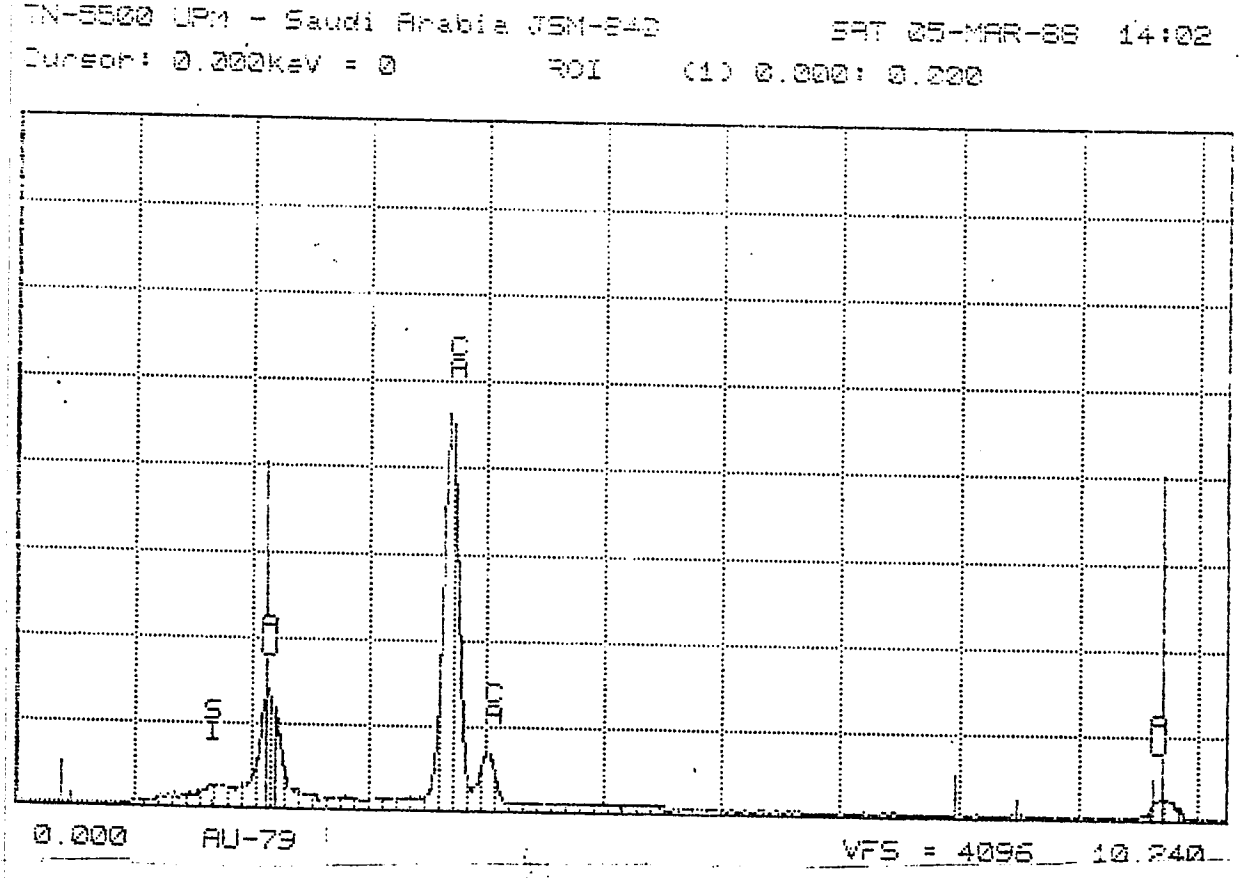

Fig. C5 -SEM compositional data by energy dispersive XRF analysis. Spot analysis for calcite crystals in dolomitic groundmass, dolomitic green mudstone No. 3/44.3(37m).

APPENDIX D

METAL CONCENTRATION

Inductively-Coupled Plasma Emission Spectroscopic (ICP-ES) analysis of rock samples from three boreholes.

Sample ID		K %	Ca %	Fe %	Mg %	Mn (ppm)	Sr (ppm)
AS	1/1(.5)	0.79	12.00	2.35	0.45	241	1286
AS	1/1(2)B	0.42	17.01	1.03	1.23	215	1972
AS	1/1(2)	0.48	22.83	1.26	1.49	221	2403
AS	1/1(2.6)	0.64	05.97	0.35	0.31	063	0877
CGS	1/1(5.5)	0.14	20.03	0.21	1.42	041	0690
CGS	1/1(6)	0.09	20.85	0.31	0.45	34	0640
CGS	1/1(7)	0.09	17.59	0.09	0.33	015	0648
CGS	1/1(8)	0.14	17.09	0.40	0.29	038	0457
WD	1/1(10)	0.07	14.01	0.06	3.13	062	0080
WD	1/1(12)	0.69	14.09	0.42	5.36	089	0068
WD	1/1(12.5)	0.39	06.30	0.18	2.39	048	0029
WD	1/1(13)	0.38	07.36	0.17	1.02	053	0032
WD	1/1(16.3)	0.24	08.73	0.09	1.00	063	0052
GMS	1/1(18.9)	1.36	03.38	1.42	2.49	201	0031
GMS	1/1(19)	2.52	01.33	2.75	1.44	114	0029
GMS	1/1(19)	2.74	01.44	2.68	1.58	129	0030
WD	1/1(19.3)	0.30	13.62	0.28	4.99	091	0068
WD	1/1(20)	0.37	16.15	0.27	7.99	091	0068
WD	1/1(20)B	0.44	14.45	0.18	3.68	063	0062
WD	1/1(20.5)	0.43	13.70	0.17	0.03	057	0065
WD	1/1(25)	1.12	12.89	0.44	3.57	029	0098
WD	1/7(16)	0.11	06.76	0.04	35.74	062	0043
CGS	3/44(2)	1.12	02.68	1.13	0.80	264	0130
WD	3/44(3.5)	0.29	09.07	0.08	1.40	042	0041
WD	3/44(9.5)	0.35	08.12	0.10	1.40	051	0040
WD	3/44(12.5)	0.40	07.68	0.19	2.93	049	0033
WD	3/44(13)	0.31	05.55	0.18	3.65	081	0031
WD	3/44(15.5)	0.40	09.16	0.12	1.38	050	0044
WD	3/44(25)	0.15	08.46	0.23	4.03	054	0054
WD	3/44(27.5)	0.40	08.13	0.16	19.09	034	0037
WD	3/44(33.5)	0.24	04.65	0.09	2.47	054	0029
GMS	3/44(36.5)	1.24	05.50	1.17	0.18	179	0042
WD	3/44(39.2)	0.16	06.75	0.30	4.76	102	0052
GMS	3/44(42M)	1.01	06.26	0.60	0.52	150	0034
WD	3/44(6)	0.64	07.69	0.16	1.80	064	0069
WD	3/44(7.5)	1.05	12.54	0.50	5.51	092	0056
WD	3/44(10.5)	0.26	10.86	0.12	5.11	039	0055
WD	3/44(11.3)	0.29	08.16	0.10	1.21	027	0045
WD	3/44(11.3)B	0.45	09.28	0.11	1.61	027	0051
WD	3/44(13)	0.30	07.43	0.15	1.93	051	0033
GMS	3/44(14.5)	1.76	06.11	2.12	0.98	213	0052
WD	3/44(16.5)	0.06	07.20	0.02	1.12	039	0034

Sample Id		K %	Ca %	Fe %	Mg %	Mn (ppm)	Sr (ppm)
WD	3/44(17)	0.13	08.55	0.04	1.09	043	0038
WD	3/44(18.5)	0.06	10.15	0.01	1.61	030	0043
WD	3/44(21.7)	1.03	10.55	0.44	1.69	099	0046
WD	3/44(24)	0.31	10.54	0.11	0.11	040	0051
GMS	3/44(38)	1.21	08.42	1.25	0.14	205	0077
AS	3/102(1.5)	0.82	08.54	0.52	0.11	107	0884
AS	3/102(3)	0.39	05.59	0.06	0.29	012	1489
CGS	3/102(4.5)	0.22	09.78	0.17	0.39	040	0477
CGS	3/102(6)	0.44	11.17	0.22	4.40	060	0159
WD	3/102(7)	0.49	06.45	0.26	5.27	058	0035
WD	3/102(7.4)	0.42	10.26	0.26	4.67	082	0042
WD	3/102(8.9)	1.18	04.91	0.40	2.08	101	0040
GMS	3/102(10)	0.52	03.36	2.38	1.68	180	0042
GMS	3/102(10)B	0.12	03.09	2.12	0.27	187	0036
WD	3/102(10)	0.45	00.09	0.03	0.10	050	0002

AS=Aragonitic sand CGS= Cal.sk. grainstone
WD=White dol. lithofacies GMS= Dol.green mudstone

APPENDIX E

AN EXAMPLE OF ROCK DESCRIPTION PROFILE, DONE BY Balast-nedam group n.v. (KING FAHD CAUSEWAY CONTRACTOR).

ballast-nedam groep n.v.

Saudi Arabia – Bahrain Causeway

LEGENDS TO THE GEOLOGICAL PROFILES

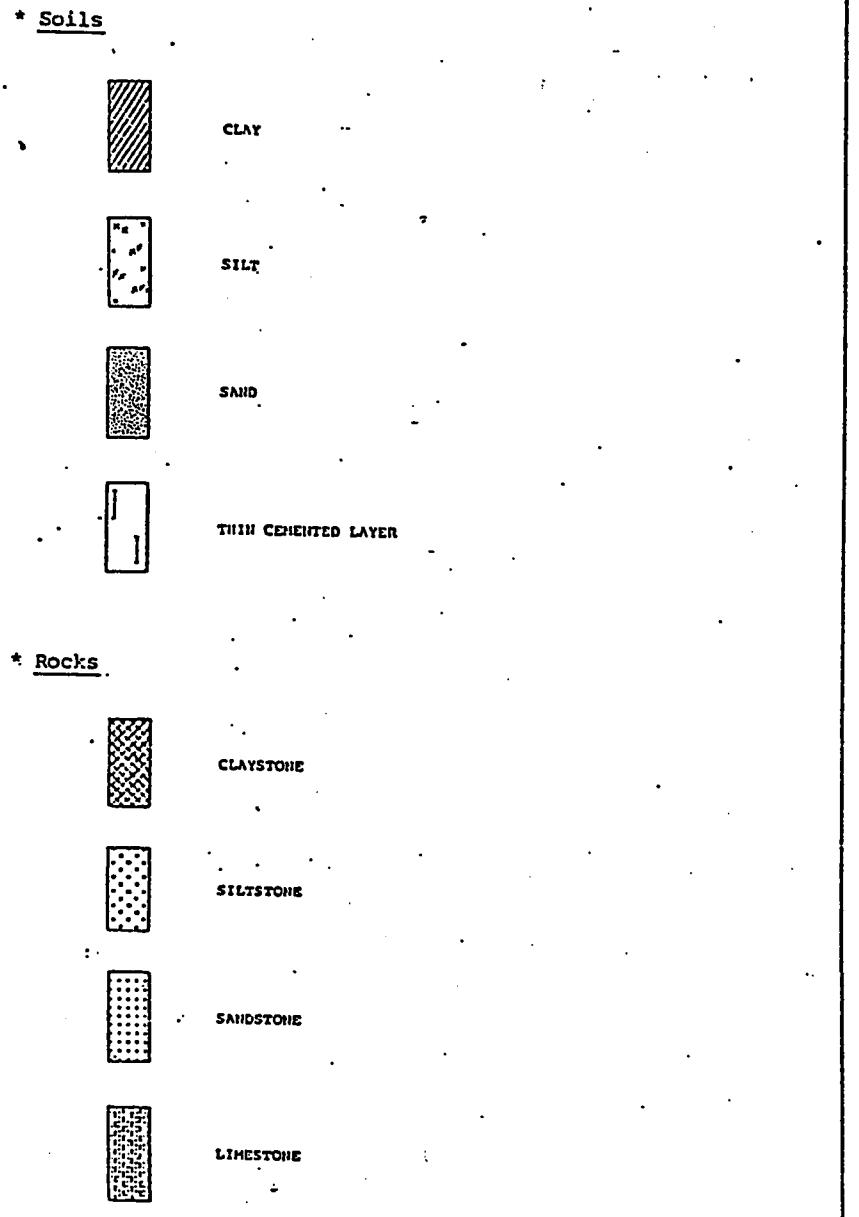

Figure E1 . Legends of rock description which were used by Balast-nedam groep n.v.

BRIDGE No.: 3	PIER No.: 44	Date:

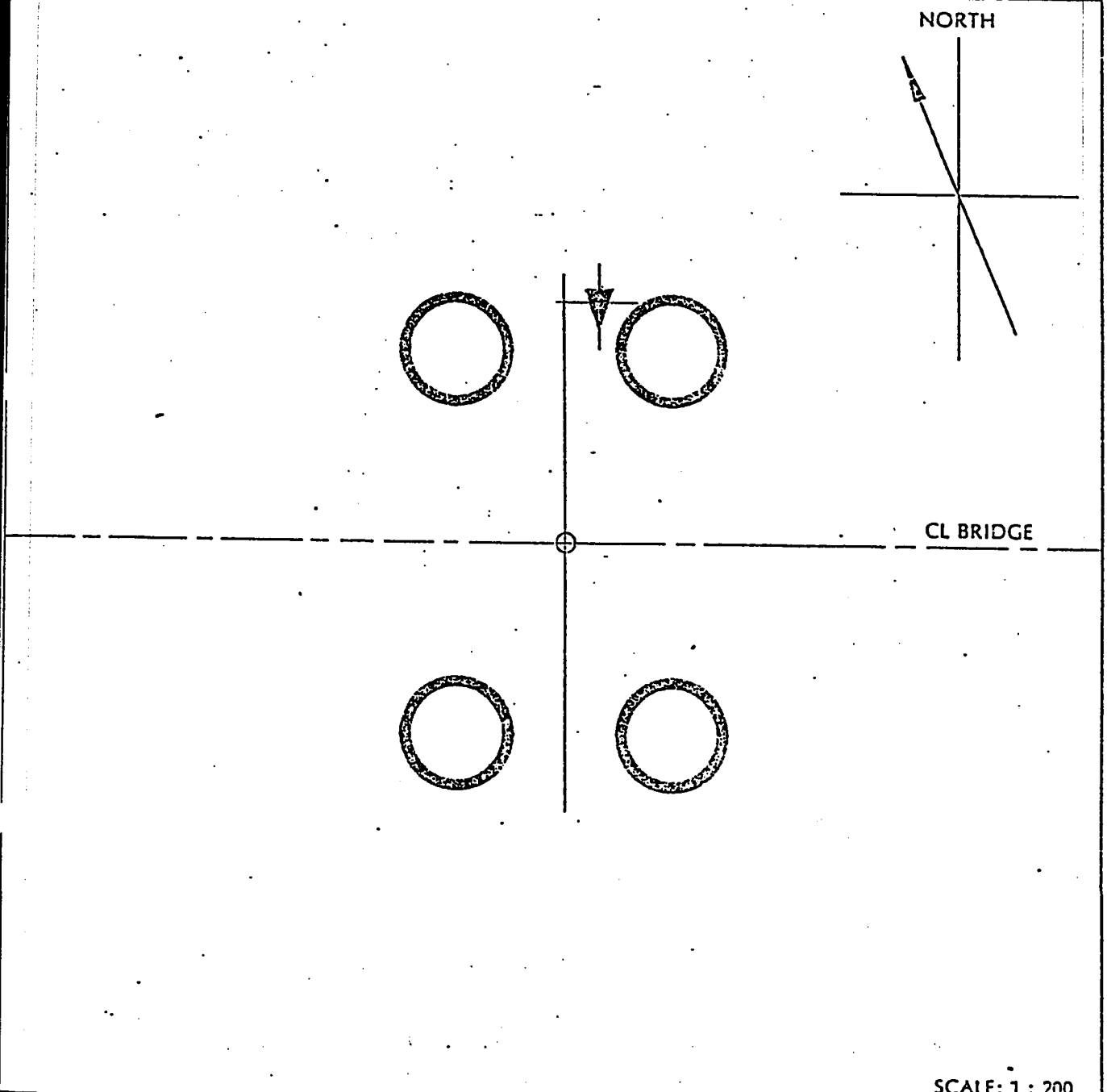

SCALE: 1 : 200

LOCATION	CHAINAGE	OFSET	EASTING	NORTHING
as planned ⊕	33850.0	0	28960.012	98155.194
as drilled ✝	33851.15	7.90 N	28964.81	98161.58

REMARKS: Seabed level 9.20 m - CD

Figure E2 . Location of borehole number 3/44 by latitude and longitude.

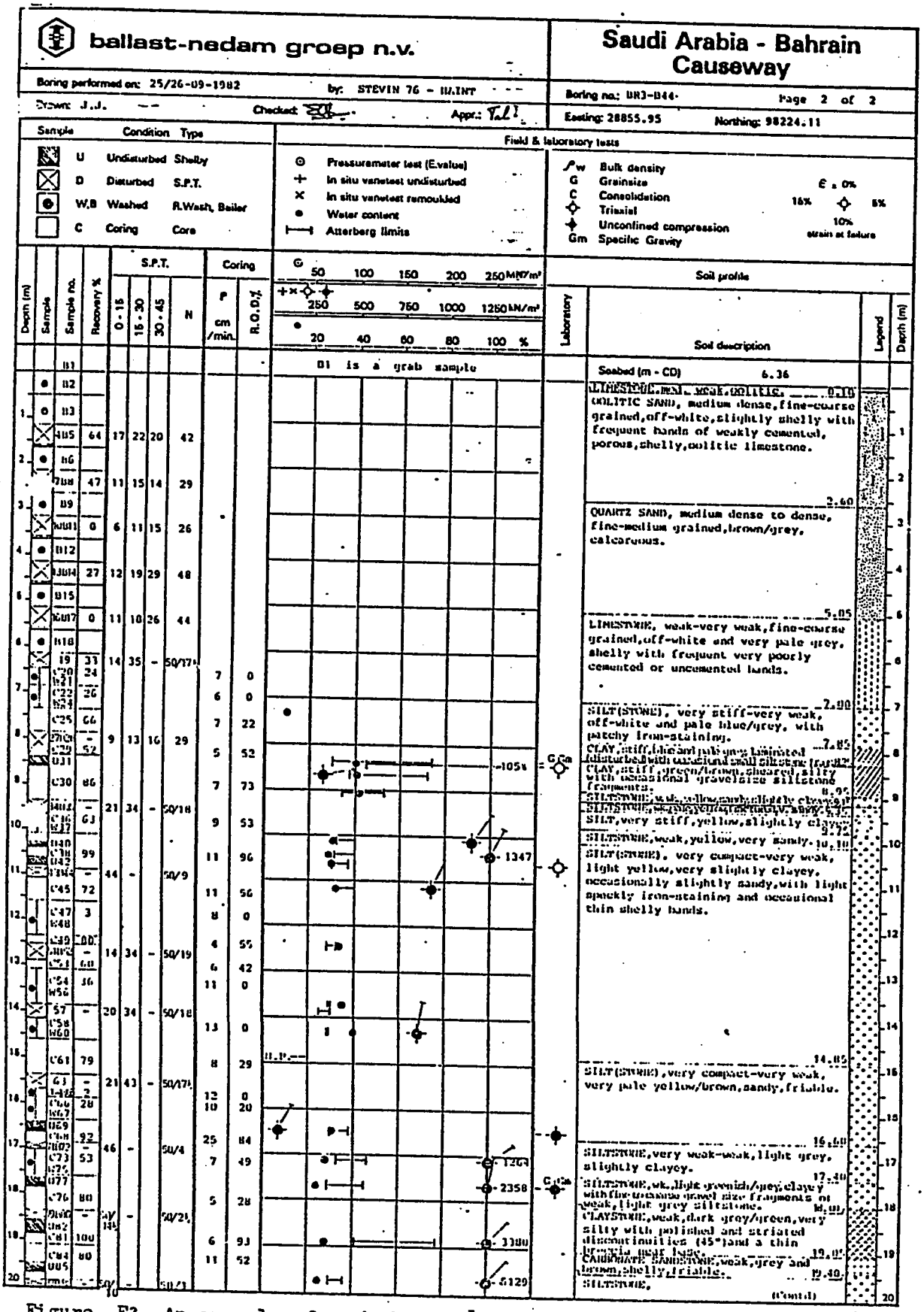

Figure E3. An example of rock description profile including most of the engineering properties of soil and rocks. It was done by Balast-nedam groep n.v.

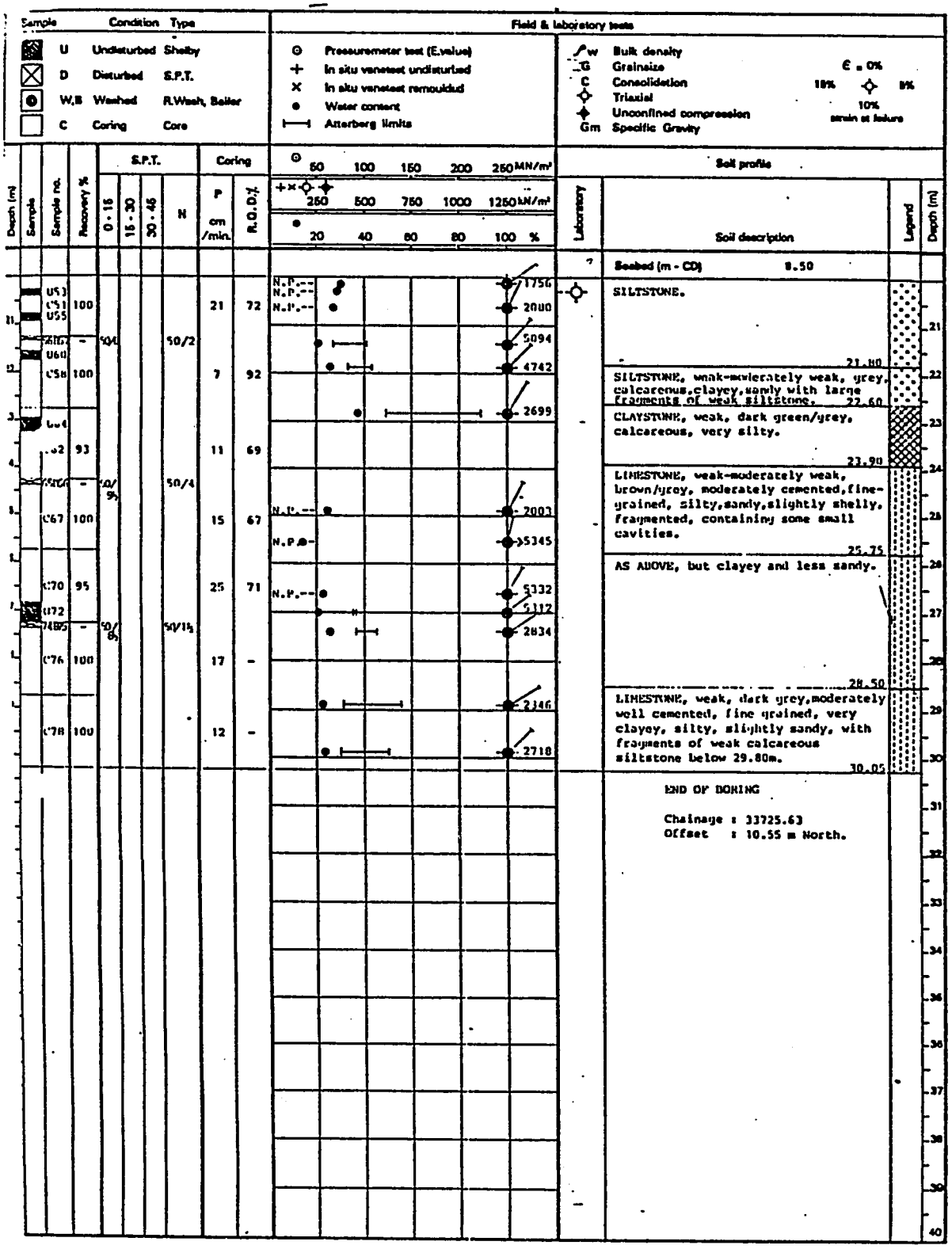
Sample
Condition
Type
U Undisturbed Shelby
D Disturbed S.P.T.
W,B Washed R.Wash, Baller
C Coring Core
Field & laboratory tests
Pressuremeter test (E.value)
In situ vanetest undisturbed
In situ vanetest remoulded
Water content
Atterberg limits
w Bulk density
G Grainsize
c Consolidation
Triaxial
Unconfined compression
Gm Specific Gravity
ε = 0%
18%
8%
10%
strain at failure
Depth (m)
Sample
Sample no.
Recovery %
S.P.T.
0 - 15
15 - 30
30 - 45
N
Coring
P cm /min.
R.Q.D.%
Soil profile
Laboratory
Soil description
Legend
Depth (m)
Seabed (m - CD) 8.50
SILTSTONE.
21.80
SILTSTONE, weak-moderately weak, grey, calcareous,clayey,sandy with large fragments of weak siltstone. 22.60
CLAYSTONE, weak, dark green/grey, calcareous, very silty.
23.90
LIMESTONE, weak-moderately weak, brown/grey, moderately cemented,fine-grained, silty,sandy,slightly shelly, fragmented, containing some small cavities.
25.75
AS ABOVE, but clayey and less sandy.
28.50
LIMESTONE, weak, dark grey,moderately well cemented, fine grained, very clayey, silty, slightly sandy, with fragments of weak calcareous siltstone below 29.80m.
30.05
END OF BORING
Chainage : 33725.63
Offset : 10.55 m North.

APPENDIX F

ACID WASH RESULTS FOR 8 ROCK SAMPLES TREATED BY DILUTED ACID (1 n HCL).

Table f Acid wash (1 N HCL) results for 8 rock samples.

	ROCK NAME	No. & DEPTH	RESIDUE %	RESIDUE TYPES
1	Calcitic skeletal grainstone	1/7 (2m)	21%	Quartz sand, sub-rounded, with some silt.
2	Calcitic skeletal grainstone	2/1 (5m)	26%	Quartz sand, sub-rounded
3	Aragonitic skeletal grainstone	3/9 (.5m)	35%	Quartz sand, rounded to sub-rou--nded.
4	Dolomitic green mudstone	3/44.3 (24)	31%	Mainly fine clay (undefined) and quartz silt, with traces of gypsum.
5	Dolomitic wackestone	2/16 (10)	4%	Quartz silts with some gypsum
6	Dolomitic wackestone	3/1 (22m)	8%	Mainly quartz silt, with some gypsum crystals.
7	Dolomitic green mudstone	3/32	20%	Mainly fine clay (undefined), with quartz silt.
8	Aragonitic skeletal grainstone	3/32 1m	32%	Quartz sand, sub-rounded to sub-angular.

REFERENCES

Adams, J.E. and Rhodes, M.L., 1960, Dolomitization by seepage refluxion. Bull. Am. Assoc. Petrol. Geologists, No. 44, p. 1912-1920.

Al-Asfour, T.A., 1982, Changing sea-level along the north coast of Kuwait Bay. Kegan Paul International, London, 250 p.

Badiozamani, K., 1973, The Dorag dolomitization model - application to the Middle Ordovician of Wisconsin: Jour. Sed. Petrology, V. 43, p. 965-984.

Balast-needam groep n. v., 1983, Site Investigation report for Saudi-Bahrain Causeway, Saudi Arabia: Unpublished report.

Bathurst, R.G.C., 1971, Carbonate sediments and their diagenesis: Developments in Sedimentology, V. 12, Amsterdam, Elsevier, 658 p.

Bricker, O.P., 1971, Carbonate Cement, Johns Hopkins University Studies in Geology, No. 19, London, 376 p.

Butler, G.P., 1971, Recent gypsum and anhydrite of the Abu Dhabi Sabkha, Trucial Coast: Northern Ohio Geol. Soc., p.120-152.

Doornkamp, J.C., Brunsden, D. and Jones, K.C, 1980, Geology, Geomorphology, and Pedology of Bahrain. University of East Anglia, Norwich, Geo Abstracts Ltd., U.K., 443 p.

Dunham, R.J., 1962, Classification of carbonate rocks according to depositional texture. Am. Assoc. Petrol. Geologist, Mem. 1, p. 108-120.

Dunham, R.J. and Olson E.R.,1978, Diagenetic Dolomite Formation Related to Paleozoic Paleogeography of the Cordilleran Miogeocline in Nevada, Geology, V. 6, p. 556-559.

Ehlers, E.G. and Blatt, H., 1980, Petrology, Igneous, Sedimentary and Metamorphic, W.H. Freeman, SanFrancisco, 732 p.

Evans, G., Kinsman, D.J. and Shearman, D.J.,1964, A reconnaissance surve of the environment of recent carbonate sedimentation along the Trucial coast, Persian Gulf. In: Deltaic and Shallow marine deposits, ed. by L.M.J.U. Van Straaten. Elsevier, Amsterdam, p.129-135.

Evans, G., Schmidt, V., Bush, P. and Nelson, H., 1969, Stratigraphy and geologic history of the Sabkha, Abu Dhabi, Persian Gulf, Sedimentology, V. 12, p. 145-159.

Evans, G., 1970, Coastal and nearshore sedimentation: A comparison of clastic and carbonate deposition. Proc. Geol. Assoc. London 81, p. 493-508.

Fairbridge, R.W., 1961, Eustatic changes in sea level. In: Physics and Chemistry of the earth, V. 4, Pergamon Press.

Folk, R.L., 1962, Special subdivision of Limestone types, In:
Classification of Carbonate Rocks: A Symposium, W.E. Ham (Ed.), Am. Assoc. Petrol. Geol., Mem. 1, p. 62-84.

Folk, R.L., 1974, The natural history of crystalline calcium carbonate, effect of magnesium content and salinity, Jour. Sed. Petrology, V. 44, p. 40-53.

Folk, R.A. and Land, A.S., 1975. Mg/Ca ratio and salinity: two controls over crystallization of dolomite: Am. Assoc. Petroleum Geologists Bull., V. 59, p. 60-68.

Gunatilika, A., 1986, Kuwait and Northern Arabian Gulf: A study in Quaternary Sedimentation, Episodes, V. 9, No. 4, December.

Houbolt, J.J.H.C., 1957. Surface sediments of the Persian Gulf near the Qatar Peninsula. Doctoral thesis, University of Utrecht. Den Haag: Monton & Co.

Hsu, K.J., 1966, Origin of dolomite in sedimentary sequences: A critical analysis. Mineralium Deposit, No. 2, p. 133-138.

Illing, L.V., Wells, A.J. and Taylor, J.C.M., 1965, Penecontemporary dolomite in the Persian Gulf. In: Dolomitization and Limestone diagenesis, ed. by L.C. Pray and R.C. Murray. S.E.P.M., Spec. Pub., No. 13, p. 89-111.

Kassler, P., 1973, The Structural and geomorphic evaluation of the Persian Gulf. In: The Persian Gulf: Holocene carbonate sedimentation and their diagenesis, by B.H. Purser (ed.), Springer-Verlag, Berlin, 472 p.

KFAS, 1987, Conference on Quaternary Sediments in the Arabian Gulf and Mesopotamian Region, Abstracts, Kuwait University, 74 p.

Kinsman, D.J.J., 1964, The Recent Carbonate Sediments near Halal el Bahraini, Trucial Coast, Persian Gulf. In: Developments in Sedimentolog 1, Deltaic and Shallow Marine Deposits, ed. by L.M.J.U. Van Straaten, p. 189-192.

Land, L.S. and Epstein S.,1970, Late Pleistocene diagenesis and dolomitization, North Jamaica, Sedimentology, V. 14, p. 187-200.

Land, L.S., 1970, Phreatic versus vadose meteoric diagenesis of limestones: evidence from a fossil water table. Sedimentology, V. 14, p. 175-185.

Land, L.S., Salem, M.I. and Morrow, D.W., 1975, Paleohydrology of ancient dolomites: geochemical evidence: Am. Assoc. Petroleum Geologists Bull., V. 49, p.1602-1625.

Loreau, J.P. and Purser, B.H., 1973, Distribution and ultrastructure of Holocene ooids in the Persian Gulf, p.233-379. In: Persian Gulf by B.H. Purser (ed.), Springer-Verlag, Berlin, 471 p.

Morrow, D.W., 1978. The influence of the Mg/Ca ratio and salinity on dolomitization in evaporite basins. Bull.

Canad. Petroleum Geol., V. 26, No. 3, Sep., p. 389-392.

Milliman, J.D., 1974, Marine Carbonate, 375 p. Berlin-Heidelberg, New York: Springer-Verlag.

Purser, B.H., ed., 1973. The Persian Gulf: Holocene carbonate sedimentation and diagenesis in a shallow Epicontinental Sea, Springer-Verlag, Berlin, 471 p.

Purser, B.H., and Seibold, E., 1973, The principal environmental factors influencing Holocene sedimentation and diagenesis in the Persian Gulf, pp.1-11. In: Persian Gulf by B.H. Purser (ed.), Springer-Verlag, Berlin, 471 p.

Scoffin, P.S., 1987, An Introduction to carbonate sediments and rocks, Chapman and Hall, New York, 274 p.

Seibold, E. and Volbrecht, K., 1969, Dia Bodengestalt des Persischen Golfs "METEOR" Forsch. Ergebnisse, Reihe, C., No. 2, p. 29-56.

Shadfan, H., Mashhady, A.S., Dixon, J.B. and Hussen, A.A., 1985. Palygorskite from Tertiary Formations of Eastern Saudi Arabia, Clays and Clay Minerals, V.33, No.5, p. 451-457.

Shinn, E.A., 1969, Submarine lithification of Holocene carbonate sediments in the Persian Gulf. Sedimentology, V. 12, p. 109-144.

Shinn, E.A., 1973, Carbonate coastal accretion in an area of Longshore transport, NE Qater, Persian Gulf. In: B.H. Purser (ed.), The Persian Gulf-Holocene Carbonate Sedimentation, Berlin, Springer-Verlag, p. 179-191.

Shinn, E.A., 1984, Tidal flat environment. In: Scholle, Bebout and Moore (ed.), Carbonate depositional environment, Am. Assoc. Petroleum Geologists, Mem. 33, p. 171-210.

Sugden, W., 1963a, Some aspects of sedimentation in the Persian Gulf. J. Sediment. Petrol., V. 33, p. 171-210.

Wagner, C.W. and Togt, C.V., 1973, Holocene sediment types and their distribution in the southern Persian Gulf. In: B.H. Purser (ed.), The Persian Gulf-Holocene Carbonate Sedimentation: Berlin, Springer-Verlag, p. 123-155.

Warshaw, C.M. and Roy R., 1961, Classification and scheme for the identification of layered silicates. Bull. Geol. Soc. Am., No. 72, p. 1455-1492.

Weaver, C.E., and Beck, K.C., 1977, Miocene of the S.E. United States. A model for chemical sedimentation in a peri-marine environment, Amsterdam, p. 201-225.

Wells, A.J., and Illing, L.V., 1964, Present-day precipitation of calcium carbonate in the Persian Gulf. In: L.M.J.U. Van Straaten (ed.), Deltaic and shallow marine deposits. Elsevier, Amsterdam, p. 429-435.

Zenger, D.H., 1972, Dolomitization and Uniformitarianism. J. Geol. Educ., No. 20, p. 107-124.